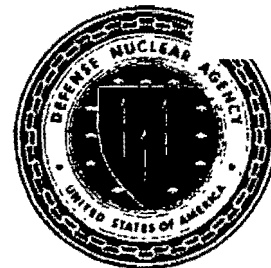




~~UNCLASSIFIED~~
UNCLASSIFIED

Defense Nuclear Agency
Alexandria, VA 22310-3398



DNA-TR-93-2

Influence of Ingested Nuclear Cloud Dust and Overpressure Waves on Gas Turbine Engine Behavior (U)

Michael G. Dunn
Calspan Corporation
P.O. Box 400
Buffalo, NY 14225

November 1993

Technical Report

CONTRACT No. DNA 001-89-C-0060

STATEMENT A

Approved for public release;
distribution is unlimited.

DECLASSIFIED

Authority EO 13526

Air Force AFRL/RZ 11 June 2010

DTRA 7540 Date 15 June 2010

THIS DOCUMENT CONSISTS OF 100 PAGES

COPY 35 OF 58 COPIES, SERIES A

~~CLASSIFIED BY DO Form 254 dated 6 May 1988. Control No. DNA 001-89-C-0060. F-16 Tactical Fighter (FA) SCG dated 15 October 1986 (U); F-16 Multimission (FM) SCG dated 20 June 1986 (U), and the B-1B Program SCG dated 31 October 1984 (U).
DECLASSIFY ON OADR.~~

~~UNCLASSIFIED~~
UNCLASSIFIED

DNA 93 002

DESTRUCTION NOTICE:

FOR CLASSIFIED documents, follow the procedures in DoD 5200.22-M, Industrial Security Manual, Section II-19.

FOR UNCLASSIFIED, limited documents, destroy by any method that will prevent disclosure of contents or reconstruction of the document.

Retention of this document by DoD contractors is authorized in accordance with DoD 5220.22-M, Industrial Security Manual.

PLEASE NOTIFY THE DEFENSE NUCLEAR AGENCY, ATTN: CSTI, 6801 TELEGRAPH ROAD, ALEXANDRIA, VA 22310-3398, IF YOUR ADDRESS IS INCORRECT, IF YOU WISH IT DELETED FROM THE DISTRIBUTION LIST, OR IF THE ADDRESSEE IS NO LONGER EMPLOYED BY YOUR ORGANIZATION.



From: Freeman, Betsy L. CIV
Sent: Thursday, September 09, 2010 11:13 AM
To: Lindsey, Robert H. MAJ USA
Cc: Hoppe, Herbert CONTRACTOR; Cole, Richard M. CIV
Subject: Fw: SAF/PA Case Completed: Case Number 2010-0507

Maj Lindsey,

Please forward this note to DTRIAC as official clearance from DTRA/PA that the AF/OSR clearance below has been verified and is final step in public release process. The documents should now be marked for Distribution A Public Release, Unlimited Distribution.

Thank you,
Betsy Freeman
Deputy Director
Public Affairs
Defense Threat Reduction Agency

----- Original Message -----

From: Devalee.Pridgen-Gattison@pentagon.af.mil
<Devalee.Pridgen-Gattison@pentagon.af.mil>
To: Freeman, Betsy L. CIV; dick.cole@dtra.mil <dick.cole@dtra.mil>
Sent: Thu Sep 09 08:50:35 2010
Subject: SAF/PA Case Completed: Case Number 2010-0507

SAF/PA has completed the review process for your case on 09 Sep 2010:

Subject: Report - Volcanic Ash Engine Data (Report)

Case Reviewer: Devalee Pridgen-Gattison
Case Number: 2010-0507

The material was assigned a clearance of AF NO OBJECTION on 09 Sep 2010. If local policy permits, the Review Manager for your case, Devalee Pridgen-Gattison, Devalee.Pridgen-Gattison@pentagon.af.mil, will prepare a hard copy of the review and will forward it via mail or prepare it for pick up.

DISTRIBUTION LIST UPDATE

This mailer is provided to enable DNA to maintain current distribution lists for reports. (We would appreciate your providing the requested information.)

- ☐ Add the individual listed to your distribution list.
- ☐ Delete the cited organization/individual.
- ☐ Change of address.

NOTE:

Please return the mailing label from the document so that any additions, changes, corrections or deletions can be made easily.

NAME: _____

ORGANIZATION: _____

OLD ADDRESS**CURRENT ADDRESS**

TELEPHONE NUMBER: () _____

DNA PUBLICATION NUMBER/TITLE**CHANGES/DELETIONS/ADDITIONS, etc.)**

(Attach Sheet if more Space is Required)

DNA OR OTHER GOVERNMENT CONTRACT NUMBER: _____

CERTIFICATION OF NEED-TO-KNOW BY GOVERNMENT SPONSOR (if other than DNA): _____

SPONSORING ORGANIZATION: _____

CONTRACTING OFFICER OR REPRESENTATIVE: _____

SIGNATURE: _____

CUT HERE AND RETURN



DEFENSE NUCLEAR AGENCY
ATTN: TITL
6801 TELEGRAPH ROAD
ALEXANDRIA, VA 22310-3398

DEFENSE NUCLEAR AGENCY
ATTN: TITL
6801 TELEGRAPH ROAD
ALEXANDRIA, VA 22310-3398

DECLASSIFIED

REPORT DOCUMENTATION PAGE			Form Approved OMB No. 0704-0188	
<small>Public reporting burden for this collection of information is estimated to average 1 hour per response including the time for reviewing instructions, searching existing data sources, gathering and maintaining the data needed, and completing and reviewing the collection of information. Send comments regarding this burden estimate or any other aspect of this collection of information, including suggestions for reducing this burden, to Washington Headquarters Services, Directorate for Information Operations and Reports, 1215 Jefferson Davis Highway, Suite 1204, Arlington, VA 22202-4302, and to the Office of Management and Budget, Paperwork Reduction Project (0704-0188), Washington, DC 20503</small>				
1. AGENCY USE ONLY (Leave blank)	2. REPORT DATE 931101	3. REPORT TYPE AND DATES COVERED Technical 910110 - 923006		
4. TITLE AND SUBTITLE Influence of Ingested Nuclear Cloud Dust and Overpressure Waves on Gas Turbine Engine Behavior (U)		5. FUNDING NUMBERS C - DNA 001-89-C-0060 PE - 62715H PR - N99QMXA, RA, A TA - J, RJ, J WU - DH056830		
6. AUTHOR(S) Michael G. Dunn				
7. PERFORMING ORGANIZATION NAME(S) AND ADDRESS(ES) Calspan Corporation P.O. Box 400 Buffalo, NY 14225		8. PERFORMING ORGANIZATION REPORT NUMBER 7749-6		
9. SPONSORING/MONITORING AGENCY NAME(S) AND ADDRESS(ES) Defense Nuclear Agency 6801 Telegraph Road Alexandria, VA 22310-3398 SPWE/Miatech		10. SPONSORING/MONITORING AGENCY REPORT NUMBER DNA-TR-93-2		
11. SUPPLEMENTARY NOTES This work was sponsored by the Defense Nuclear Agency under RDT&E RMSS and RMC Codes B342085466 N99QMXAJ00002 H2590D, B4662D RA RJ 00173 SPWE 4400A 25904D, and B342085466 AJ00168 25904D.				
12a. DISTRIBUTION/AVAILABILITY STATEMENT STATEMENT A Approved for public release; distribution is unlimited.		12b. DISTRIBUTION CODE		
13. ABSTRACT (Maximum 200 words) The material contained in this report was prepared as an input to EM-1, Chapter 20. In the editing necessary for construction of that volume, the material was so reduced that it was considered worthwhile to present the text in complete form. This technical report is composed of two parts. The main report presents the experimental data pertaining to the response of gas turbine engines when exposed to a nuclear dust cloud. All of these data have been obtained by Cal-span utilizing engines that are still active in the military inventory. The Appendix presents experimental data obtained at Calspan that are relevant to the operation of gas turbine engines when subjected to overpressure waves. Several of the same type of engines used in the main report were used in the Appendix.				
14. SUBJECT TERMS Overpressure Pulse Deposition (Glassification)		Erosion Surge		15. NUMBER OF PAGES 100
				16. PRICE CODE
17. SECURITY CLASSIFICATION OF REPORT [REDACTED] (U)	18. SECURITY CLASSIFICATION OF THIS PAGE UNCLASSIFIED	19. SECURITY CLASSIFICATION OF ABSTRACT UNCLASSIFIED	20. LIMITATION OF ABSTRACT SAR	

NSN 7540-280-5500

Standard Form 298 (Rev.2-89)
Prescribed by ANSI Std. Z39-18
298-102

UNCLASSIFIED

[REDACTED]

UNCLASSIFIED

SECURITY CLASSIFICATION OF THIS PAGE

CLASSIFIED BY:

[REDACTED] 5
[REDACTED]

DECLASSIFY ON:

[REDACTED]

[REDACTED]

SECURITY CLASSIFICATION OF THIS PAGE

UNCLASSIFIED



PREFACE

(This Preface is Unclassified)

This study was performed by the Calspan Corporation, Advanced Technology Center. The material represents a summary of research performed by Calspan for the Defense Nuclear Agency under several contracts over a number of years. The comparison of material is Calspan's input to the construction of EM1, Chapter 20. During the course of editing for EM1, Chapter 20, it became clear that significant portions of the material presented herein would be deleted by the editors. A decision was, therefore, made to keep the assembled material together and to make it available as a technical report. The author gratefully acknowledges the contributions made to the success of this effort by the DNA technical monitor, Lt. Col. Jerry Miatech. Thanks are also extended to Mr. Jack Lotsof, Consultant to Calspan, for his help in putting these two parts together.

UNCLASSIFIED

CONVERSION TABLE

Conversion factors for U.S. customary to metric (SI) units of measurement

To Convert From	To	Multiply
angstrom	meters (m)	1.000 000 X E-10
atmosphere (normal)	kilo pascal (kPa)	1.013 25 X E+2
bar	kilo pascal (kPa)	1.000 000 X E+2
barn	meter ² (m ²)	1.000 000 X E-28
British Thermal unit (thermochemical)	joule (J)	1.054 350 X E+3
calorie (thermochemical)	joule (J)	4.184 000
cal (thermochemical)/cm ²	mega joule/m ² (MJ/m ²)	4.184 000 X E-2
curie	giga becquerel (GBq)*	3.700 000 X E+1
degree (angle)	radian (rad)	1.745 329 X E-2
degree Fahrenheit	degree kelvin (K)	$t_K = (t_F + 459.67)/1.8$
electron volt	joule (J)	1.602 19 X E-19
erg	joule (J)	1.000 000 X E-7
erg/second	watt (W)	1.000 000 X E-7
foot	meter (m)	3.048 000 X E-1
foot-pound-force	joule (J)	1.355 818
gallon (U.S. liquid)	meter ³ (m ³)	3.785 412 X E-3
inch	meter (m)	2.540 000 X E-2
jerk	joule (J)	1.000 000 X E+9
joule/kilogram (J/Kg) (radiation dose absorbed)	Gray (Gy)	1.000 000
kilotons	terajoules	4.183
kip (1000 lbf)	newton (N)	4.448 222 X E+3
kip/inch ² (ksi)	kilo pascal (kPa)	6.894 757 X E+3
ktap	newton-second/m ² (N-s/m ²)	1.000 000 X E+2
micron	meter (m)	1.000 000 X E-6
mil	meter (m)	2.540 000 X E-5
mile (international)	meter (m)	1.609 344 X E+3
ounce	kilogram (kg)	2.834 952 X E-2
pound-force (lbf avoirdupois)	newton (N)	4.448 222
pound-force inch	newton-meter (N·m)	1.129 848 X E-1
pound-force/inch	newton/meter (N/m)	1.751 268 X E+2
pound-force/foot ²	kilo pascal (kPa)	4.788 026 X E-2
pound-force/inch ² (psi)	kilo pascal (kPa)	6.894 757
pound-mass (lbm avoirdupois)	kilogram (kg)	4.535 924 X E-1
pound-mass-foot ² (moment of inertia)	kilogram-meter ² (kg·m ²)	4.214 011 X E-2
pound-mass/foot ³	kilogram/meter ³ (kg/m ³)	1.601 846 X E+1
rad (radiation dose absorbed)	Gray (Gy)**	1.000 000 X E-2
roentgen	coulomb/kilogram (C/kg)	2.579 760 X E-4
shake	second (s)	1.000 000 X E-8
slug	kilogram (kg)	1.459 390 X E+1
torr (mm Hg, 0°C)	kilo pascal (kPa)	1.333 22 X E-1

*The becquerel (Bq) is the SI unit of radioactivity; Bq = 1 event/s.

**The Gray (Gy) is the SI unit of absorbed radiation.

UNCLASSIFIED

TABLE OF CONTENTS (This Table of Contents is Unclassified)

Section	Page
PREFACE	iii
CONVERSION TABLE	iv
FIGURES	vi
1 INTRODUCTION	1
2 DAMAGE PHENOMENOLOGY	3
2.1 Engine Damage	3
2.2 Other Dust Damage	7
3 IN-FLIGHT AND LABORATORY DATA	9
3.1 Experimental Apparatus and Procedure	10
3.2 Cloud Description, Preparation, and Analysis	10
4 EXPERIMENTAL RESULTS	13
4.1 Pratt and Whitney F-100-PW-100 Turbofan12 Results	13
4.2 General Electric YF-101-GE-100 Turbofan Engine Results	16
4.3 Williams International F-107-WR-102 Turbofan Engine Results	20
4.4 Pratt and Whitney TF-33-P-3 Turbofan Engine Results	21
4.4 Laboratory Results With an Engine Combustor Rig	22
5 COPING WITH THE DUST CLOUD ENVIRONMENT	23
5.1 Air Crew Actions	23
5.2 Modifications to Existing Engines	24
5.3 Comments About Future Engines	25
6 CONCLUSIONS	26
7 REFERENCES	27
APPENDIX - INFLUENCE OF OVERPRESSURE PULSE ON THE OPERATION OF A GAS TURBINE ENGINE	55

UNCLASSIFIED

FIGURES

(This list of Figures is Unclassified)

Figure		Page
2.1	Photograph of St. Elmo's glow at fan face of P/W TF-33 turbofan	31
2.2	Closeup photograph of St. Elmo's glow at fan face of P/W TF-33 turbofan	32
2.3	Post-test photograph of ECS plumbing for TF-33 engine after dust exposure	33
3.4	Large engine research cell	34
3.5	Schematic of dust injection system	34
3.6	Scanning electron microscope micrograph and composition spectrum of black scoria	35
4.7	Time history of F-100-PW-100 engine parameters during dust exposure	36
4.8	Time history of F-100-PW-100 engine parameters during dust exposure	38
4.9	Time history of F-100-PW-100 engine parameters during dust exposure	40
4.10	Photograph of first vane for F-100-PW-100 high-pressure turbine after dust exposure	42
4.11	Close-up of photograph of F-100-PW-100 fuel nozzles after dust exposure	43
4.12	Rear view photograph of second stage fan rotor of F-100-PW-100 after dust exposure	44
4.13	Photograph of F-100-PW-100 high-pressure compressor ninth-stage rotor after dust exposure	45
4.14	Pre-test photograph of inlet to first vane of YF-101-GE-100 high pressure turbine	46
4.15	Post-test photograph of YF-101-GE-100 hp turbine vane	47
4.16	Close-up post-test photograph of YF-101-GE-100 hp turbine guide vane	48
4.17	Post-test photograph of YF-101-GE-100 hp turbine vane cooling air inlet filter	49
4.18	Post-test view photograph of first vane of YF-	

UNCLASSIFIED

FIGURES (Continued)

Figure		Page
	101-GE-100 high pressure turbine	50
4.19	Post-test photograph of three blades from YF-101-GE-100 high pressure turbine	51
4.20	Post-test photograph of YF-101-GE-100 blade suction surface	52
4.21	Post-test photograph of 6th stage blade of YF-101-GE-100 high pressure compressor	53
4.22	Post-test photograph of fuel nozzles from YF-101-GE-100 combustor	54
A-1	Nuclear weapons effects	74
A-2	Pulse requirements	75
A-3	Sketch of shock tube and test cell configuration	76
A-4	Sketch of test cell configuration	77
A-5	Typical shock tube and fan face static pressure records for TF33 at MRT setting	78
A-6	Typical pressure history	79
A-7	Typical pressure-data history for station #1 in S-type inlet at 0 deg. yaw	80
A-8	Typical pressure-data history for station #3 in S-type inlet at 0 deg. yaw	81
A-9	Typical pressure-data history for station #3 in S-type inlet at 20 deg. yaw	82
A-10	Engine pressure results for core speed of 55,000 rpm	83
A-11	Distortion inlet for S-type inlet at 0 deg. yaw	84
A-12	Distortion index for S-type inlet at 20 deg. yaw	85
A-13	Typical component radial displacement histories for TF33 at MRT setting	86
A-14	Influence of overpressure on TF33 inlet, diffuser, and casing displacement	87
A-15	Influence of overpressure on J57 inlet, diffuser, and turbine casing displacement	88

UNCLASSIFIED

FIGURES (Continued)

Figure		Page
A-16	Photograph of initial tailpipe flame for 2.1 psi overpressure	90
A-17	Photograph of tailpipe surge during acceleration	90

UNCLASSIFIED

SECTION 1

(This Section is Unclassified)

INTRODUCTION

During the past ten years, there have been several instances in which commercial aircraft have inadvertently flown through volcanic dust clouds with potentially disastrous results. Some notable instances are (a) the 1980 Trans America Lockheed L-382 aircraft (Allison T56 turboprop engines) encounter with the Mt. St. Helens cloud near Seattle, Washington; (b) the June 1982 encounter of a British Airways Boeing 747 aircraft (Rolls Royce RB211 turbofan engines) with a cloud from Mt. Galunggung near Bandung, Indonesia; (c) the July 1982 encounter of a Singapore Airlines Boeing 747 aircraft (Pratt/Whitney JT9D turbofan engines) with a volcanic cloud also from Mt. Galunggung; (d) the May 1985 encounter of a Qantas Airlines (RB211 engines) with a volcanic cloud from Mt. Soputan near Salawesi, Indonesia; and (e) the December 1989 encounter of a KLM Boeing 747 aircraft (General Electric CF6 turbofan engines) with the Mt. Readout cloud near Anchorage, Alaska. In all of these cases, substantial deposition of material occurred on the high pressure turbine first vane which caused significant difficulty in operating the engines, Campbell, 1990. With the exception of the Trans America and The Qantas aircrafts, the engines had to be shut down. Attempts at high altitude restart failed, and it was not possible to restart the engines until lower altitudes. The turboprop engines of the Trans America aircraft were destroyed by the time the aircraft returned to the airport and portion of the turbofan engines of the British Airways, the Singapore Airlines, the KLM Airlines and the Qantas Airlines aircraft had to be replaced.

The incidents described above have demonstrated that lofted earth materials can result in gas turbine engine distress. The detonation of a nuclear device or any other mechanism that may cause amounts of earth material to become airborne must be considered from the viewpoint of survivability of the aircraft propulsion systems. The particular engine involved is of obvious importance. In addition, the composition, concentration and movement of the lofted material become very important in terms of determining how to cope with the situation. These considerations will be treated more fully below.

The remainder of this section will present a description of the damage mechanisms in Section 2, a discussion of the source of the experimental data in

UNCLASSIFIED

Section 3, a review of the experimental results in Section 4, and a brief discussion of how to cope with the engine degradation problem in Section 5.

UNCLASSIFIED

SECTION 2

(This Section is Unclassified)

DAMAGE PHENOMENOLOGY

This section of the report focuses on engine degradation due to dust ingestion, but it should be noted that the dust will scrub exposed external surfaces of the aircraft and, in addition, will find its way into the cabin via the environmental control system (ECS). Engine damage mechanisms will be discussed next; other types of damage will be covered later.

2.1 ENGINE DAMAGE.

Several different mechanisms may be active in altering engine performance during or after exposure to a nuclear dust cloud and the potential of each should be recognized. Depending upon the particular engine and the particular dust, damage to the engine may be manifested in one or more of the following ways: (a) erosion of compressor blading, (b) melting in the combustor of one or more of the ingested components and subsequent deposition of material on hot section components, (c) blockage of turbine vane and blade cooling holes, (d) blockage of fuel nozzle swirl vanes, and (e) oil system contamination. It should also be pointed out at this juncture that the various engines in the military inventory have been designed and built by several different manufacturers at different time periods. Because of this, the individual engines will respond to the same environment in very different ways. As this discussion proceeds, these design differences and the behaviors that they cause will be highlighted.

For a turbofan engine, the first encounter of the dust particles with the engine is at the fan stage. An immediate effect is that the larger particles are pulverized upon impact with the rotating blades with the result that there are few particles remaining larger than about 10 microns in diameter. At the same time, the impact of the dust particles on the moving metallic surfaces creates an electrostatic charge which, upon discharge, generates a striking glow (the intensity of which depends upon dust concentration) at the fan face. This glow, which has been identified as the well-known St. Elmo's fire, has been observed in all laboratory tests, and was also observed by the British Airways crew during their encounter with the Galunggung volcano cloud, Private Communication, Dunn and Moody. To a crew, the first indication of the dust cloud would be "fire flies" on the wind screen. The crew may incorrectly attribute this "fire fly"

observation to ice crystals in the air stream since they are accustomed to the ice crystal scenario. If they can see the engine face, then they would also see the glow at the engine nacelle.

This glow has been photographed for each of the laboratory measurement programs performed by Calspan and typical pictures are given in Figures 2-1 and 2-2. Figure 2-1 is a wide angle photograph of the dust tube, the dust injection nozzles, and the fan face glow recorded on video tape for a TF33 turbofan (Dunn, Padova, and Moller, 1986(a)) operating in a dust cloud of concentration on the order of 500 mg/M^3 ($5 \times 10^{-7} \text{ gm/cm}^3$). Figure 2-2 is a close-up photograph of the fan face. The first fan stage rotor fence and the first stage inlet guide vane are not obscured by the glow because the momentum exchange between these surfaces and the dust particles is too low to cause charge accumulation. The second stage inlet guide vane appears as a shadow in the illumination field of the first and second rotors. Three silhouettes in Figure 2-2 are due to the dust injection nozzles. The location of these nozzles can be more clearly seen on Figure 2-1. A very bright ring of light appears at the first and second rotor tip/shroud region. The illumination in this region may be brighter for several reasons, e.g., (a) higher dust particle concentrations due to centrifuging, (b) greater optical depth and unobstructed view of the illumination, and (c) scintillation at the rotor tip. Also visible in this photograph is the stationary nose and a total pressure probe.

Dust cloud material ingested by a gas turbine engine acts as an abrasive which polishes surfaces and removes metal in the process. After passing through the fan, the dust enters the compressor. Although it has been pulverized into fine particles, they are not so fine that they can follow flow streamlines and thus have a tendency to be centrifuged towards the outer portion of the flow. One should not be misled by this comment into concluding that, for a high-bypass-ratio engine, the majority of the dust will be centrifuged in the fan stage into the bypass duct; experimental evidence demonstrates that such is not the case.

Major erosion of the fan and the compressor occurs in the tip region on the rotating components. The stationary guide vanes are polished, but not much material is removed. However, for the blades, a significant amount of material is removed in the tip region causing significant increases in the tip gap and blade profile. These changes result in loss of compressor performance and loss of surge margin.

UNCLASSIFIED

Erosion of compressor components represents an irreversible loss of engine capability which can only be regained by replacing the damaged parts. The erosion process appears to be relatively independent of blade material, e.g., titanium or steel. On the encouraging side, for compressor erosion to render the engine inoperable generally requires more dust loading (and thus exposure time) than is required for some of the other damage modes to be discussed later. In the older engines, compressor erosion becomes the major damage mechanism.

A small amount of air exiting the high pressure compressor (on the order of 5% to 10%) is bled off for cooling the blades and vanes of the turbine, oil sump pressurization, and for the ECS. The effects of dust particles on blade and vane cooling and on the oil system will be described later; the focus at this point is on fuel nozzle deposits.

Deposits of carbon-like material on the engine fuel nozzles have been observed in the laboratory and in flight. It is difficult to generalize about this problem since there are as many different fuel nozzle configurations as there are engines. Whether or not deposits will form on a particular fuel nozzle depends upon the configuration. In cases where deposits have been observed, they form on the air swirl vanes, not over the hole through which the fuel flows. The mechanism for these deposits is not clearly understood, but the available evidence suggests that it is associated with a rich fuel-to-air mixture ratio arising from the fact that the ability of the compressor to produce compressed air has been compromised by blade erosion and the control system does not recognize the problem and thus reduce the fuel flow rate. For some engines, the fuel flow was observed to increase with continued dust exposure (and thus decreased compressor performance) and in these cases carbon deposits were found on the fuel nozzles. For another engine, the control system decreased the fuel flow rate and the carbon deposits on the fuel nozzles were present, but not as extensive.

As far as the air crew is concerned, the problems associated with fuel nozzle deposits come about if the engine flames out. As noted above, the fuel hole is not blocked and fuel will flow at the normal flow rate. However, the air swirl vanes may be partially blocked and thus fuel atomization is significantly reduced. A modern annular combustor normally has two igniters and about sixteen to twenty fuel nozzles. If, for some reason, the fuel is not atomized, then

it is very difficult to initiate and sustain proper combustion. Experimental data pertinent to this difficulty will also be presented in Section 4.

Most modern gas turbine engines use air bled from the high pressure compressor to pressurize the oil sump. For the situation under discussion here, this air contains dust particles. The oil system has one or more filters that will collect particles larger than about 30 microns in diameter. The pressurized air contains some particles in the 30 micron range but many more in the 5 to 10 micron range. These smaller particles pass through the filter and on into the lubrication system. The larger particles collect on the filter causing the back pressure to increase and thus the system diverts oil to the sump. In the first case, the dust material finds its way to the bearings and in the second case the supply of oil to the bearings is reduced. Damage to the bearing system can survive longer exposure than the other engine damage modes. Upon landing the aircraft, the oil system should be drained and flushed, new oil added to the engine, and the filters should be replaced. By contrast, the older engines do not appear to be as sensitive to this damage mechanism because of the design and construction techniques used at that time.

As mentioned above, air for film cooling turbine blades and vanes is bled from the high pressure compressor. Older engines (e.g., J57, TF33, F107, etc.) do not rely heavily on film cooling and thus the discussion of this subsection is not as important for those engines. However, all modern gas turbine engines (e.g., F100, F101, F110, F119, etc.) rely on extensive film cooling of the high pressure turbine first vane and first blade in order to achieve the required thrust.

(U) Unless the turbine designer considers the implications of flying through a dust cloud, he will design the cooling system with a large number of small, closely-spaced cooling holes in order to achieve higher cooling efficiency. Experimental data (Baran and Dunn, 1992 and Kim, Baran, and Dunn, 1991(a)) for modern engines (F101 and F100) demonstrate that the vane and blade cooling holes can be blocked from the inside by ingested dust with the result that the component is destroyed by excess heating. Further, the passages leading the cooling air to the vane or blade cooling passage inlet are relatively small and can also become compacted with the dust material. If the cooling holes or the passages to these holes become blocked, then the flow rate of cooling air is reduced. Continued operation of the engine at high thrust level will cause the turbine components to be destroyed and the engine will lose performance rapidly. This problem will be addressed more fully in Section 4.

Only a portion of the air leaving the compressor passes through the very hot zone of the combustor. The remainder is used for combustor dilution or for turbine cooling. In this discussion, hot is a relative term which, from a damage mechanism viewpoint, really requires one to determine over which portion of the combustor a particular component of the ingested material will melt. Melting also depends upon the time spent by the entrained particles in the hot zone. This time must be sufficiently long to absorb sufficient heat which then requires that their thermal characteristics be within a given range if the particles are to melt. After leaving the combustor, the particles are directed to the first vane of the high pressure turbine. Whether or not the particles that have melted adhere to the first vane depends upon several factors, e.g., the properties of the melted material, the local shear stress on the surface, and the surface temperature of that vane. However, those melted particles that do not adhere to the first vane have an opportunity to adhere to the first blade. The first blade operates at a lower temperature than the first vane, but it is also rotating at relatively high speed so centrifugal force influences the ability of the particles to adhere to the blade.

The process of particle melting and subsequent deposition on turbine components is often referred to as deposition or glassification. It is the only dust-cloud damage mechanism that is, to a point, reversible in flight if the crew understands the problem. Section 5 describes the mitigation procedure in detail. By contrast, internal cooling-hole clogging is not reversible, but there may be some rather simple design changes that could help with this problem.

2.2 OTHER DUST DAMAGE.

As was pointed out above, dust will scrub external surfaces and will enter the aircraft cabin via the ECS. With respect to the ECS, the particles have the appearance of smoke and form a thin layer of dust on electronics, instruments, and all other portions of the aircraft that are exposed to ECS air. Electronic microchips are known to be adversely effected by dust material and, though the damage may not be immediate, it may occur in a relatively short time. In addition, the dust is easily taken into the lungs. If it is radioactive, then the impact on the health of the flight crew could be harsh. If such a situation is encountered, the crew should immediately transit to an oxygen supply system that is totally independent of the ECS. Such a system is normally available on both military and civilian aircraft for the cockpit crew, but not for the passengers.

UNCLASSIFIED

As illustrated by the 747 aircraft experiences described in Campbell, 1990, it is well documented that dust cloud material ingested by the engine makes its way through the ECS of modern aircraft and into the cabin. Laboratory measurements reported in Dunn, Padova, and Adams, 1987, determined the relative amount of dust material that is passed by the ECS of a TF-33 engine. Figure 2.3 is a photograph of a portion of the ECS duct (taken from a TF-33 engine) illustrating that the dust particles erode the duct wall material. For this engine, the collection efficiency was found to depend primarily on the geometry of the engine near the ECS bleed and the local air velocity. The engine geometry is fixed and the contribution of changes in the local air velocity to the collection efficiency with moderate changes in thrust setting, is expected to be small. Thus, the collection efficiency is relatively independent of thrust setting and its measured level can be used to estimate the absolute level of contamination for the bleed air at power settings other than cruise. For example, at a high thrust condition an increase in ECS airflow of about 50% would produce an absolute level of contamination for the bleed air equal to 3.4 parts per thousand of input dust feed rate compared with 2.2 parts per thousand at cruise.

The ECS measurements described above for the TF-33 engine were repeated for the YF101-GE-100 engine and will be reported in Baran and Dunn, 1992. Dust was collected from both the fifth and ninth stage bleeds of that engine, but the data have not yet been analyzed.

The aircraft windscreen and landing lights are directly exposed to the abrasive dust particles at high relative velocity. The result is severe pitting and/or scratching which severely reduces the crew's ability to see through the window. In-flight refueling may be difficult to complete if the crew cannot clearly see the boom extending from the tanker aircraft. Visual bomb damage assessment and landing are also harder to accomplish effectively.

UNCLASSIFIED

SECTION 3

(This Section is Unclassified)

IN-FLIGHT AND LABORATORY DATA

There are two sources of data relevant to the operation of gas turbine engines in dust-laden environments. The first comes from inadvertent encounters of commercial aircraft with volcanic clouds. These encounters are briefly described in the Introduction. The second data source is laboratory measurements performed at Calspan Advanced Technology Center under support from the Defense Nuclear Agency (DNA). The intent of these laboratory measurements has been to determine the early warning signs of incipient engine difficulties, to obtain engine operating data that allows the air crew to cope with the problem, and to obtain phenomenological information which can form the basis of a prediction capability.

Gas turbine engines are routinely tested for the effect of ingestion of solid particles according to the procedures of Military Specification MIL-E-5007D, the commonly known Arizona road-dust test. Within the past several years the material used in this test was changed from an earth-like material to a crushed quartz material. Although the Arizona road-dust test is an important one and is very applicable to many situations that a military aircraft engine might encounter under normal operating conditions, it is not representative of an encounter with a nuclear dust cloud. Nuclear cloud predictions suggest that the material composition is generally more complicated than just quartz and that the dust concentration of the cloud will, in many cases, be significantly greater than that used for MIL-E-5007D. The particle size distribution of the dust in the nuclear cloud is also different from that of MIL-E-5007D, but this difference is probably not important because of the way in which the machine pulverizes the ingested material.

The material to be presented in this discussion will be confined to results obtained from the measurement program at Calspan which is specifically directed at the nuclear cloud problem and which utilizes both full scale operating engines and engine combustors to derive operational data. This effort has been ongoing for several years and many different engines and combustors have been used to obtain these data. The particular engines that have been used are as follows: (a) Pratt/Whitney J57 turbojet (B-52G, EC/KC-135) Dunn, Padova, and Moller, 1986(b), (b) Pratt/Whitney TF33 turbofan (B-52H, C-135, C-141) Dunn, Padova, and Moller, 1986(a) and Dunn and Padova, 1986, (c) Williams

International F107-WR-102 turbofan (Tomahawk cruise missile) Padova and Dunn, 1984 and Baran and Dunn, 1992, (d) Pratt/Whitney F100-PW-100 turbofan (F-15, F-16) Dunn, 1990(a). and Dunn, 1990(b), and (e) General Electric YF101-GE-100 (B1A) Baran and Dunn, 1992. The combustors used to obtain phenomenological data are the Allison T56 turbojet, Padova and Dunn, 1987 and Moller and Dunn, 1990 (can combustor) and the Pratt/Whitney F100 turbofan, Kim, Baran, and Dunn, 1991(a) and Kim, Baran, and Dunn 1991(b) (annular combustor).

3.1 EXPERIMENTAL APPARATUS AND PROCEDURE.

With the exception of the YF101-GE-100 engine, all engines discussed herein were operated in the Calspan Large Engine Research Cell (LERC). The LERC is described in detail in Dunn, Padova, and Moller, 1986(a), but a sketch of the facility is given in Figure 3.4. Following preliminary baseline runs, the engines were exposed to dust at concentrations, thrust settings, and exposure times given by their respective test matrices. These test matrices were constructed on the basis of knowledge of previous engine behavior and the environments the engines were postulated to experience. The individual runs within the matrix were selected to give a qualitative indication of the influence of dust concentration, turbine inlet temperature and exposure time on damage rate and damage mechanism. All engine readings are sampled and stored on an IBM compatible computer. Sampling is normally at 5 second intervals.

The Dust Injection System (DIS) is an important part of the test apparatus and was designed to achieve highly accurate regulation of the dust environment including a controlled range of mean particle sizes and dust concentrations, all evenly dispersed in the incoming air stream. The DIS is schematically shown in Figure 3.5. A more detailed description of the experimental apparatus is given in Dunn, Padova, Moller, and Adams, 1987.

3.2 CLOUD DESCRIPTION, PREPARATION, AND ANALYSIS.

Definition of the specific components that make up the nuclear dust cloud to which the engine will be exposed is an important aspect of this measurement program. It is customary for DNA to work with its consultants and provide to Calspan a description of the desired cloud composition. A joint effort among DNA, its consultants, and Calspan is then initiated to obtain the desired material. Pre-test analysis of the cloud material is performed to determine the mineral

content, the particle size distribution, and the general particle shape. During the course of this nuclear cloud definition, it was decided by the DNA community that a particular volcanic material (Twin Mountain black scoria) possessed the chemical properties of earth material that would have been processed by the nuclear fire ball. This material was, therefore, used in some of the Calspan measurement programs. Figure 3.6 is an example of a scanning electron microscope micrograph and a composition spectrum for the black scoria material.

The final task in the cloud description is to determine the dust concentration along the aircraft flight path for a given nuclear laydown and target area. This task is performed by DNA consultants and then transmitted to Calspan. In order to complete construction of the test matrix, an input from the Strategic Air Command is needed regarding a typical mission flight profile (i.e., altitude, speed, thrust setting (which can be converted to turbine inlet temperature), etc. When the information described above becomes available, the test matrix can be defined and the experiments initiated.

As the particular geographical area of interest changes so does the chemical make up of the dust cloud and thus the soil constituents to be used for the engine experiments. As noted in an earlier paragraph, prior to passing a soil through an engine, a careful analysis of the material is performed. Table 1 provides a summary of several of the different dust blends that have been used in the Calspan experiments and indicates the engine in which they have been used. A significant amount of detailed information about the constituents of these blends can be found in Dunn and Kim, 1991.

Table 3-1. Summary of Dust Constituents and Test Environments.**Unclassified**

BLEND	SOIL	GLASSY MATERIAL ADDED	ENGINE OR HSTS
#1 chosen to reflect a flyout scenario	Wyoming (Warren AFB) clay, sand, Bentonite	Mount St. Helens ash (near Seattle, Washington)	TF-33, F-107
#2 chosen for a penetration scenario	Hollywood Sand Corona clay Bentonite	Black scoria (Twin Mountain, N.M.)	TF33, F-107 YF-101, F-100
#19	Red art clay Ottawa sand Peat moss Feldspar	Synthetic glass* (Laboratory constructed)	F-107 YF-101, F-100 Hot Section Test System
#15	Red art clay Ottawa sand Feldspar	Synthetic glass* (Laboratory constructed)	Hot Section Test System
#17	Red art clay Ottawa sand Feldspar	Black scoria (Twin Mountain, N.M.)	Hot Section Test System
* Synthetic glass was made by melting together constituents of soil, cooling mix, pulverizing material and sifting.			

SECTION 4

(U) EXPERIMENTAL RESULTS

(U) Because of space limitations, only selected results from the engine test program can be presented. Emphasis will be given to the modern engines, the tactical F-100-PW-100, the strategic F-101-GE-100, and the strategic F-107-WR-102. The F-100 has been used in this research because it has been the only large modern engine available. The F-107 is an older version of the Cruise missile engine, but many F-107's are still in use in the Tomahawk missile. A decision has also been made to include a brief discussion regarding the strategic TF-33 engine. The YF-101 used here is a pre-production version and has only recently become available. Though the information presented here is abbreviated, the proper references are cited for anyone interested in more detail.

4.1 (U) PRATT AND WHITNEY F-100-PW-100 TURBOFAN ENGINE RESULTS.

(U) The potential damage mechanisms for a gas turbine engine operating in a nuclear dust environment have been described earlier. The manner by which these mechanisms show up in the instruments available to the air crew has not been described. This information is, however, known and will be presented here. It has been observed that a selected few of the engine readout parameters respond very quickly when an engine encounters a dust cloud environment. To illustrate this point it is appropriate to present data for a modern engine operating in a representative environment. Figures 4.7 were obtained for an F-100 engine (Dunn, 1990(a)) for which the turbine inlet temperature was 2345°F, the dust was blend #2 (see Table 1 for constituents), the dust concentration was 250 mg/M³, and the exposure time was 5 minutes. Note that the burner static pressure (P_B) and the high compressor static discharge pressure (P_{S3}) respond immediately in almost identical fashion as soon as the dust is turned on. This figure illustrates that the pressure increase can be very rapid (The CF6 engines described in Campbell, 1990 flamed out after about 1 minute of exposure to a volcanic cloud). It is also known that the particular response shown above is due to the melting and subsequent deposition on the high pressure turbine vane of a portion of the ingested material. Unfortunately, neither the burner pressure nor the compressor discharge pressure are read out on the instrument panel. (For the F-101

engine, they are measured and are included in the available data bank, but they would need to be interrogated by the weapons officer upon request from the pilot. This request would occur at a time when everyone is very busy. A green, yellow, red light system connected to the pressure read out system would be much easier to cope with.)

(U) Figure 4.7 also includes the fuel flow rate and the fan total pressure ratio, both of which reflect the presence of the dust cloud, but not as dramatically. The rate of rise of the pressure is a strong function of the turbine inlet temperature, the chemical properties of the dust material, and the dust cloud concentration. A continuation of Figure 4.7 presents the corrected fan total inlet temperature (FTIT), the engine pressure ratio (EPR), and the core speed (N_2). The FTIT and EPR are both parameters available to the air crew on the instrument panel. Note that the FTIT is a very good indication of impending problems. The change in EPR would be much more difficult to observe especially during times of heavy work load. Changes in the core speed (N_2) and the fan speed (N_1) are indirect indicators of the deposition or erosion as seen through the response of the control system. However, these changes are so small that they would not be observed by the air crew.

(U) On several occasions, the importance of dust concentration and exposure time has been mentioned. Figures 4.8 present parameters similar to those presented in Figures 4.7 for a similar engine operating point. The primary difference between these results is that the dust concentration has been increased by a factor of two. The burner pressure shown on Figure 4.8 increases much more rapidly than it did at the lower concentration, increasing from about 20 atm. to 22.5 atm. in three minutes. The second of Figure 4.8 shows correspondingly large increases in both EPR and FTIT.

[REDACTED] An investigation of the threshold in turbine inlet temperature necessary to avoid melting of the ingested material and/or deposition on the turbine stage was part of the study described above. Figures 4.9 present a portion of the results of that investigation. For a TIT of 2135°F, there is a relatively small increase in compressor discharge pressure and in FTIT which occurs near the end of the dust exposure time. Subsequent measurements demonstrated that for the particular dust blend being used (blend #2), deposition did not occur if the TIT was maintained at 2000°F or less.

(U) All engines tested are torn down for inspection when they can no longer be operated safely. Experience in the laboratory has demonstrated that if the

engine continues to operate at representative thrust levels in a nuclear dust cloud environment, it will eventually lose thrust and surge. An attempt at advancing the throttle will result in continued surging with no increase in thrust, thus making it necessary to shut down. As noted earlier, many factors are involved in causing this engine distress, but the ones which are of immediate concern to the air crew are deposition of foreign material on the first vane and/or first blade of the turbine, erosion of the fan and compressor blading, and formation of carbon-like material on the fuel nozzles.

(u) As was noted above, the buildup of material on the first vane causes the very rapid increase in burner static pressure and in compressor discharge static pressure shown in Figures 4.7. At high altitude, this pressure increase can lead to surge and engine flame-out. If the engine surges at high altitude, then flame-out is more likely than at low altitude. The air crew must be aware that a high-altitude engine restart is significantly different from a low-altitude restart. Boeing Commercial Airplane Company has recently changed their procedure instructions to airmen regarding this event and it is anticipated that other companies will soon follow suit. In addition, Boeing has made a videotape for air crews that treats this problem in some detail.

(u) Figure 4.10 is a photograph of a portion of a first vane row taken from a Pratt/Whitney F-100-PW-100 engine that was subjected to blend #2 (see Table 3.1) as part of the work reported in Dunn, 1990(b). This figure illustrates the typical heavy deposits on the leading edge and on the pressure surface. It also shows that the cooling holes near the tip endwall are blocked. The deposits near the tip endwall are generally heavier because of the tendency of the foreign material to be centrifuged outward. For this particular case, the cooling holes near the hub endwall are still open. Once the cooling holes become blocked, cooling effectiveness is dramatically reduced and the vane will burn through.

(u) It has been observed that the deposited material is relatively brittle and that its thermal properties are different from those of the metal airfoils. In the laboratory, it has been possible to remove large amounts of deposited material by cycling the throttle and in this way rapidly changing the turbine inlet temperature and the corresponding vane temperature as well as the shear forces acting on the surface. Evidence of material removal from the NGV's can be seen on Figure 4.10. The rate at which these throttle excursions are performed is very important. They should be performed slowly. Rapid throttle

excursion has been shown in the laboratory to cause uncontrollable engine surge and subsequent tailpipe fire.

(U) Figure 4.11 is a photograph of three fuel nozzles taken from the same F-100 engine. The material on these nozzles was removed and subsequent analysis indicated that it was carbon. The center hole of the nozzle from which the fuel is sprayed was open and was found to be capable of passing fuel at the design flow rate. However, the air swirl vanes were plugged thus inhibiting atomization of the fuel. The engine from which these fuel nozzles were taken surged violently and had to be shut down because of an excessive tailpipe fire (due to the rapid throttle movement described above). After putting the fire out, which was done without damage to the engine, many unsuccessful attempts were made at restarting.

(S) In addition to the difficulties caused in the hot section of the machine as a result of exposure to the dust environment, the fan, and the high pressure compressor may also sustain severe damage when operating in a dust laden environment. Figure 4.12 is a photograph of the tip region of the second stage fan of another F-100 engine that was also subjected to blend #2, but under different operating conditions than the components shown in Figures 4.10 and 4.11. This engine test program is reported in detail in Dunn, 1990(a). A new blade has been inserted into the photograph for comparison purposes. The leading edge of the blade is noted on the airfoil and the tip erosion is evident. Tip region erosion occurred on almost every stage throughout the compressor. Figure 4.13 is an example of the ninth-stage compressor blade row taken from this same machine. The trailing edge of the airfoil in the tip region became so thin that the material folded away from the pressure surface.

(U) This engine also surged violently followed by a tailpipe fire and had to be shut down. Attempts at restarting were unsuccessful. Upon teardown, deposition was found on the first vane and the fuel nozzles looked like those shown in Figure 4.11.

4.2 (U) GENERAL ELECTRIC YF-101-GE-100 TURBOFAN ENGINE RESULTS.

(U) Recently, two YF-101-GE-100 pre-production engines became available for use on the DNA experimental program. These engines have some notable features that are not present in the production engine (e.g., a dust filter located at the entrance to the high pressure turbine cooling passage) and lack other

features that are present in the production engines (e.g., a different fuel nozzle configuration, a dust deflector in the combustor at the turbine rotor cooling air pickoff location, and larger cooling holes in the rotor blade tips.) The engines came from a B-1A aircraft. Prior to initiating the measurement program, DNA and its consultants reviewed the dust blend that would be used in this test program. The intent was to build a soil representative of a most probable encounter environment and then to construct a synthetic "pumice glass" that could be mixed with the other ingredients of the cloud constituents. In determining this dust blend, the specific region of study was bounded by 54-56°N. latitude and 35-40°E. longitude. The soil types in this region are mainly sod-podzolic and grey forest. The portion of ground soil that was of most interest was the top 10 cm. After careful consideration of the region described above, the decision was made that the specific ingredients to be blended for the "most probable" dust cloud (see Table 3.1) were: (a) red art clay, (b) minspar 200 feldspar, (c) Ottawa quartz, (d) peat moss, and (e) a glass made from constituents (a) - (d). A detailed description of this blend is given in Dunn and Kim, 1991. In preparation for the YF-101-100 engine tests, this new blend was studied using the T-56 combustor (Dunn and Kim, 1991) and the F-100 combustor (Kim, Dunn, and Barton, 1991). These combustor studies will be discussed in more detail in Section 4.5.

(U) The test matrix for the first YF-101 engine included points for which the "most probable" blend would be used and others for which blend #2 would be used. Measurements for the initial engine have been completed and the results are described in Padova and Dunn, 1984. Analysis of the experimental data has not been completed. A brief summary of what is known and selected photographs from the post-test inspection of the engine will be provided in this section.

u The engine consumed about 176 Kg. of material (various versions of the "most probable" blend) over a time period of approximately three hours. During the course of the dust exposure runs, several throttle excursions (slow) were successfully performed in order to remove deposited material from the machine (see Section 5). At about 2.5 hours into the test, the engine control system assumed responsibility and the engine began to spool down (decreasing core speed) with associated loss in fuel flow rate and thrust. At about the 3 hour point, the engine surged while at high thrust setting. The PLA was retarded by the operator in order to stop the surging. Subsequent operator advances of the

PLA in attempts to regain the thrust level resulted in multiple surging. After many attempts to regain thrust, the engine was shut down, removed from the test cell, and torn down for inspection. The photographs shown in this section were taken during teardown. It should be noted that pre-dust exposure photographs are also available for comparison purposes in Baran and Dunn, 1992.

u [REDACTED] Figure 4.14 is a pre-test photograph of the entrance to the high pressure turbine first vane which illustrates that the turbine was in excellent shape prior to initiation of the dust ingestion program. The second figure of Figure 4.14 is a post-test photograph of a portion of the first vane row of the high pressure turbine which illustrates severe deposition on the vane leading edge, pressure surface, and a portion of the suction surface. As shown, the build-up of material is present not only on the vane leading edge and pressure surface but also on the hub endwall. Also note that the deposits are very heavy near the tip endwall, even more so than observed for the F100 engine. Figure 4.15 is a close-up post-test photograph of one of the first vane leading edges that was typical of most vanes; it illustrates that the cooling holes were completely blocked and no cooling air was exiting the vane. It was noted earlier that the YF engines had a dust filter at the entrance to the vane cooling passages that the production engines do not have. Figure 4.16 is a post-test photograph of this filter illustrating that it is heavily contaminated with dust material. It is probable that this filter is severely blocked so that very little air was actually getting into the vane cooling passages. This reduced air flow resulted in increased vane metal surface temperature which then caused the very heavy deposits observed. This effect also reduced our ability to clear the turbine of deposits for any significant length of time by cycling the engine.

u [REDACTED] Figure 4.17 is a post-test photograph taken from the rear of the first vane. The heavy deposits on the vane pressure surface can be seen clearly. The trailing edge cooling holes are also shown and appear to be open. However, several of the vanes show significant damage at the trailing edge and in many cases the material has broken.

u [REDACTED] The blades of the high pressure turbine rotor of the YF-101 stage sustained more damage than those of other engines that have been tested. Several of the blades from this rotor were removed and Figure 4.18 is a close-up photograph of three of them. The leading edges of the two blades on the outer portion of the photograph are clearly destroyed from about 10 percent span to

[REDACTED]

the tip. The portion of the blade from the leading edge to the first row of cooling holes on both the suction and pressure surface has been burned away. This pattern of damage is not an accident. The cooling air for the leading edge comes from an insert tube which can clearly be seen for the blade on the right, and once the holes are blocked the cooling effect is severely decreased. Also note the white deposit on the internal cooling air passage tube. This internal tube has been destroyed for the blade shown on the left of the photograph. Also shown on this photograph is some deposit on the blade pressure surface. The blade in the middle of the photograph has a burn-through in the tip midspan region and at the tip trailing edge. However, the leading edge of the blade has not been destroyed. A close look at the cooling holes indicates that many of them are blocked and that burn-through has begun at about 30 percent span.

u [REDACTED] The turbine exit (pyrometer) temperature for this machine is measured by a pyrometer looking at the trailing edge of the rotor blades. Figure 4.19 is a photograph of the suction surface side of the blade at which the pyrometer is looking. Also shown in this photograph are two blades which have a white patch for reference purposes. The characteristics of the blade surface have been altered by the dust environment. However, the degree to which this has influenced the indicated pyrometer temperature is unknown.

u [REDACTED] The YF-101 engine described in this section suffered extensive deposition on the first vane row and damage to several of the blades of the high pressure turbine stage. At the time the test was terminated, it was not possible for the engine to generate significant thrust. The fan and compressor were highly polished and sustained some damage, but not enough to have rendered the machine inoperable. Figure 4.20 is a photograph of a blade from the 6th stage of the high pressure compressor. This blade has some erosion in the trailing edge tip region, but it does not appear to be severe.

u [REDACTED] The fuel nozzles on this engine are of an entirely different construction from those for the F100-PW-100 engine described earlier and are also very different from the production engine. Figure 4.21 is a post-test photograph of one of these fuel nozzles. There is some carbon build-up as might have been expected, but the unit appeared to be functional at shutdown. Prior to the last test matrix point, difficulty was experienced in starting the engine. However, in order to avoid further damage to the engine by a possible tailpipe fire and subsequent burn down, no attempt was made to restart the engine after encountering the difficulties described in the previous paragraph.

4.3 (U) WILLIAMS INTERNATIONAL F-107-WR-102 TURBOFAN ENGINE RESULTS.

(U) Two different F-107 engines (S/N WR-0000110 and S/N WR-0000111) have been exposed to nuclear dust environments in the Calspan facilities. The first of these measurement programs was conducted in 1984 using engine S/N WR-0000110 and the results are reported in Padova and Dunn, 1984. Measurements for this engine were carried out using a significantly different dust mixture and dust profile time history than was used for a more recent F-107 test series reported in Baran and Dunn, 1992 which utilized engine S/N WR-0000111. The results reported in Padova and Dunn, 1984 utilized a dust mixture (composed of a mixture of Warren Air Force Base soil and Mt. St. Helens ash) which was significantly different as well as a much lower dust concentrations than used for the more recent experiments. The results described in Baran and Dunn, 1992 used a dust cloud blend felt to be representative of a laydown in the vicinity bounded by 54°-56° N. latitude and 35°-40° E. longitude. The discussion presented here will concentrate on the results of the most recent measurements.

Three failure modes were observed for engine S/N WR 0000111: (1) contamination of the oil lubrication system, (2) deposition of material on the turbine inlet nozzle guide vane, and (3) burnout of the combustor. Erosion of the fan, centrifugal compressor, diffuser, and turbine was also evident; however, it had no significant effect on engine performance.

The most apparent effect that dust exposure had on engine performance was the contamination of the oil lubrication system. Oil supply pressure was progressively lost as oil flow was continually restricted by accumulated dust particles in the oil filter. This resulted in the gradual loss in oil supply to the bearings and gearbox and subsequent bypass of most of the lubrication system by increasingly contaminated oil. Occasionally, some bearings exhibited a rise in temperature, but the engine was never run beyond manufacturer specifications. During the experiment, periodic oil and filter changes were performed in order to extend the usable life of the engine. Had the engine been run without continued maintenance, as during a mission, continued contamination of the lubrication system would have ultimately resulted in seizure of the bearings and a catastrophic failure of the engine.

(U) A second potential problem was an accumulation of material on the turbine inlet nozzle guide vanes. This deposition was responsible for terminating the test and rendering the engine inoperable by choking off flow to the turbine. This failure mode was found at teardown.

(U) The third damage mode was found during teardown. Along with material deposition in the hot section, there was evidence of burn through in the combustor. At the time of test termination, it was not obvious that this burn through was causing any problem. However, had the combustor burning been allowed to continue, it probably would have had a mission limiting influence.

4.4 (U) PRATT AND WHITNEY TF-33-P-3 TURBOFAN ENGINE RESULTS.

(U) Measurements designed to determine the operability of the TF-33 turbofan engine (B52 H-model) in a dust laden environment have also been performed. For detailed descriptions of these results, one is referred to Dunn, Padova, and Moller, 1986(a) and Dunn and Padova, 1986. Because the TF-33 is a much older engine, it operates at much lower turbine inlet temperatures than either the F-100 or the F-101. Mainly because of this factor, the damage mechanism of primary importance is different than it was for the F-100 or F-101. That is, in the case of the TF-33 compressor erosion, instead of material deposition, becomes the dominant damage mechanism. Like all other control systems, the one used on the TF-33 doesn't cope well with damage due to erosion. With increased exposure to the dust environment, several observations can be made: (1) the fuel flow rate required to maintain engine pressure ratio (EPR) increases significantly, (2) the exhaust gas temperature (at constant EPR) increases, (3) a mismatch between the core and fan speed occurs, and (4) the engine becomes difficult to operate if the power lever angle (PLA) is retarded to the point where the compressor interstage bleed valves open.

(U) Many laboratory experiments have resulted in the determination of a technique for operating a badly damaged engine. The best advice is that if the aircraft has been flying in a dust laden environment, then don't retard the PLA to the point where the interstage bleed valve opens. If the bleed valve is inadvertently allowed to open, then a procedure that may help to regain thrust is as follows; (a) turn on the deicer system, (b) lock the bleed valve in the open position (this can now be done on the B52 (H-model only) when weight is on the landing gear. However, it is a relatively simple fix to be able to do so in flight), and (c) advance the throttle slowly until the EPR levels out, then close the bleed

valve rapidly. Generally, a simple surge will be experienced, but the core will then accelerate to give essentially full thrust. The references cited above provide a more complete description of this technique.

4.5 (U) LABORATORY RESULTS WITH AN ENGINE COMBUSTOR RIG.

(U) It is important to have the ability to test the influence of different dust constituents under realistic engine conditions without destroying an engine in the process. Modern engines are difficult to obtain and, typically, only one or two of a particular type may be available. In order to make the best possible use of an engine, Calspan has constructed two hot-section test systems that are routinely used to define dust component behavior and engine parameter influences on this behavior. One of these uses an Allison T56 combustor can and associated first vane of the high pressure turbine hardware. The second uses a sector of a F-100 annular combustor and the associated first vane hardware. Padova and Dunn, 1987, Moller and Dunn, 1990, and Dunn and Kim, 1991 describe measurement programs conducted with the T56 system and Kim, Dunn, and Baran, 1991(a) and Kim, Baran, and Dunn, 1991(b) describe measurements obtained with the F-100 system.

(U) In preparation for the YF-101-GE-100 engine measurements described in Section 4.2, extensive measurements concerned with the behavior of the "most probable" blend were performed in the F-100 hot-section test system. The information obtained in these tests proved to be very helpful in planning for both the just completed YF-101 engine test series and an upcoming F-100 engine test series. The combustor test system allows one to quickly and inexpensively test the parameters thought to control particle melting and subsequent deposition on hot section components. It is also possible to control the surface temperature of individual vanes (which cannot be done in an engine) to determine the influence of surface temperature on the tendency of a melted material to deposit. The specific parameters tested were: (a) the amount of free water in the dust blend, (b) the amount of bound water in the dust blend, (c) the amount of already glassy material in the ingested air, (d) the turbine inlet temperature, and (e) the vane metal temperature. The tests reported in Kim, Dunn, and Baran, 1991(a) produced internal cooling hole blocking and subsequent leading edge burn through similar to that shown in Figure 4.18. The dust blends used in the hot-section test experiments and in the full-scale engine experiments were the same.

[REDACTED]

SECTION 5

COPING WITH THE DUST CLOUD ENVIRONMENT

5.1 (U) AIR CREW ACTIONS.

(U) In the case of commercial airliners inadvertently encountering volcanic ash clouds along their flight path, the solution is relatively easy: reduce power significantly, make a 180 degree descending turn, and return in the direction from which you have come. However, for a military aircraft encountering a nuclear dust cloud, it may not be acceptable to abort the mission and execute the maneuver just described. There are, however, several things that the crew can do to maximize engine lifetime and thus to increase the probability of a successful mission. The things that must be done are as follows:

(U) (1) The crew must recognize the threat. If they can see outside, then they should see "fire flies" on the windscreen and, if they can see the engine nacelles, then they should see St. Elmo's glow. If it is not possible to see outside, then it is very important to monitor either exhaust gas temperature, fan turbine inlet temperature, or pyrometer temperature (depending upon the particular engine). If the engine is a F-101, then the co-pilot may have to increase his already heavy workload and carefully monitor the burner pressure and the compressor discharge pressure.

(U) (2) Melting and subsequent deposition of cloud material on hot section components is a temperature-dependent phenomenon. The combustor temperature must be sufficiently high to melt a significant amount of material and the vane metal temperature must be sufficiently high to allow for deposition. By reducing the thrust setting sufficiently to reduce the turbine inlet temperature to 2000°F (the manufacturer can provide a conversion to pyrometer temperature) or less, particle melting is significantly reduced and the vane metal temperature falls sufficiently low that deposition is significantly retarded.

(U) (3) Reducing the thrust setting also reduces the engine speed and thereby reduces the erosion damage to the fan and compressor stages. It must be kept in mind that erosion damage is irreversible and can only be repaired by replacing components.

[REDACTED] (4) If the air crew does not recognize the dust cloud early or if it is not possible to reduce the thrust setting, then particle melting and subsequent deposition on the first vane can be cleared up to a point by cycling the throttle one engine at a time. This throttle motion should be relatively slow so as to not

[REDACTED]

surge the engine. When the thrust setting is reduced, the temperature of the vane and the deposited material is decreased. Because of the difference in the thermal expansion coefficients, severe stresses are induced at the interface, and the bond between the materials is weakened. During the low-thrust portion of the excursion external shear stress is relatively low. On the throttle advance portion of the excursion, the shear stress builds rapidly, the bond between the vane wall and the deposited material fails, and at least a portion of the deposited material is blown away. It is important to point out that if internal plugging of the cooling air holes has occurred, then removing the external material is not very helpful since, as illustrated in Section 4.3, internal blocking of the cooling holes with dust results in total destruction of the components. Additionally, if the cooling holes become blocked or if cooling air flow rate is reduced (by a blocked filter in the case of the YF101-GE-100) then the vane metal temperature increases resulting in a greater potential for deposition of material.

5.2 (U) MODIFICATIONS TO EXISTING ENGINES.

[REDACTED] There are some potential fixes to modern engines that could reduce the probability of blocking the cooling holes from the inside. In principle, one could do the following; (1) deflect the dust away from the intake to the cooling passage bleed, (2) increase the diameter of the cooling air passages and of the cooling holes, and (3) install a filter in the cooling air passage to collect a portion of the dust material. To make changes to an engine like those just described requires careful coordination between the engine designer and the user. For example, the turbine designer will not be happy with the film cooling problems introduced by increasing the size of the cooling holes. For the F-101-GE-102 engine, the manufacturer has incorporated a dust deflector in the combustor for the air that is directed to the rotor portion of the stage and increased the size of the cooling holes in the blade tip, but in going to the production engine the vane cooling passage filter was removed. As illustrated in Section 4.2 the vane suffered very heavy deposits and the blade burned for the YF-101-GE-100 which did not have the dust deflector, but did have the vane filter. However, no experimental data relevant to a nuclear dust cloud are available which demonstrate that the -102 fix actually performs as intended or that, by removing the vane cooling passage filter, another problem wasn't introduced.

5.3 (U) COMMENTS ABOUT FUTURE ENGINES.

(U) The trend in modern engines has been to increase both the turbine inlet temperature (TIT) and the hot-section component surface temperature. Increasing the TIT also increases the likelihood of melting the ingested material. The laboratory experiments performed to date suggest that the higher the surface temperature of the component, the greater the likelihood for deposition to occur. To date, the hot-section components have been metal and not ceramic. With the advent of ceramics, it may become possible for hot-section components to operate at temperatures above the melting point of the dust material. The ceramic will also have different surface characteristics than the metal and thus it is dangerous to speculate as to whether or not the material deposition problem will become better or worse.

SECTION 6

CONCLUSIONS

(U) This portion of the report has been devoted to a description of the current state of the art as it applies to operating gas turbine engines in a nuclear dust cloud environment. Experimental data obtained for engines flying through volcanic clouds and in the laboratory for engines operating in predicted nuclear cloud environments have been presented. The knowns and unknowns concerning the environment and the operation of the engines have been described.

■ The overwhelming conclusion for the air crew is that it is a dangerous practice to operate a gas turbine engine in a particle-laden environment. However, if one is forced to do so, then it is very important to recognize the situation as soon as possible and then to operate the engine in such a way as to maximize lifetime. To ignore the existence of a major operational problem may lead to an abrupt end to an otherwise successful mission. Techniques for recognizing a potentially dangerous environment and procedures for operating in it are known, at least for some modern engines, and are described herein. It is difficult to generalize because engine configurations and control systems differ from one manufacturer to the next. Nevertheless, reasonable operational rules of thumb derived on the basis of laboratory experiments are provided.

(U) There are still many aspects of operating gas turbine engines in a nuclear dust cloud environment that require further investigation, e.g., the effects of such parameters as: (a) surface properties of materials, (b) cooling hole size and configuration, (c) chemical and physical properties of the ingested material, etc. on the deposition process.

UNCLASSIFIED

SECTION 7

REFERENCES

Adams, R.M. and Dunn, M.G., 1987, "Response of a Turbofan Engine to a Simulated Nuclear Blast," 10th International Symposium on Military Application of Blast Simulation, Bad Reichenhall, Federal Republic of Germany (UNCLASSIFIED).

Baran, A.J. and Dunn, M.G. (1992), "The Response of a F107 Engine to a "Most Probable" Nuclear Dust Environment (U)," DNA-TR-92-(in review) (SECRET).

Baran, A.J. and Dunn, M.G. (1992), "The Response of a YF101-100 Engine to a "Most Probable" Nuclear Dust Environment (U)," DNA-TR-92-(in preparation) (SECRET).

Campbell, E.E. (1990) Volcanic Ash, Proceedings of the 747 Flight Operations Symposium, pp 2.3.1 - 2.3.34, Seattle, Washington, Oct. 9-11, Boeing Commercial Aircraft Company (UNCLASSIFIED).

Dunn, M.G., 1980, "Nuclear Blast Vulnerability of Airbreathing Propulsion Systems: Laboratory Measurements With an Operational J-85-5 Turbojet Engine," Calspan Rept. No. 6484-A-1 (UNCLASSIFIED).

Dunn, M.G., 1981, "Response of an Operational Turbofan Engine to a Simulated Nuclear Blast (U)," DNA-TR-81-135 (SECRET).

Dunn, M.G. (1990(a)), "Performance Deterioration of an Operational F100 Turbofan Engine Upon Exposure to a Simulated Nuclear Dust Environment (U)," DNA-TR-90-72-V1 (SECRET).

Dunn, M.G. (1990(b)), "Performance Deterioration of a Second F100 Turbofan Engine Upon Exposure to a Simulated Nuclear Dust Environment (U)," DNA-TR-90-72-V3 (SECRET).

UNCLASSIFIED

Dunn, M.G., Adams, R.M., and Oxford, V.S., 1989, "Response of Large Turbofan and Turbojet Engines to a Short-Duration Overpressure," J. of Engineering for Gas Turbines and Power, Vol. III, pp. 740-747 (UNCLASSIFIED).

Dunn, M.G., Davis, A.O., and Rafferty, J.M., 1979, "Nuclear Blast Vulnerability of Airbreathing Propulsion Systems: Laboratory Measurements and Predictive Modeling," 6th International Symposium on Military Applications of Blast Simulation, Cahors, France (UNCLASSIFIED).

Dunn, M.G. and Kim, J. (1991), "The "Most Probable" Dust Blend and its Response in the T56 Hot Section Test Section (HSTS)," DNA-TR-91-234 (UNCLASSIFIED).

Dunn, M.G., Padova, C., and Adams, R.M., 1987, "Response of an Operational Turbofan Engine to a Simulated Nuclear Blast," J. of Fluids Engineering, Vol. 109, pp. 121-129 (UNCLASSIFIED).

Dunn, M.G. and Padova, C. (1986), "Deterioration of a TF33 Turbofan When Exposed to a Scoria-Laden Dust Environment," DNA-TR-86-62-V3 (UNCLASSIFIED).

Dunn, M.G., Padova, C., and Adams, R.M. (1987), "Operation of Gas Turbine Engines in Dust-Laden Environments," AGARD-Advanced Technology of Aero Engine Components, Paris, France (UNCLASSIFIED).

Dunn, M.G., Padova, C., and Moller, J.C. (1986(a)), "Performance Deterioration of an Operational TF33 Turbofan Engine Upon Exposure to a Simulated Nuclear Dust Environment," DNA-TR-86-62-V1 (UNCLASSIFIED).

Dunn, M.G., Padova, C., and Moller, J.C. (1986(b)), "Performance Deterioration of a Turbojet Engine Upon Exposure to a Dust Environment," DNA-TR-86-62-V2 (UNCLASSIFIED).

UNCLASSIFIED

Dunn, M.G., Padova, C., Moller, J.C., and Adams, R.E. (1987), "Performance Deterioration of a Turbofan and a Turbojet Engine Upon Exposure to a Dust Environment," ASME Journal of Engr. for Gas Turbines and Power, Vol. 109, pp 336-343 (UNCLASSIFIED).

Dunn, M.G. and Rafferty, J.M., 1982, "Nuclear Blast Response of Airbreathing Propulsion Systems: Laboratory Measurements With an Operational J-85-5 Turbojet Engine," J. of Engineering for Power, Vol. 104, pp. 624-632 (UNCLASSIFIED).

Glasstone, S. and Dolan, P.J., 1977, The Effects of Nuclear Weapons, 3rd Edition, Dept. of Defense and Dept. of Energy (UNCLASSIFIED).

Jansen, W., Swarden, M.C., and Carlson, A.W., 1971, "Compressor Sensitivity to Transient and Distorted Transient Flows, Vol. II - Mathematical Details and Computer Programs," Northern Research and Engineering Corporation, Cambridge, MA, AD728024 (UNCLASSIFIED).

Kim J., Baran, A.J., and Dunn, M.G. (1991(b)), "Design and Construction of a F-100 Engine Hot-Section Rig for Dust Phenomenology Testing," DNA-TR-91-159 (UNCLASSIFIED).

Kim, J., Dunn, M.G., and Baran, A.J. (1991(a)), "The 'Most Probable' Dust Blend and Its Response in the F-100 Combustor," DNA-TR-91-160 (UNCLASSIFIED).

Kleppin, D.A., Ruetenik, J.R., Smiley, R.F., and Treimanis, G., 1982, "Measurement of Blast Pressures on a Cruise Missile Airframe and Engine at Mach 0.62 From Rocket Propelled Sled Tests," DNA-TR-82-198 (UNCLASSIFIED).

Moller, J.C. and Dunn, M.G. (1990), "Dust and Smoke Phenomenology Testing in a Gas Turbine Hot Section Simulator," DNA-TR-90-72-V2 (UNCLASSIFIED).

Padova, C. and Dunn, M.G., 1983, "Weak Shock Propagation into a Cross-Junction Against a Jet," 14th International Symposium on Shock Tubes and Waves, Sydney, Australia (UNCLASSIFIED).

UNCLASSIFIED

Padova, C. and Dunn, M.G. (1984), "Response of an Operational Turbofan Engine to a Simulated Nuclear Dust Environment (U)," DNA-TR-91-26 (SECRET) (UNCLASSIFIED).

Padova, C. and Dunn, M.G. (1987), "Dust Phenomenology Testing in the Hot-Section Simulator of an Allison T56 Gas Turbine," DNA-TR-87-71 (UNCLASSIFIED).

Peacock, R.E., Das, D.K., and Erlap, O.C., 1980, "Compressor Response to Pulsed Transients," AIAA-80-1080 (UNCLASSIFIED).

Private correspondence; M.G. Dunn, Calspan and Capt. E. Moody, British Airways (UNCLASSIFIED).

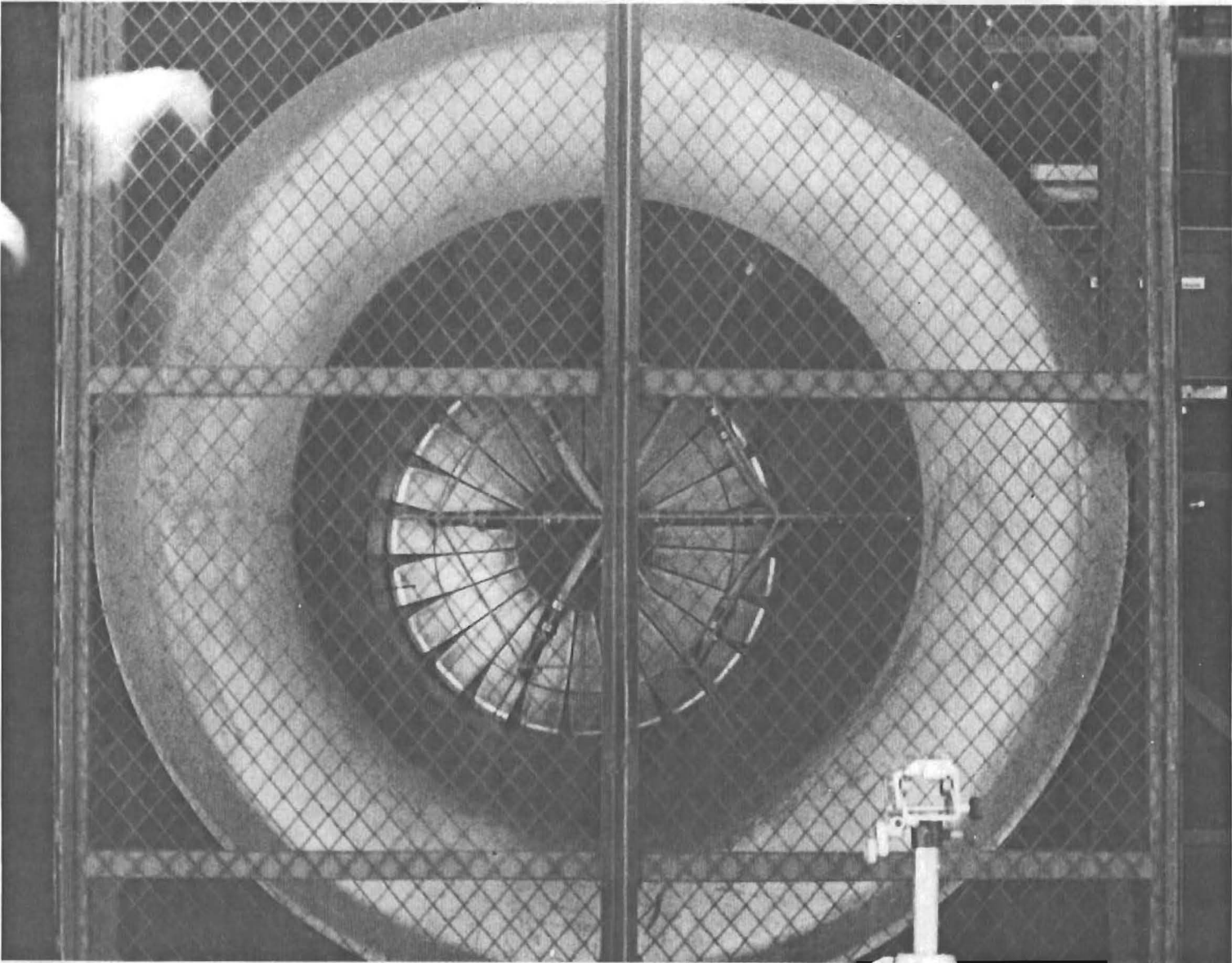
Rae, W.J., Batcho, P.J., and Dunn, M.G., 1988, "Transmission and Reflection of Pressure Waves by Compressor and Turbine Stages, Based on an Actuator Disk Model," DNA-TR-88-58 (UNCLASSIFIED).

Reynolds, G.G. and Steenken, W.G., 1976, "Dynamic Digital Blade Row Compression Component Stability Model," AFAPL-TR-76-76 (UNCLASSIFIED).

Sugiyama, Y., Hamed, A., and Tabakoff, W., 1978, "A Study of Compressor Surge Due to Inlet Pressure Disturbances," AIAA Paper 78-246 (UNCLASSIFIED).

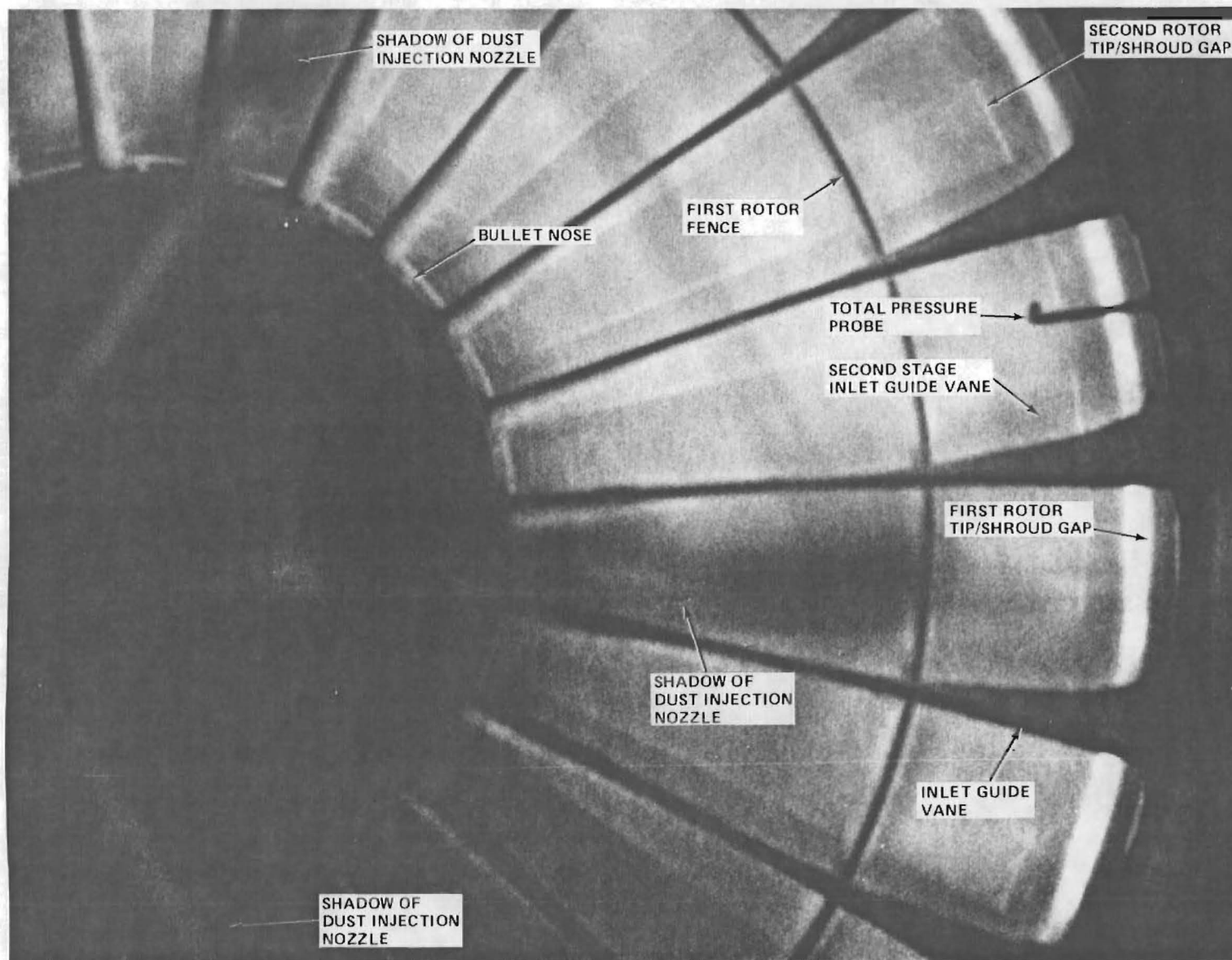
Tesch, W.A. and Steenken, W.G., 1976, "Blade Row Dynamic Digital Compressor Program," NASA CR134978 (UNCLASSIFIED).

UNCLASSIFIED



UNCLASSIFIED

Figure 2.1. (U) Photograph of St. Elmo's glow at fan face of P/W TF-33 turbofan.

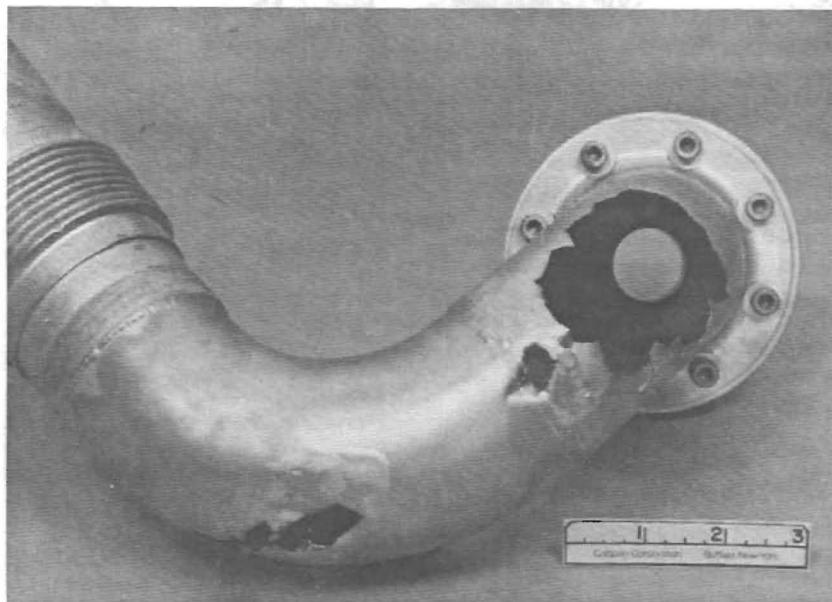


UNCLASSIFIED

Figure 2.2. (U) Closeup photograph of St. Elmo's glow at fan face of P/W TF-33 turbofan.

UNCLASSIFIED

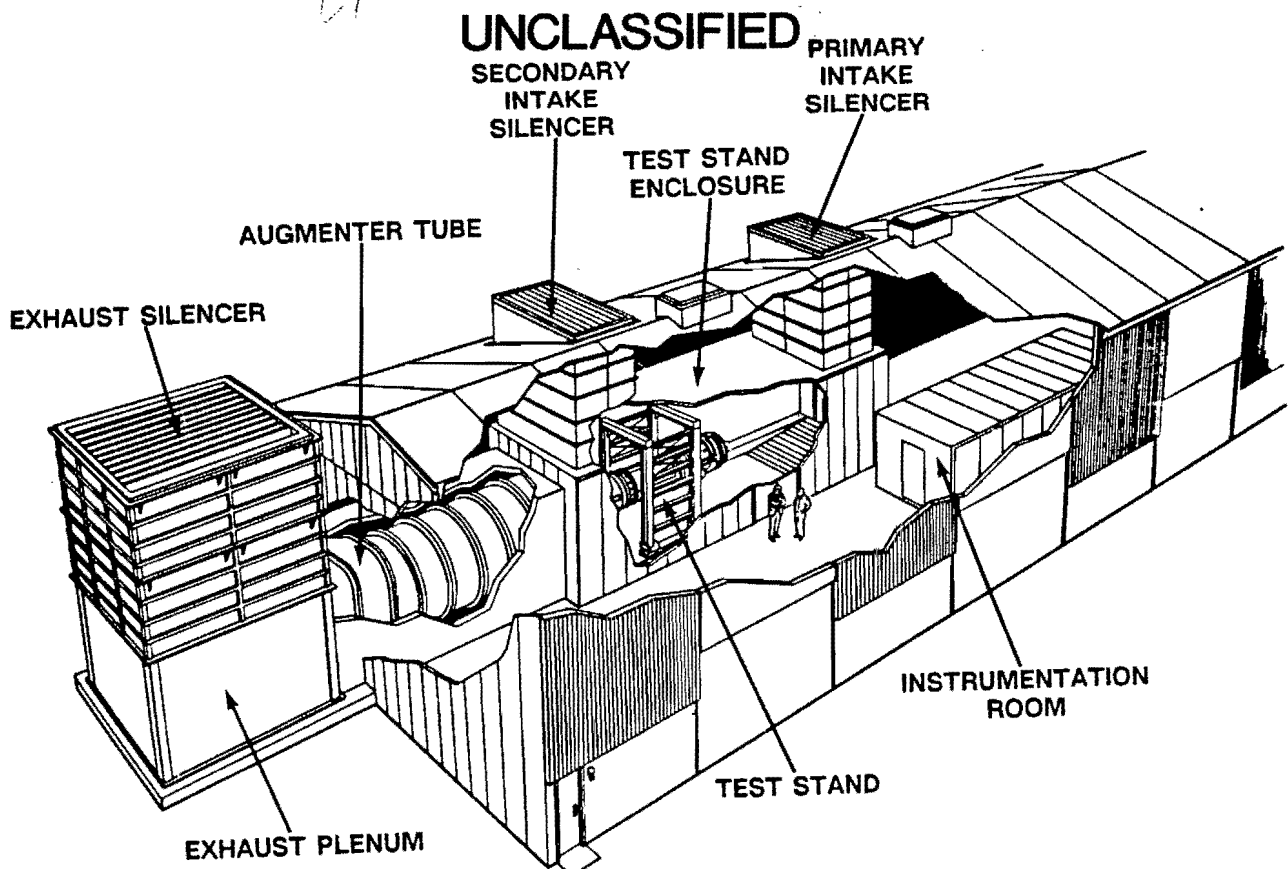
POST-TEST PHOTOGRAPH
P/W TF-33
BLEND #2
EXPOSURE TIME \cong 16 minutes
AMOUNT OF DUST COLLECT \cong 10 g



UNCLASSIFIED

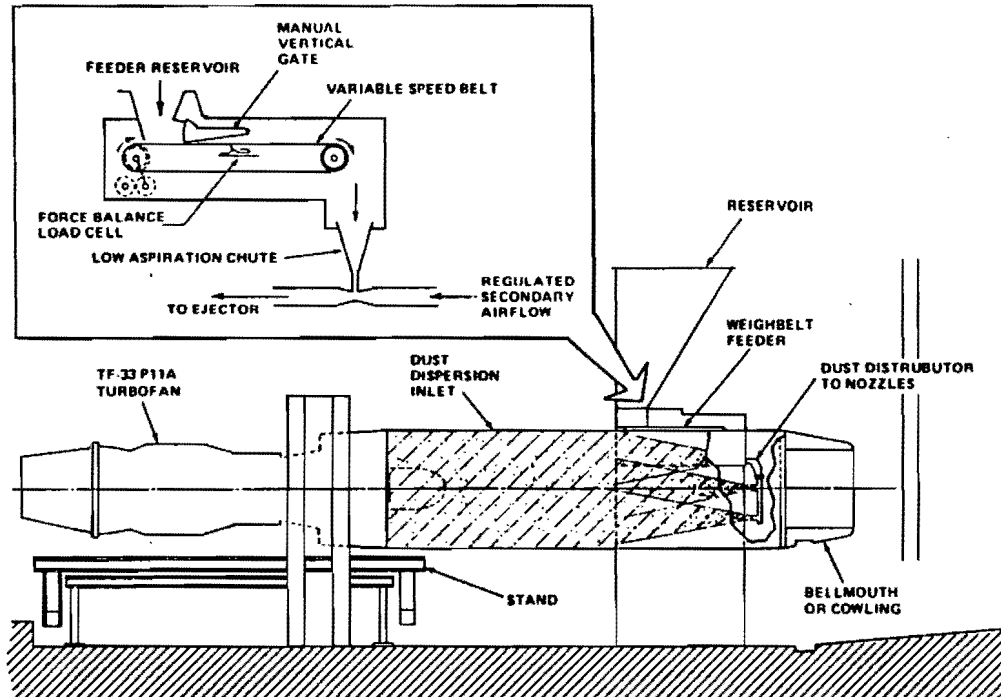
Figure 2.3. (U) Post-test photograph of ECS plumbing for TF-33 engine after dust exposure.

UNCLASSIFIED



UNCLASSIFIED

Figure 3.4. (U) Large engine research cell.



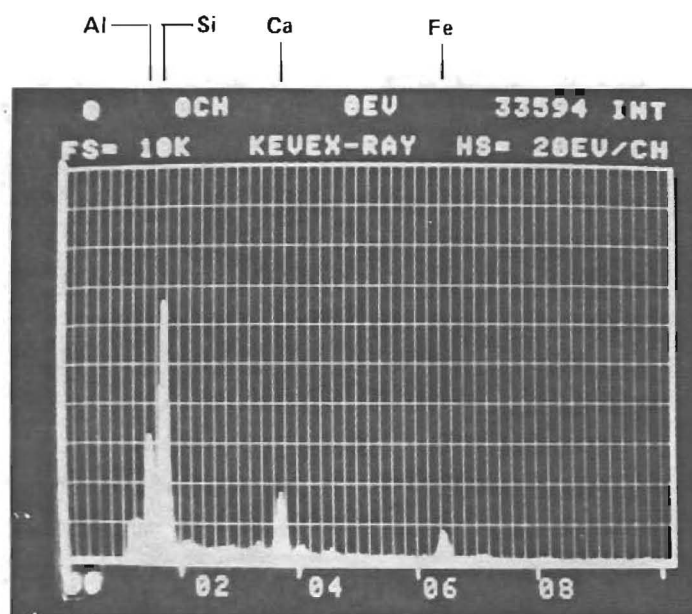
UNCLASSIFIED

Figure 3.5. (U) Schematic of dust injection system.

UNCLASSIFIED



(a) MICROGRAPH OF SAMPLE MAGNIFIED 100 TIMES



(b) ELEMENTAL COMPOSITION SPECTRUM

UNCLASSIFIED

Figure 3.6. (U) Scanning electron microscope micrograph and composition spectrum of black scoria.

UNCLASSIFIED

UNCLASSIFIED

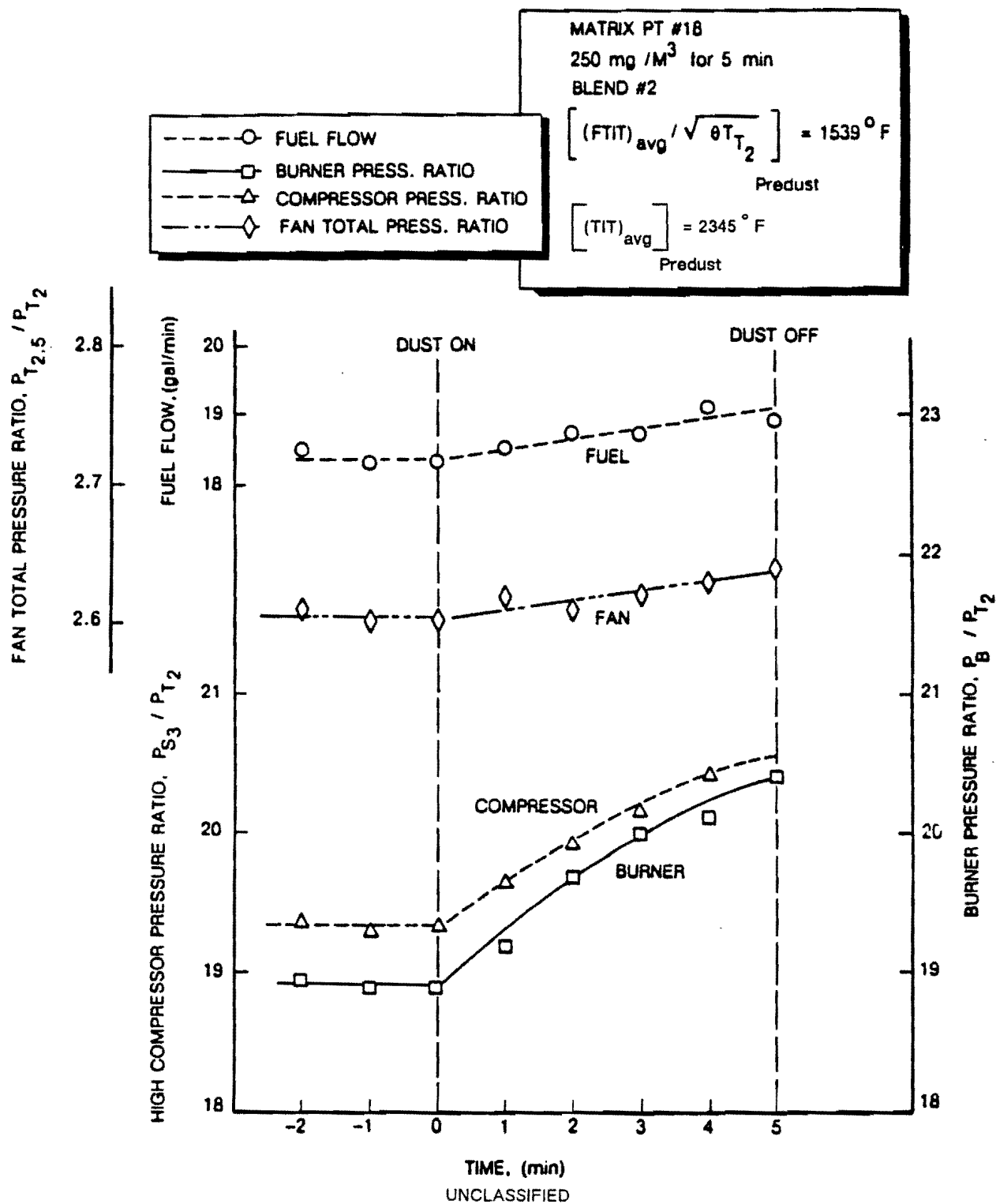


Figure 4.7. (U) Time history of F-100-PW-100 engine parameters during dust exposure.

UNCLASSIFIED

UNCLASSIFIED

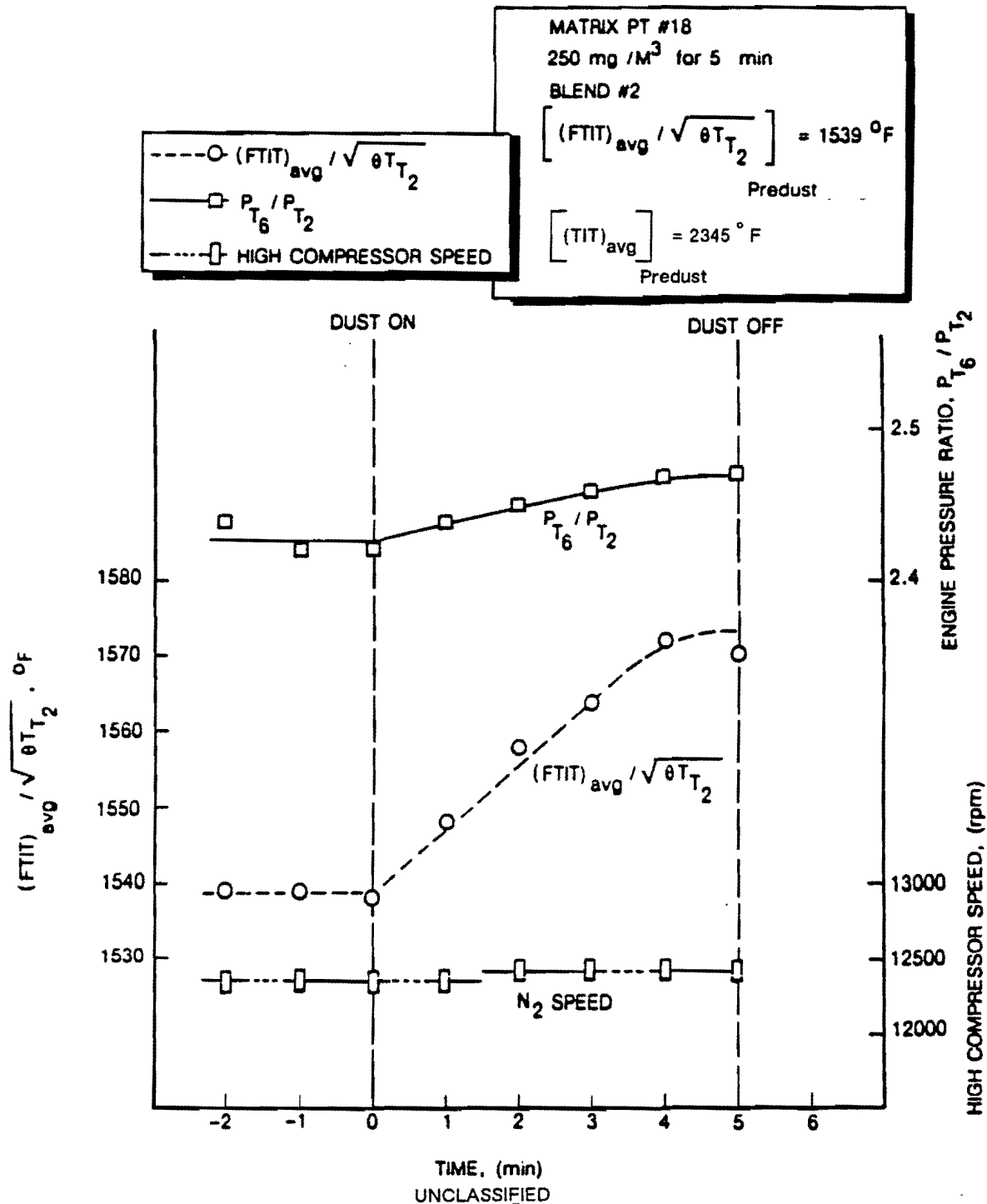


Figure 4.7. (U) Time history of F-100-PW-100 engine parameters during dust exposure (Continued).

UNCLASSIFIED

UNCLASSIFIED

MATRIX PT #14

500 mg / M³ for 3 min

BLEND #2

$$\left[(FTIT)_{avg} / \sqrt{\theta T_{T_2}} \right] = 1607^{\circ}F$$

Predust

$$\left[(TIT)_{avg} \right] = 2425^{\circ}F$$

Predust

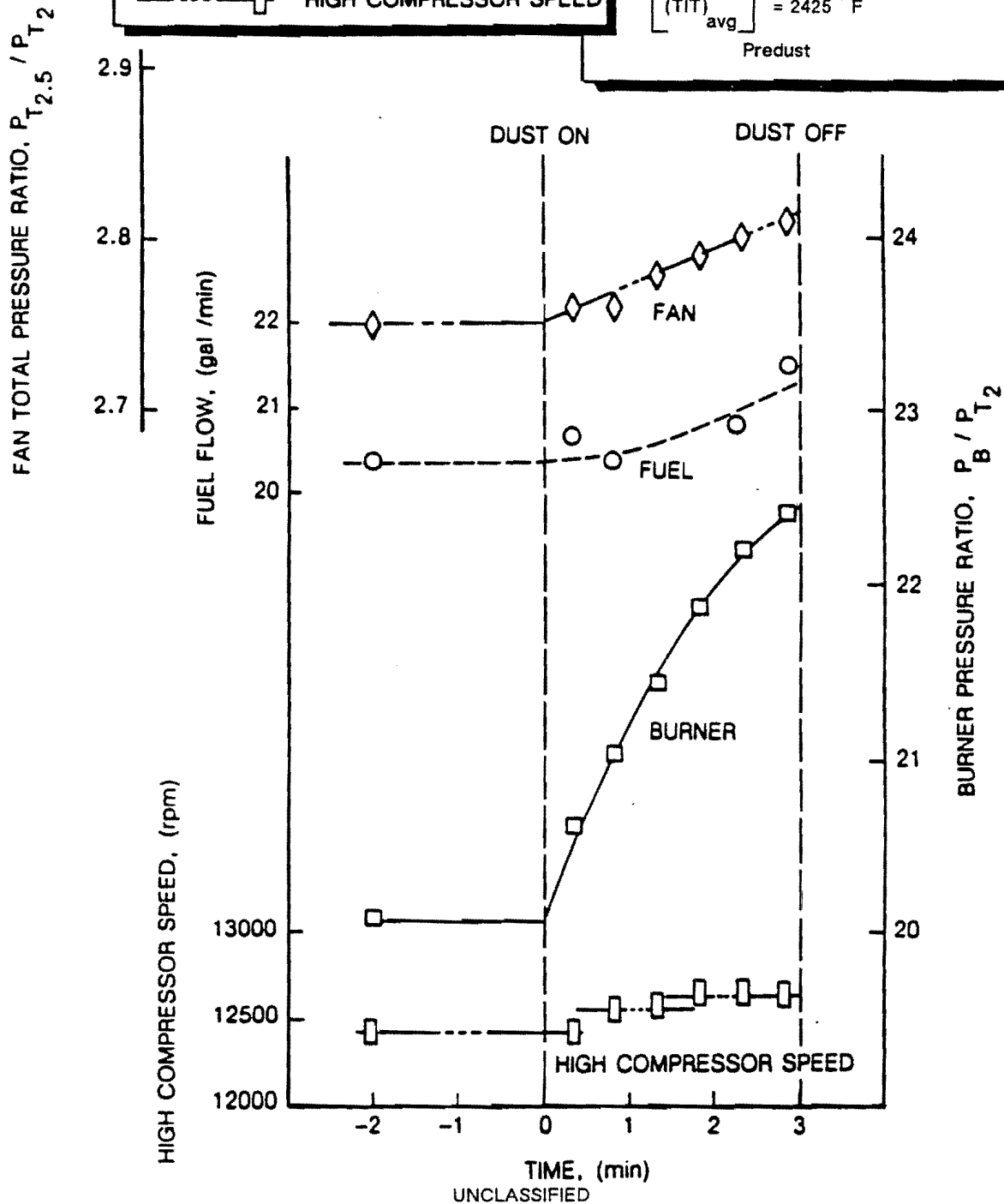


Figure 4.8. (U) Time history of F-100-PW-100 engine parameters during dust exposure.

UNCLASSIFIED

UNCLASSIFIED

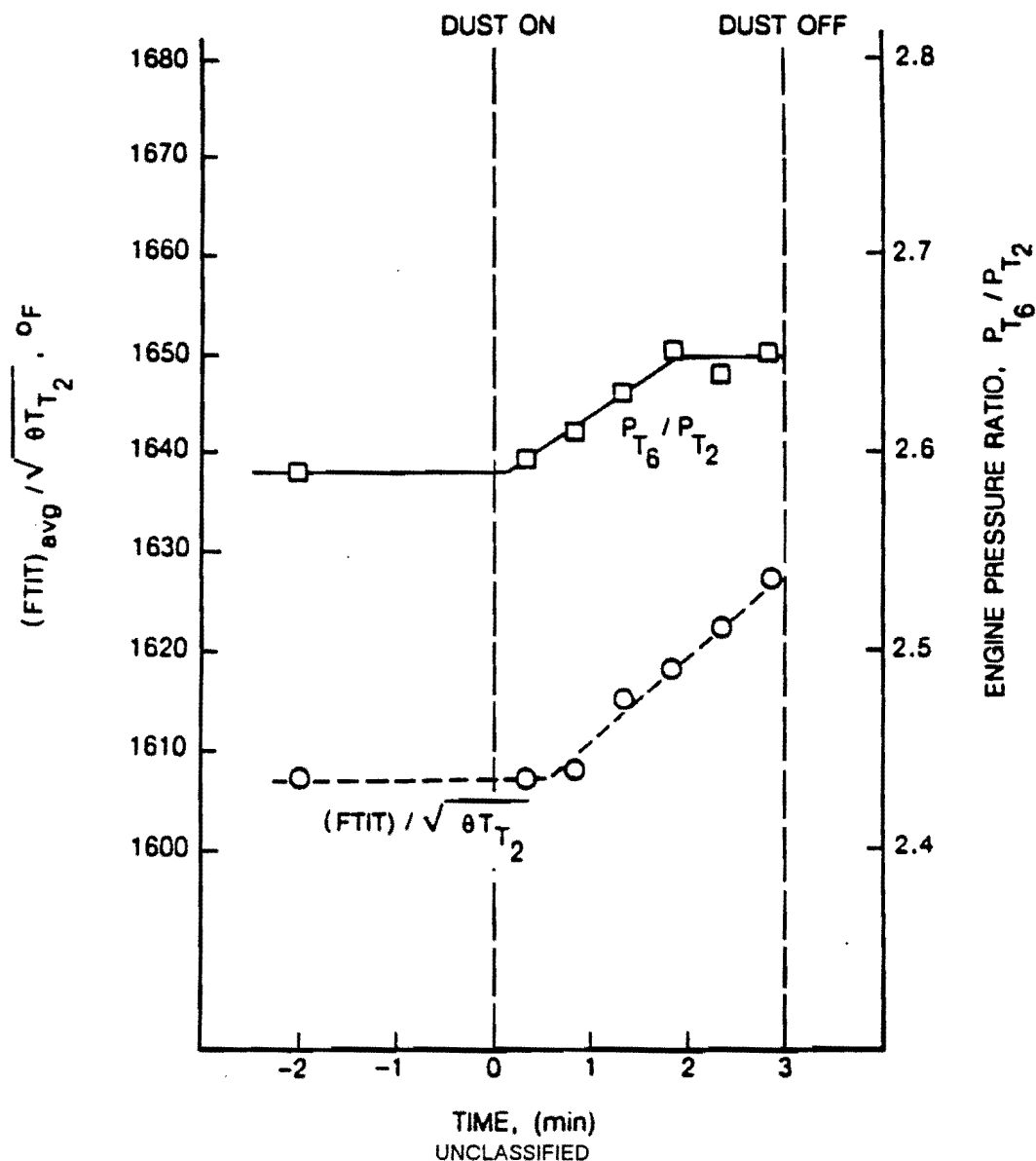
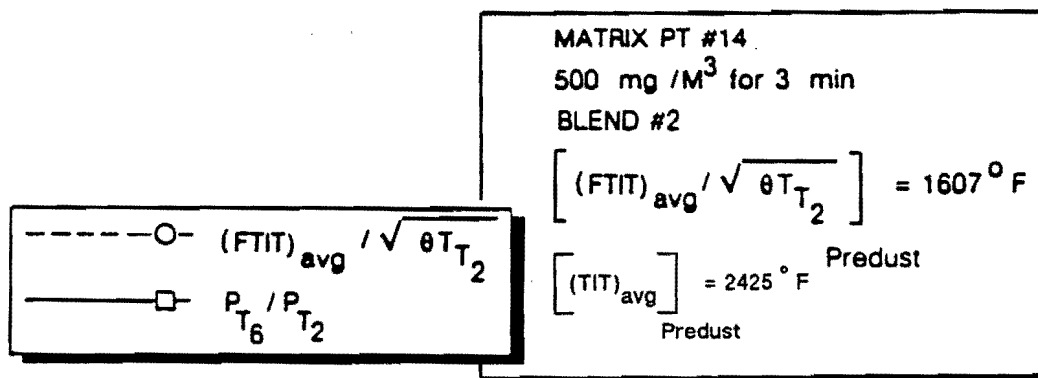


Figure 4.8. (U) Time history of F-100-PW-100 engine parameters during dust exposure (Continued).

UNCLASSIFIED

UNCLASSIFIED

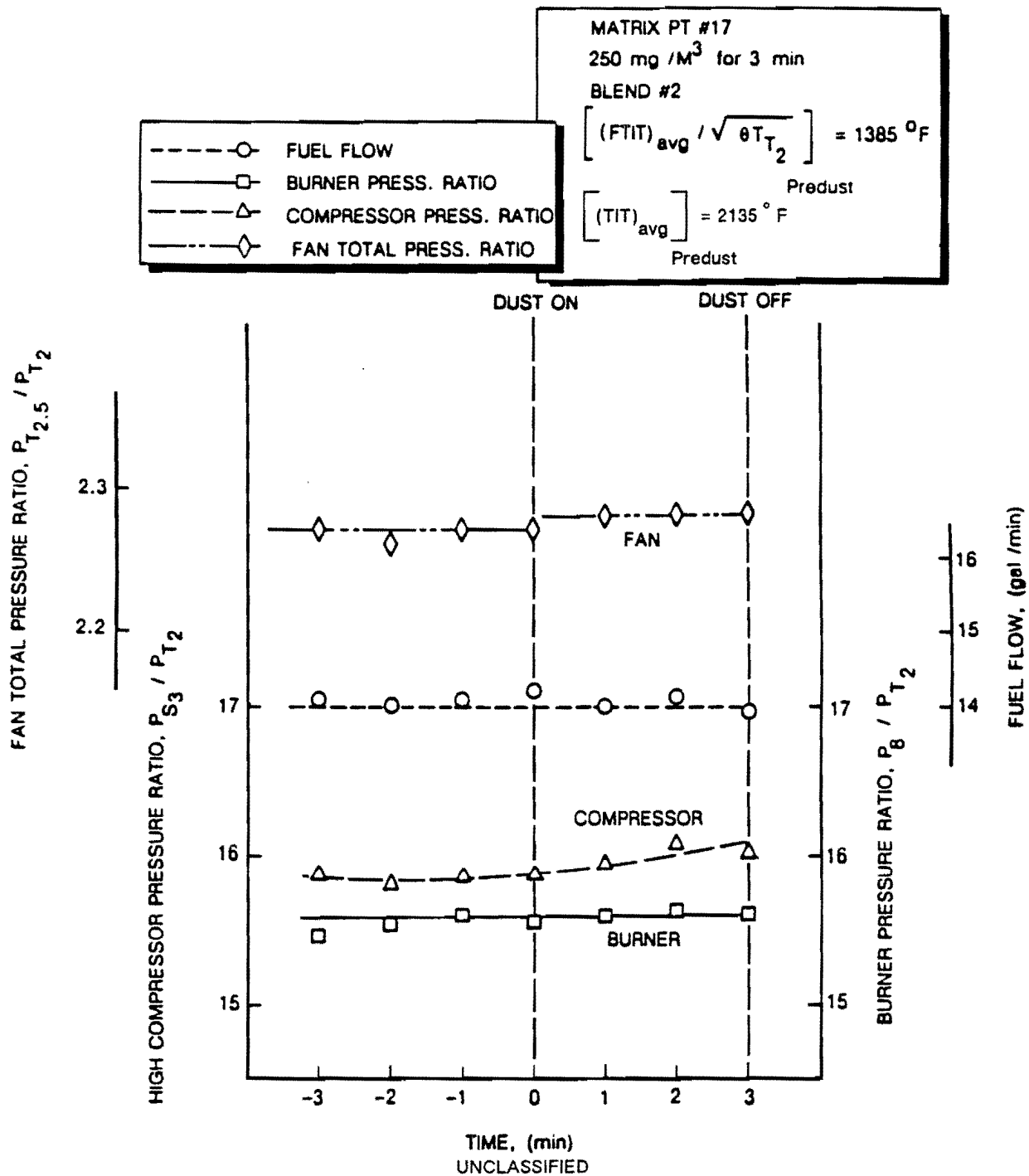


Figure 4.9. (U) Time history of F-100-PW-100 engine parameters during dust exposure.

UNCLASSIFIED

UNCLASSIFIED

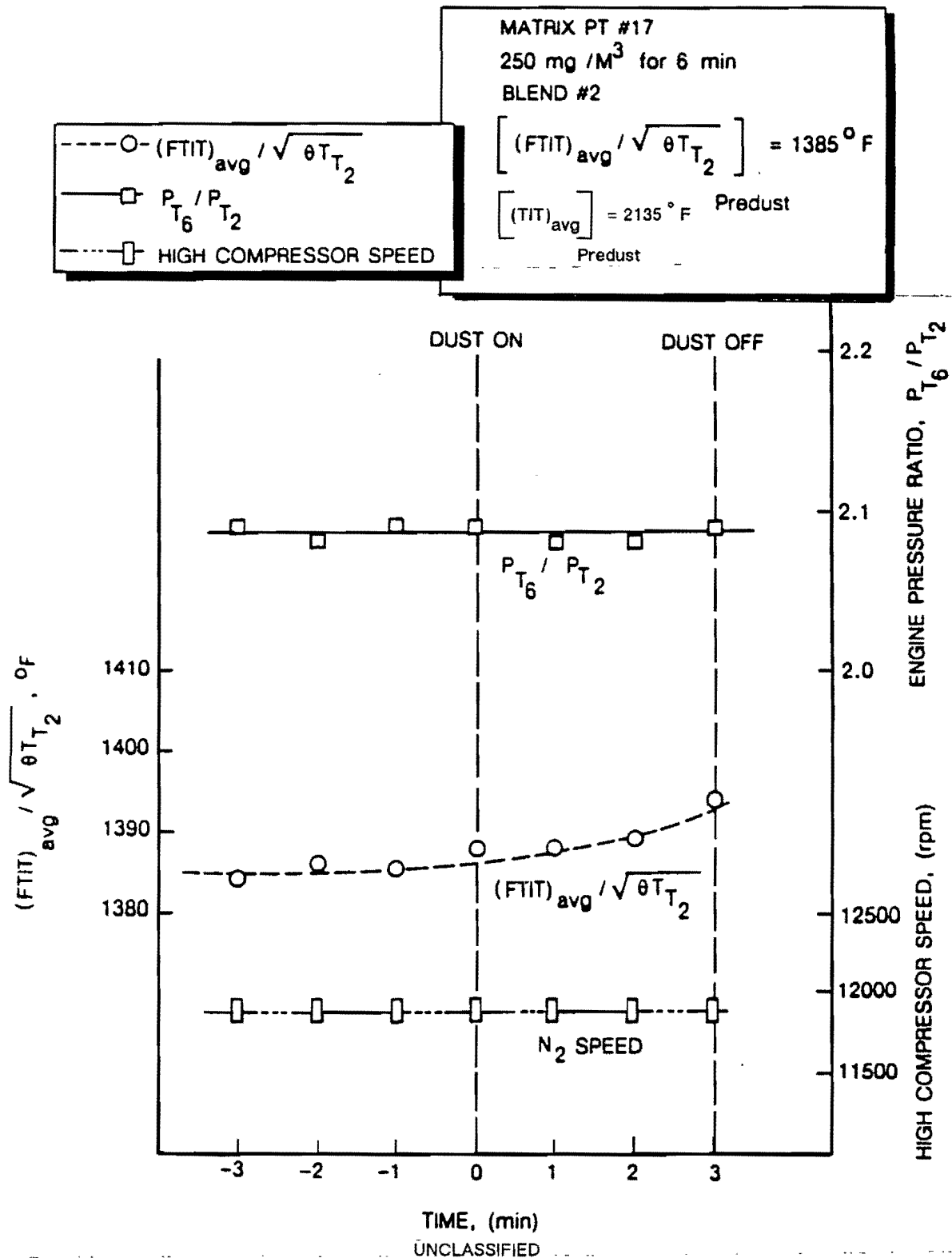


Figure 4.9. (U) Time history of F-100-PW-100 engine parameters during dust exposure (Continued).

UNCLASSIFIED

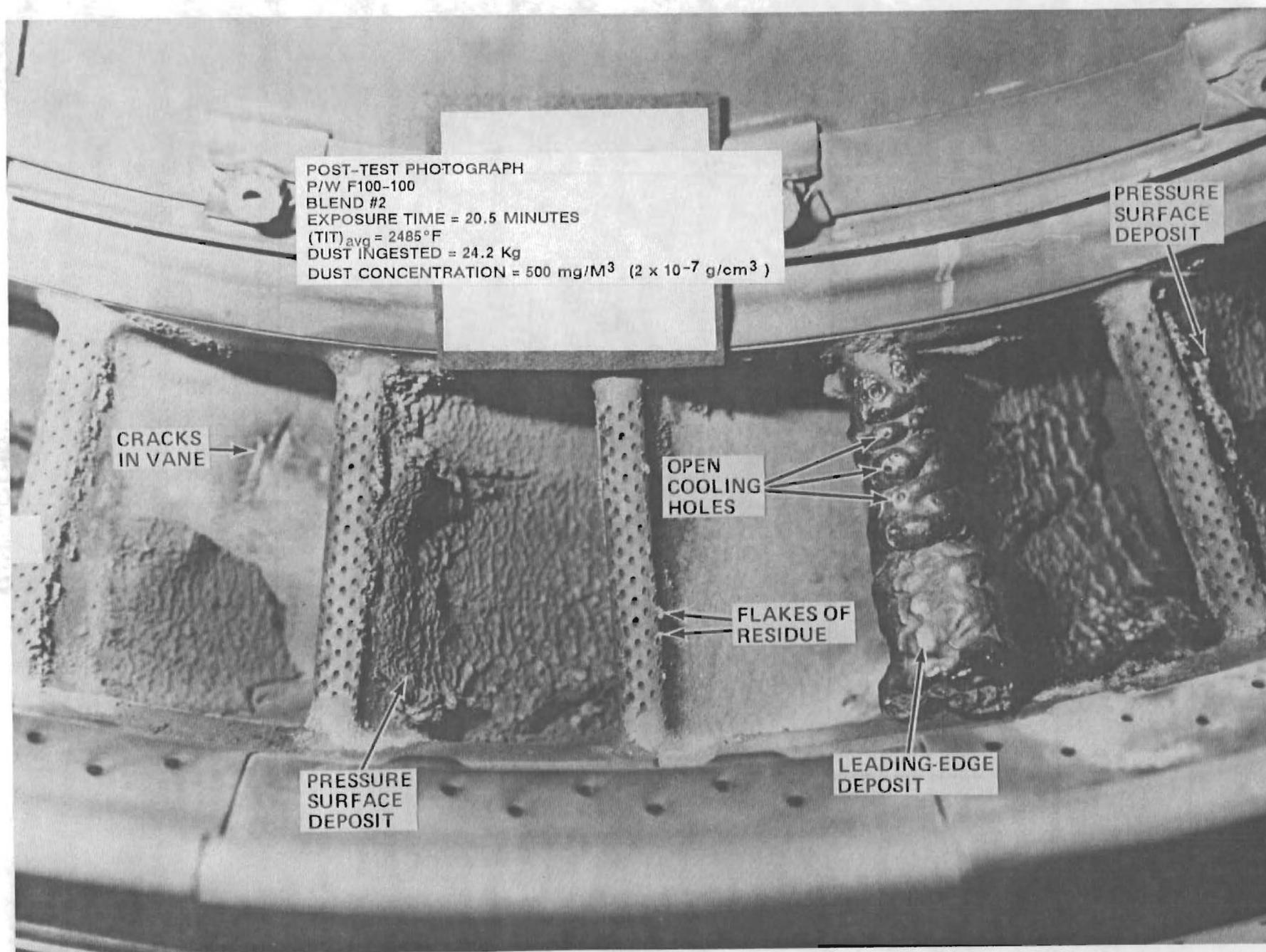


Figure 4.10. (U) Photograph of first vane for F-100-PW-100 high-pressure turbine after dust exposure.

POST-TEST PHOTOGRAPH
P/W F100-100
BLEND #2
EXPOSURE TIME = 20.5 MINUTES
(TIT)_{avg} = 2485°F
DUST INGESTED = 24.2 Kg
DUST CONCENTRATION = 500 mg/M³ (2×10^{-7} g/cm³)

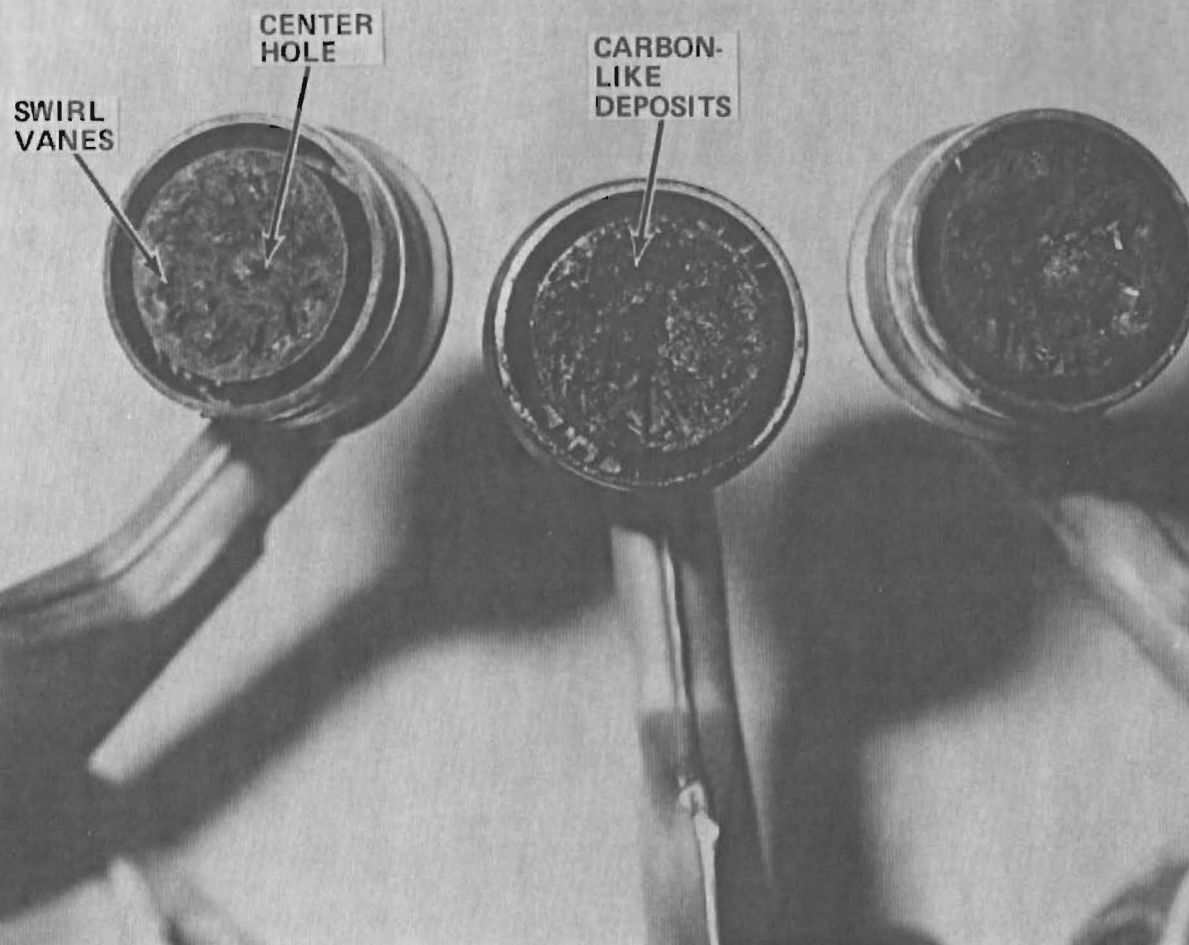
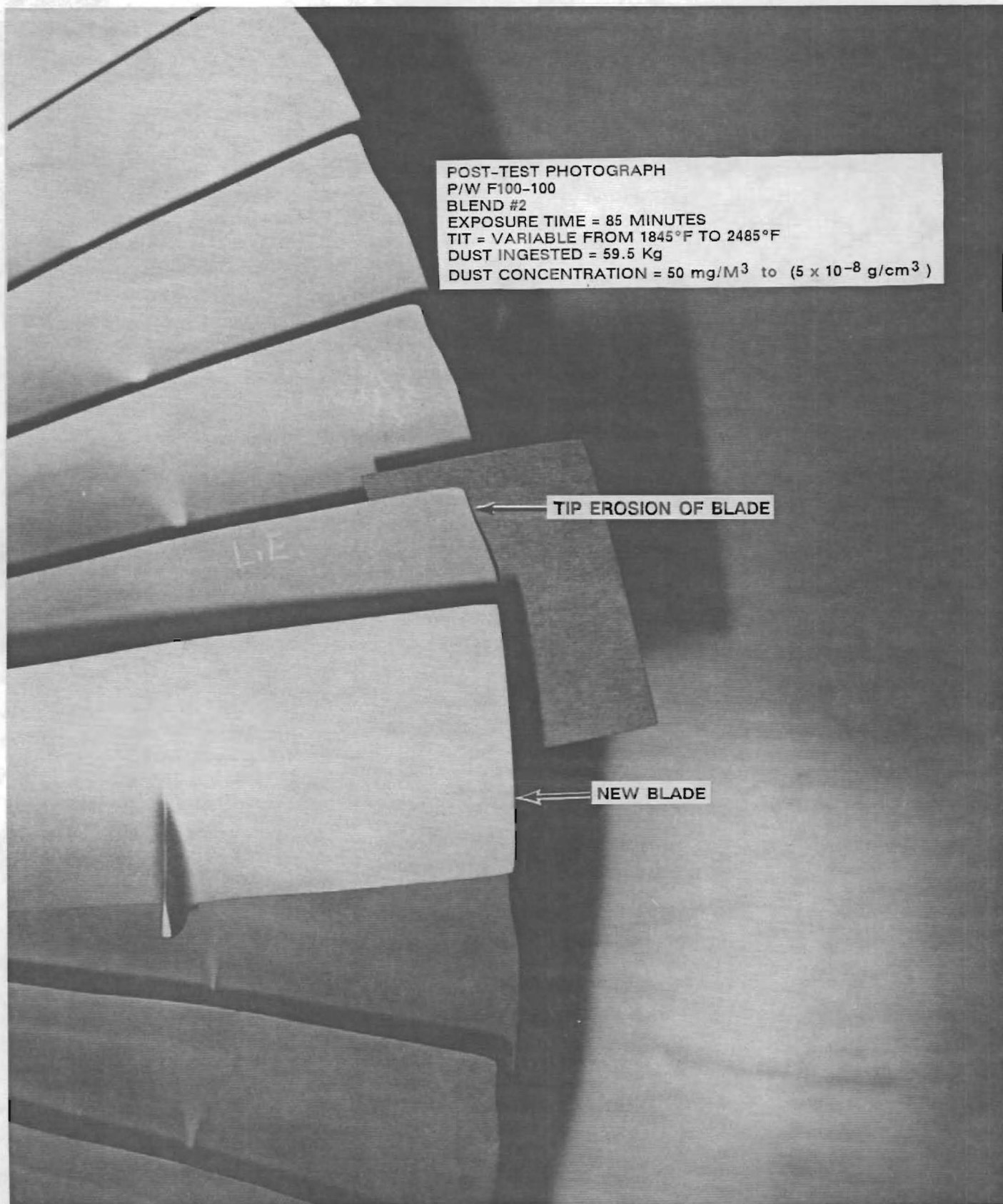


Figure 4.11. (U) Close-up of photograph of F-100-PW-100 fuel nozzles after dust exposure.

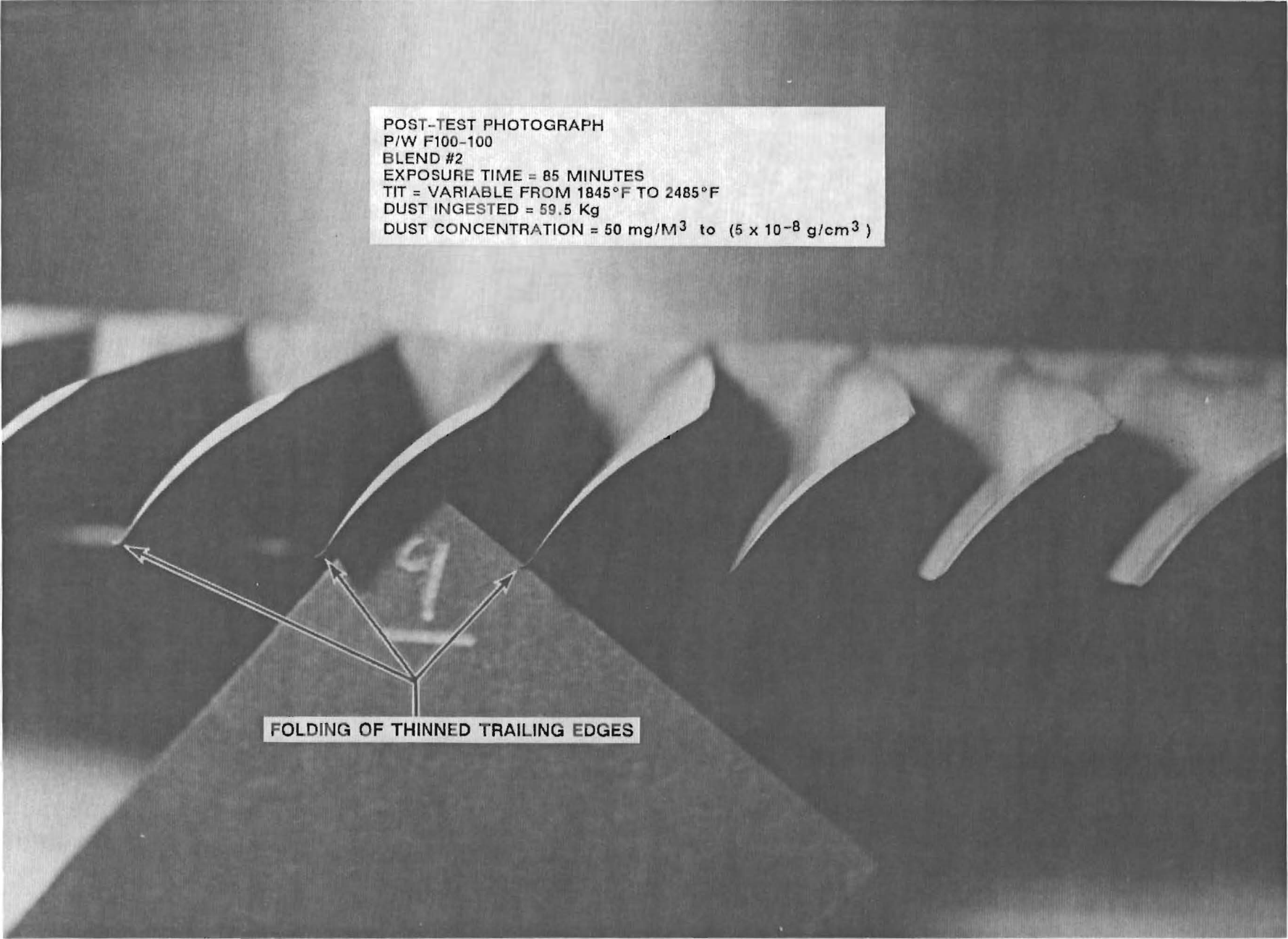


SECRET

Figure 4.12. (U) Rear view photograph of second stage fan rotor of F-100-PW-100 after dust exposure.

POST-TEST PHOTOGRAPH
P/W F100-100
BLEND #2
EXPOSURE TIME = 85 MINUTES
TIT = VARIABLE FROM 1845°F TO 2485°F
DUST INGESTED = 59.5 Kg
DUST CONCENTRATION = 50 mg/M³ to (5 x 10⁻⁸ g/cm³)

45

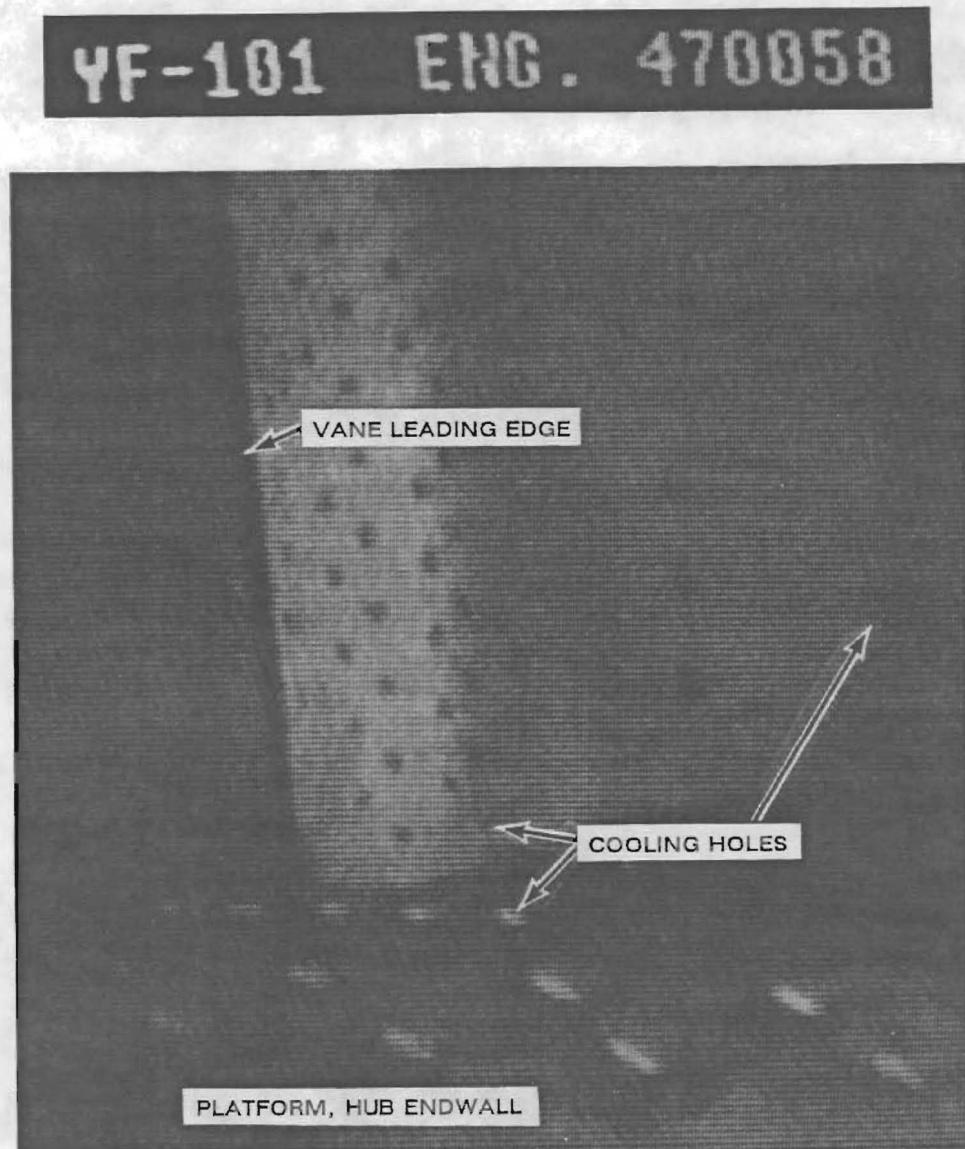


FOLDING OF THINNED TRAILING EDGES

SECRET

Figure 4.13. (U) Photograph of F-100-PW-100 high-pressure compressor ninth-stage rotor after dust exposure.

UNCLASSIFIED



UNCLASSIFIED

Figure 4.14. (U) Pre-test photograph of inlet to first vane of YF-101-GE-100 high pressure turbine.

UNCLASSIFIED

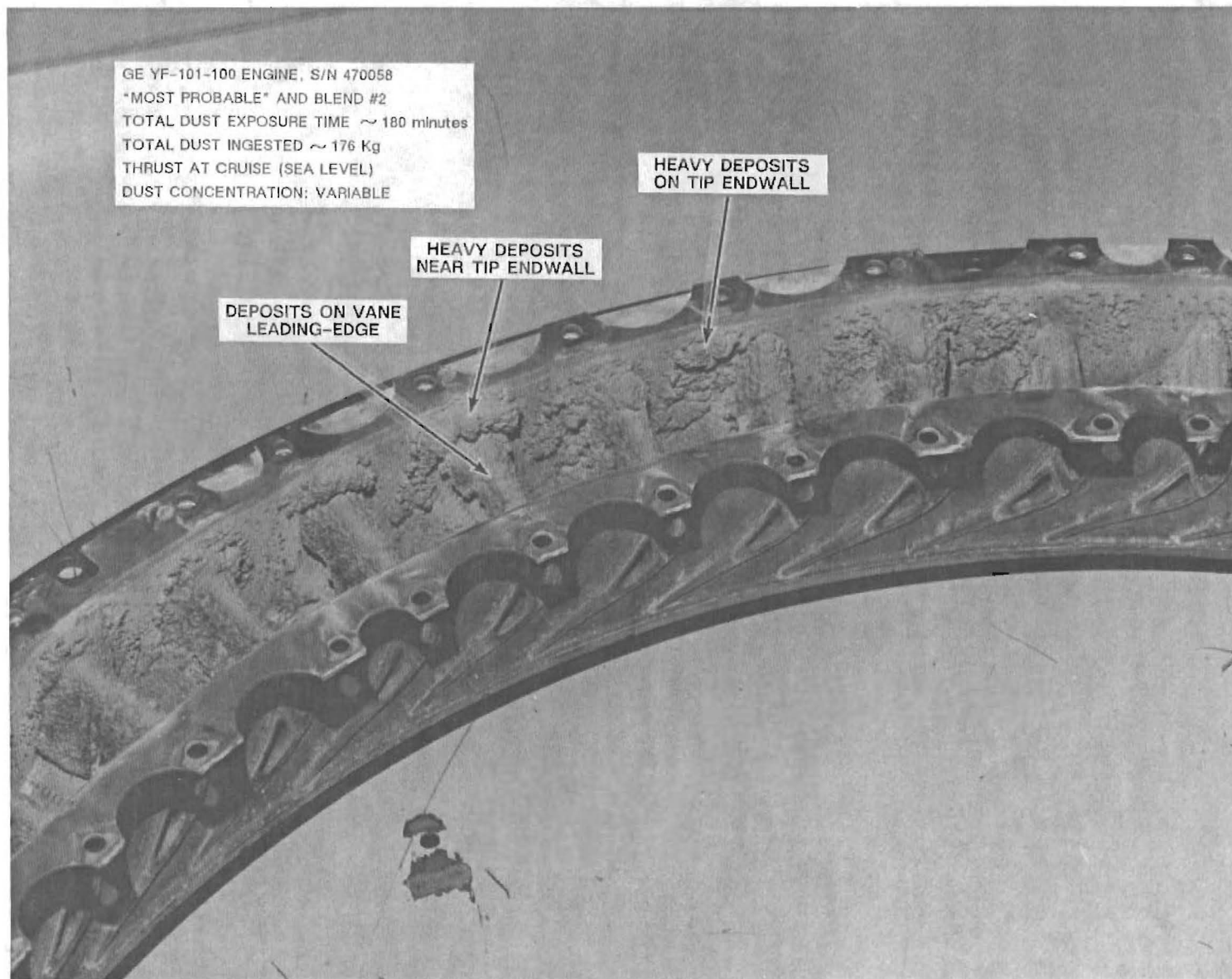


Figure 4.15. (U) Post-test photograph of YF-101-GE-100 hp turbine vane.

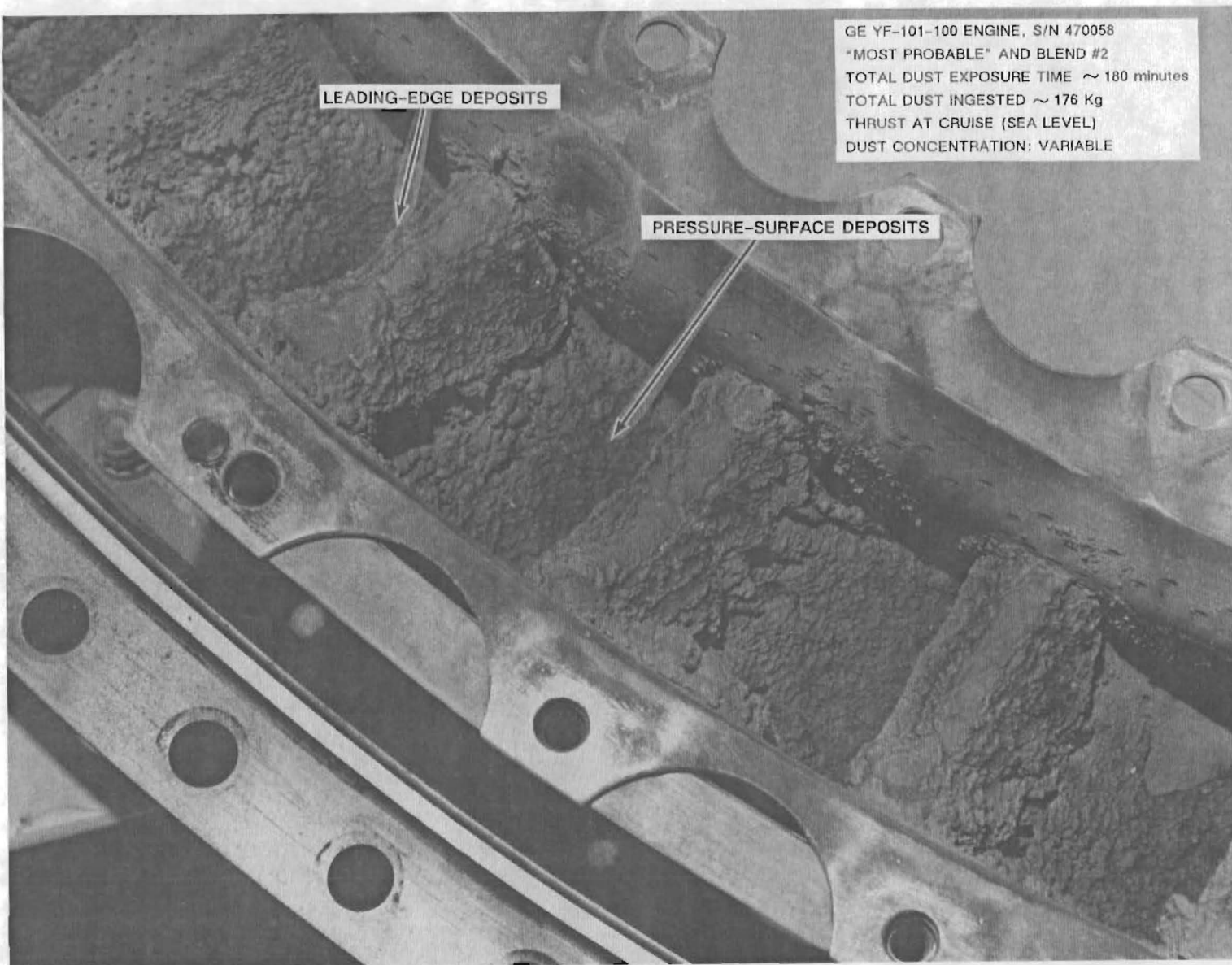


Figure 4.16. (U) Close-up post-test photograph of YF-101-GE-100 hp turbine guide vane.

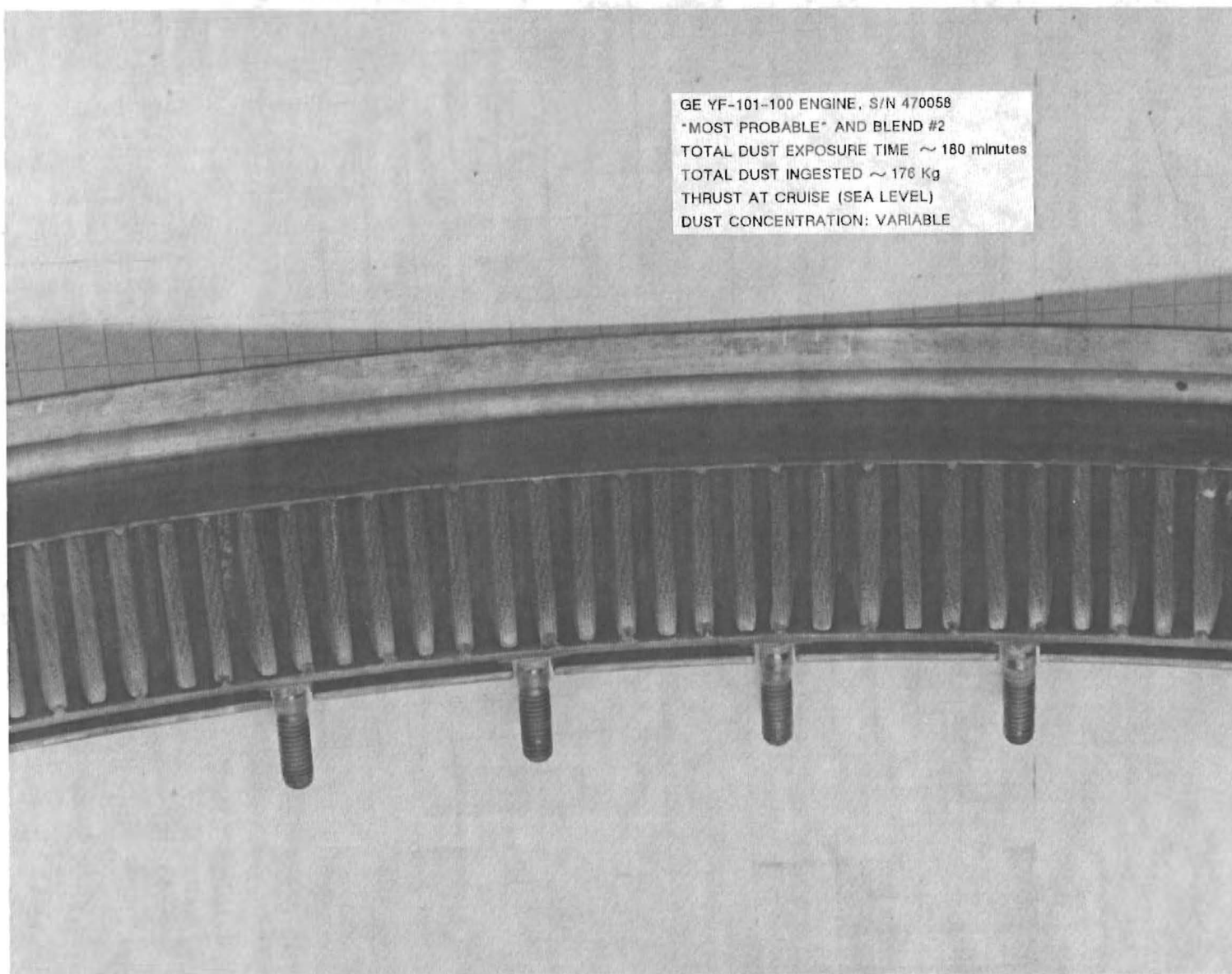


Figure 4.17. (U) Post-test photograph of YF-101-GE-100 hp turbine vane cooling air inlet filter.

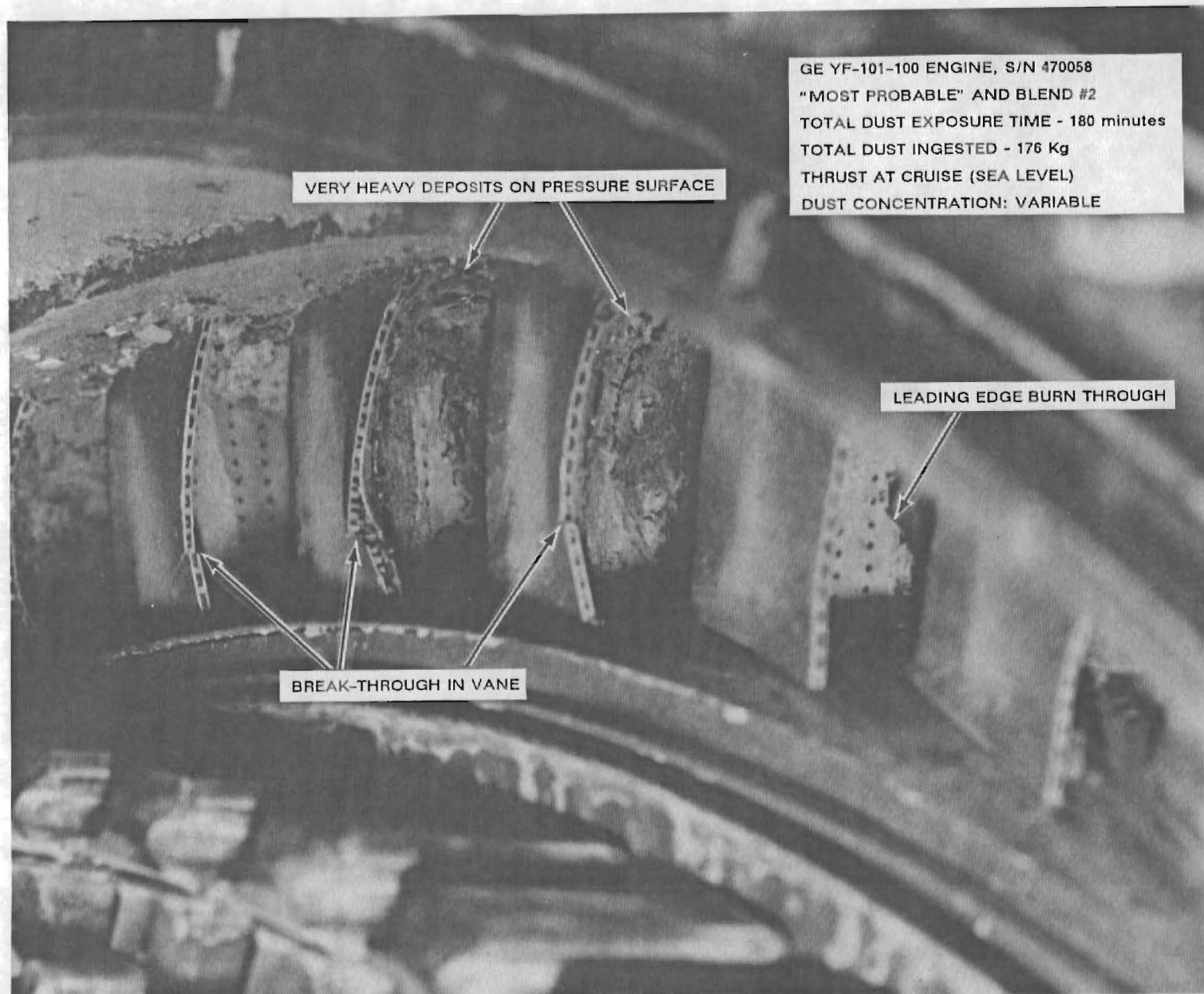


Figure 4.18. (U) Post-test view photograph of first vane of YF-101-GE-100 high pressure turbine.

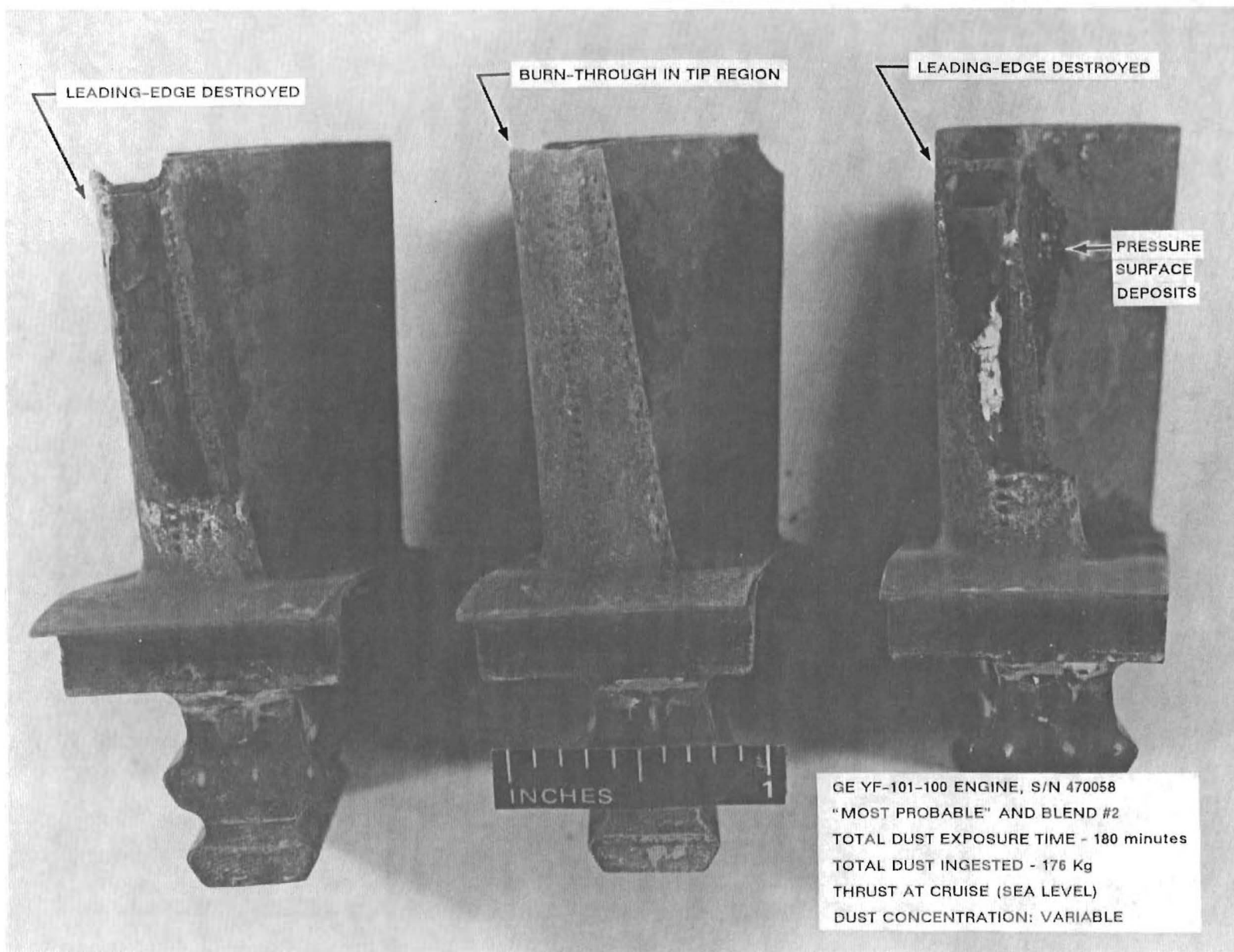


Figure 4.19. (U) Post-test photograph of three blades from YF-101-GE-100 high pressure turbine.



WHITE PATCH ON BLADE FOR
PYROMETER REFERENCE

SECRET

Figure 4.20. (U) Post-test photograph of YF-101-GE-100 blade suction surface.

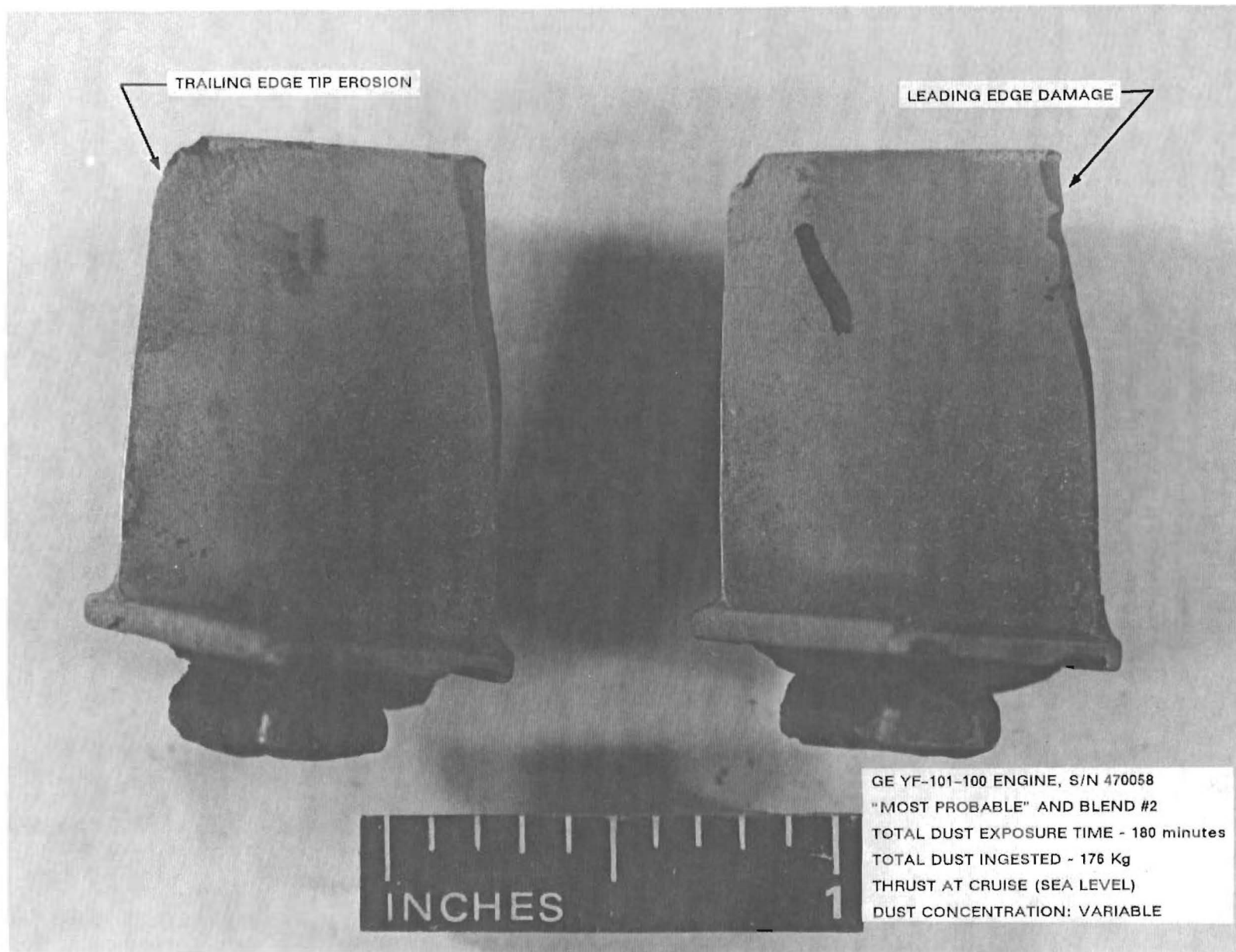


Figure 4.21. (U) Post-test photograph of 6th stage blade of YF-101-GE-100 high pressure compressor.

GE YF-101-100 ENGINE, S/N 470058
"MOST PROBABLE" AND BLEND #2
TOTAL DUST EXPOSURE TIME - 180 minutes
TOTAL DUST INGESTED - 176 Kg
THRUST AT CRUISE (SEA LEVEL)
DUST CONCENTRATION: VARIABLE

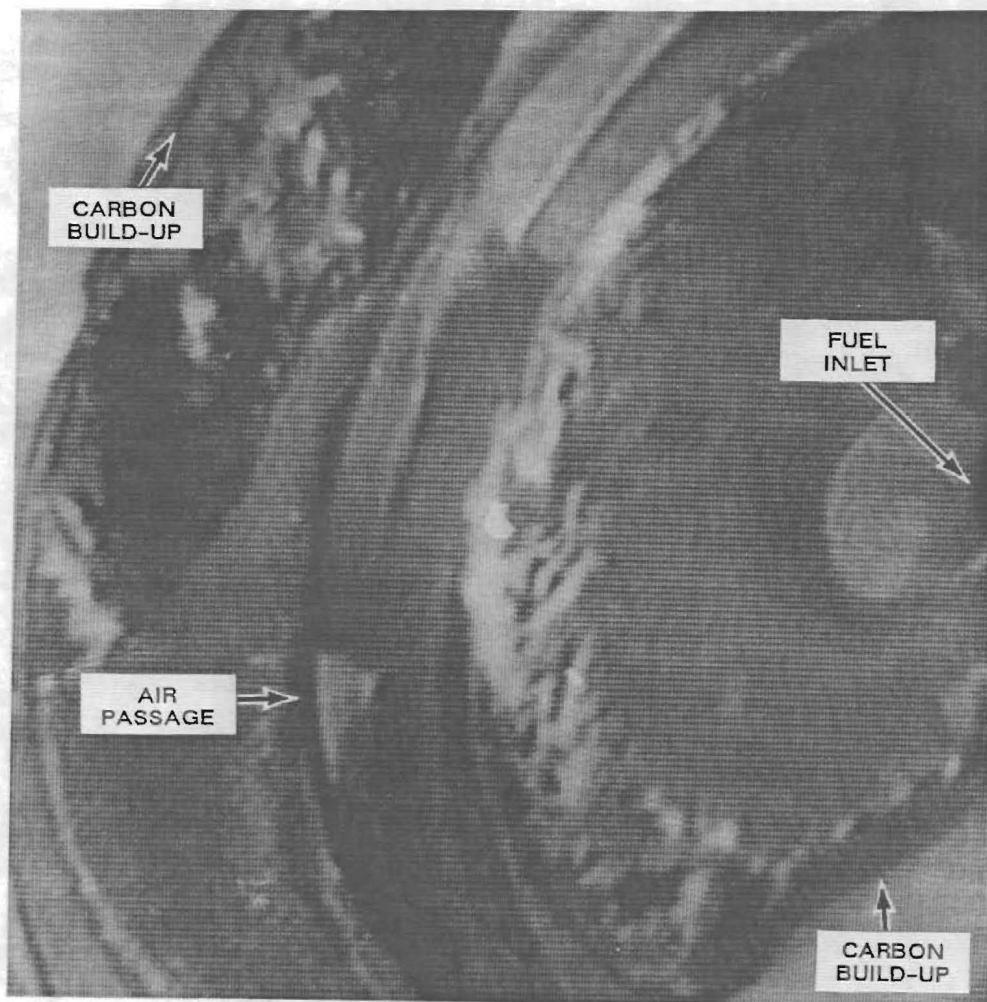


Figure 4.22. (U) Post-test photograph of fuel nozzles from YF-101-GE-100 combustor.

UNCLASSIFIED

APPENDIX

(This Appendix Is Unclassified)

Influence of Overpressure Pulse on the Operation of a Gas Turbine Engine

A.1 INTRODUCTION.

The operation of gas turbine engines in regions subject to nuclear detonations forces one to consider the potential problems associated with dust clouds and overpressure pulses. The first part of this report dealt with the dust cloud. This part will deal with the behavior of gas turbine engines when subjected to sharp leading edge overpressure waves. This is a research area that has been investigated in some detail over the past several years at the Calspan Advanced Technology Center (ATC) under support of the Defense Nuclear Agency (DNA).

The response of a given propulsion system to inlet flow distortion and internal propagation of the overpressure pulse is governed by many factors. The strength of the pulse and its angle of incidence are very important, as are the type of inlet and engine. For a specific engine, the internal gasdynamic response is dependent upon the internal configuration (i.e., the number and type of compressor stages), the engine operating condition at the time of the encounter (overall pressure ratio and stall or surge margin) and the particular control system. The type of inlet (internal, external, or mixed compression; large or small length-to-diameter ratio; boundary-layer bleed and bypass provisions) will modify overpressure waves by changing the effective strength and by introducing flow distortion at the engine face. The altitude and airspeed at which the aircraft encounters the pressure pulse are also important parameters.

The standard practice in the Calspan ATC measurement programs has been to limit the maximum overpressure to which the engine is exposed to the value corresponding to the limit of the weakest aircraft structural component. Of critical interest is the inherent overpressure hardness of the engine when compared to the airframe structure. Intuitively, they should be equally hard, and should be no harder than the aircraft as a system. It is important to note here that none of the aircraft in the current military fleet have been experimentally demonstrated to be overpressure hard. The B-1 was designed to be so, but the propulsion system hardness was bought off by the Air Force on the basis of a Rockwell paper study. No overpressure measurements have been performed for the F-101 engine series.

The specific engines that have been subjected to overpressure pulses in the Calspan ATC test facilities are: (1) the J85-5 turbojet (F-5B, F-5E/F), Dunn, Davis, and Rafferty, 1979, Dunn, 1980, and Dunn and Rafferty, 1982, (2) the J57

turbojet (B-52G, EC/KC-135) Dunn, Adams, and Oxford, 1989, (3) the TF33 turbofan (B-52H, C-135, C-141) Dunn, Adams, and Oxford, 1989 and Adams and Dunn, 1987, and (4) the F107 turbofan (Tomahawk cruise missile) Dunn, 1981, Dunn, Padova, and Adams, 1987, and Padova and Dunn, 1983. All of these engines are relatively old and thus are more robust than the modern F-101-GE-102, the F-100-PW-229, the F-119-PW-100, etc. engines.

A.1.1 Phenomenological Description of Blast Pulse.

The subject of interest here is the response of an aircraft to the blast pulse of a nuclear weapon. Figure A-1 illustrates the many different influences that nuclear weapons can have on aircraft, missiles, and satellites. When viewed from a time- or distance-from-detonation perspective, some of these effects can be categorized as prompt while others are delayed. Examples of prompt effects on aircraft are electromagnetic radiation and thermal radiation. The delayed effects include the airblast components of overpressure and gust, plus residual radiation and lofted dust. While the height of burst influences the amount of lofted dust and the energy distribution amongst the effects, much of the energy is in thermal radiation, posing nearly instantaneous problems for aircraft structures and air crew survival. Most of the late energy is found in the airblast, again affecting the aircraft structure. For a typical one megaton weapon, about 50% of the energy is in the thermal radiation while 35% is in the blast, Glasstone and Dolan, 1977. Hardening of the airframe for these two effects constitutes a major part of the design process when hardening criteria are imposed. Under DNA sponsorship, many research projects and several structural response codes have provided insights and improved hardness. Areas lagging behind in terms of research and codes are the responses of aircraft engines to airblast overpressure and lofted dust.

Before an experimental facility can be designed for the purpose of simulating the overpressure response of an inflight engine, the overpressure levels and duration must be understood. First, it should be noted that the overpressure levels of interest are likely to be 28 kPa (~4 psi) and below since the structure will fail at higher levels. Figure A-2 illustrates several additional key points. For a nominal one megaton airburst, a 28 kPa overpressure level occurs about 18 km (9.7 NM) from the detonation at altitudes below the triple point. A typical nuclear overpressure pulse shape as a function of time is illustrated in

Figure A-2. The pulse has a very sharp rise to the peak overpressure with a decay to below ambient pressure a few seconds later.

A.1.2 Engine Response to Overpressure Wave.

An overpressure wave incident on the engine inlet represents a very sudden perturbation to the incoming flow conditions. The duration of the positive portion of the pressure pulse depends upon the strength of the nuclear explosion, the altitude and the distance of the burst from the aircraft. However, the positive portion of the pulse is always followed by a negative (or expansion) portion. These two parts of the pressure pulse can influence the engine response in different ways.

There are many factors that must be taken into account when describing the potential influence on engine operation. For example, an engine will ingest a pulse if it approaches from the forward hemisphere. However, a key parameter is the time from entrance at the fan (or compressor) to reflection at the turbine nozzle guide vane (NGV) due to choked flow, and egress back out the front of the fan (or compressor). As the wave system progresses through the machine, the local sonic velocity increases as a result of increasing local temperature. At each component stage, a transmitted and reflected wave system occurs as sketched on the inset of Figure A-2. In order to attach numbers to this discussion, several of the engines used in the Calspan experiments will be used. A simple estimate for the J85 would suggest that approximately 5 ms would be required (assuming local sonic speed) for the propagating blast wave to travel through the engine. For the F107, it is approximately 2 ms and for the TF33, approximately 7 ms. While the pulse duration will likely exceed these times, the engine responds to the higher pressure behind the blast front as a steady-state condition.

It is generally agreed within the propulsion community that the engine will achieve steady-state operation at the overpressure condition in a time period consistent with one or two revolutions of the HP compressor. For the J85 at maximum rpm, a single revolution requires about 7 ms. For the F107 fan stages, it is about 2 ms, and for the TF33 at 9945 rpm, it is about 6 ms. Because each engine is different and the range of shock parameters broad, it is not possible to state in advance how long it will take for the initial transients to decay to steady-state operation. It will be shown in Section A.3.3 that about 10 ms is required for

the TF33 engine while the smaller more compact F107 engine required longer time to accommodate to the overpressure.

The experimental facility must replicate the sharp rise in overpressure to desired test levels and provide adequate duration for full engine response. The two shock-tube systems used at Calspan have both done this, including test overpressures of over 27.6 kPa (4 psi). In fact, the J85/F107 tubes provided much longer durations than necessary, typically exceeding 70 ms. For the TF33 set-up, the space constraints in the test cell made it convenient to use an arrangement which provided a flat-top pulse of typically 22 ms duration at the fan face, still very adequate. One of the major considerations in designing the overpressure pulse is that, if the duration is excessive, one of the many stages of the compressor may go into a flutter mode and cause engine destruction before the pressure pulse is relieved. It is very difficult to predict in advance whether or not flutter will occur. It has been our experience to date that of the engines tested, only the J85 turbojet experienced this problem. However, when it does occur, it is dramatic. A typical data record of an overpressure history at the fan face is shown in Figure A-2.

It is well known that engine operation is influenced by inlet flow distortion, but in the case being discussed here the resulting distortion pattern at the engine face depends on the incidence angle, the pulse, the inlet configuration, and the altitude and airspeed at which the aircraft intercepts the pressure wave, to name but a few. Further, the function of the compressor system is to take air in at a relatively low pressure and increase the pressure to 20 or 25 times the intake value. Pressure pulses of the type under consideration here have both a positive and a negative component. The machine will handle these components differently. Now, if the positive portion of the overpressure pulse is on the order of 2.5 psi, then the resulting amplification of this pulse at the compressor discharge could result in a local pressure which may exceed the surge margin of the machine. This increased pressure into the combustor may also be more than that unit can handle from a structural point of view. When the negative portion of the pressure pulse arrives at the engine face, the compressor intake may then be starved for air and the pressure of the air reaching the combustor may be less than required to sustain combustion. Having now mentioned the intake (inlet), one of the more serious problems from the viewpoint of engine operation is inlet distortion at the engine face. At high altitude, the engine operation is sensitive to the character of this distortion.

Structural failure because of the increased pressure described above, compressor stall or surge, local increases in gas flow velocity within the combustor are all potential candidates for causing flame-out to occur. Engine flame-out either at low altitude during base escape or at high altitude is a difficulty that would tax the air crew during times of high work load.

The remainder of this section will be devoted to a discussion of the experimental facility used to perform the engine measurements in Section A.2, a presentation of results obtained to date with military engines in Section A.3, and concluding comments in Section A.4.

A.2. EXPERIMENTAL FACILITIES.

Two experimental facilities are used at Calspan to perform these measurements and they are described in detail in Dunn, Adams, and Oxford, 1989 and Dunn, Padova, and Adams, 1987. Since both work on the same principle, a brief description of only one of the two will be given here. In both experimental arrangements, the engine is at rest (no ram air) and it is operating at sea level conditions. From an engine perspective, the fact that there is no ram air is of little consequence because the corrected engine operating conditions would be the same with or without ram air. The main effect of ram air would be on inlet distortion which, depending upon the inlet configuration, could influence engine operation. Further, for the large engines, space constraints do not allow yaw or tail-on overpressure incidence angles. For the small F107 cruise missile engine, it was possible to operate with both yaw and tail-on conditions.

The overpressure pulse is generated using a modified Ludwig-type facility, which has been adapted to the Calspan engine silencer as shown in Fig. A-3. The engine draws its supply air through the open area between the shock tube and the bellmouth. The shock-generating device uses compressed air stored in a driver tube and a neoprene diaphragm to initially separate the driver gas from the shock tube. The pressure to which the driver tube is loaded determines the magnitude of the overpressure pulse. When the neoprene diaphragm is released by rapidly dropping the actuating chamber pressure, the driver-tube air expands into the shock tube, forming a shock wave within a short distance from the diaphragm, which then propagates a pulse to the operating engine. There are no fracturing diaphragm materials in the driver or driven gas supply systems, thus eliminating any foreign particles that could harm the engine.

For both the TF33 and J57 configurations, the tube was designed to deliver the shock wave directly into the inlet tube, i.e., head-on incidence angle.

For generation of pulses up to 27.6 kPa (4 psi), a driver supply tube 16.2 m (53 ft.) long and 2.44 m (8.0 ft.) in diameter was selected to achieve adequate volume while also assuring adequate length so that internal wave systems would lag well behind the shock waves. To deliver the upper limit of desired pressure pulses the driver supply tube must be pressurized to about 207 kPa (30 psi).

The modified Ludwig-tube facility uses an actuating chamber and flexible diaphragm to initially isolate the supply tube from the shock tube for pressurization. Details of this design feature are given in Dunn and Rafferty, 1982. This arrangement allows actuating chamber pressurization at a value slightly above (~0.5 psi) that of the supply tube, thus forcing the diaphragm against the shock-tube opening. To generate a shock wave, an air-operated cutter knife punctures the mylar diaphragm in the back of the actuating chamber, instantaneously releasing the supply air and generating the required sharp-rise pulse.

A final aspect of the shock-tube design is the interface at the engine inlet. Figure A-4 is a sketch of the TF33 configuration illustrating how the shock tube is inserted into the inlet tube. This setup allows the engine to operate at power settings up to take-off rated thrust (TRT) without undue restriction of airflow. Prior to performing the overpressure measurements, the engine is calibrated with and without the shock tube installed. On the basis of these measurements, it can be shown that neither of the tubes has significant influence on the engine operation.

A calibrated bellmouth is placed at the entrance of the 3.66-m (12 ft.)-long inlet duct. The overlap between shock tube exit and inlet duct entrance is critical in controlling the duration of the pulse. When the pulse exits the shock tube, an expansion wave travels back up the inlet duct toward the bellmouth. At the bellmouth, a second wave system occurs, which is then reflected back toward the engine. As this system interacts with the flow exiting the shock tube, it dissipates the sustained overpressure strength of the original shock.

The geometry of the present setup provides pulse durations on the order of 25 ms as demonstrated on Figure A-5. The upper pressure history shown in Figure A-5 was obtained in the shock tube prior to entry into the large diameter tube leading to the engine face (see Adams and Dunn, 1987 and Dunn, Padova, and Adams, 1987 for additional discussion). The lower pressure history on

Figure A-5 represents the static pressure measured at the fan face of a TF-33 engine while operating at military rated thrust (MRT). The static pressure at the fan face increases rapidly with the arrival of the shock wave. About 5 ms of flow establishment time are required for the engine to accommodate the overpressure pulse. Shortly after arrival of the shock wave (2.5 ms) the shock strength is increased by reflection of the pressure pulse from one of the internal components. This reflection is felt to have come from the first or second stage fan. The period of the test time includes a series of expansion and compression waves traveling into and out of the engine. In Section A.3.3, the discussion will return to a physical interpretation of Figure A-5 and the disturbances appearing on the lower pressure trace will be described in terms of the engine operating conditions. However, for now it suffices to note that the character of this pressure record is similar to those presented in Dunn, Padova, and Adams, 1987 which were obtained using a 40-probe distortion rake at the fan face of the F107 engine under similar experimental conditions. The F-107 measurements were performed in a different facility for which the test time was on the order of 70 ms. Returning to the lower record of Figure A-5, the pulse decays at the end of the test time in a manner similar to the shock-tube pressure. The pre-shock fan face pressure record shows evidence of more acoustic noise input than was observed at the shock-tube location, but this input does not degrade the overall signal.

A.3. DISCUSSION OF EXPERIMENTAL RESULTS.

All of the results to be presented in this section were obtained in the Calspan facilities. One of the engines used in the Calspan measurements (F-107) was subsequently used by Kaman Avidyne (Kleppin, et al. 1982) at Holloman Air Force Base in an attempt to determine the influence of ram air on the engine response to a pressure pulse. The engine and instrumented inlet were placed on a rocket driven sled and subjected to blast waves created by TNT and ANFO charges. The amount of engine data obtained from the three sled tests was limited because of unanticipated difficulties. However, on the basis of the available results, the presence of ram air at the operating condition had essentially no influence on engine response. This result was anticipated on the basis of the discussion presented earlier in this report. In the remainder of this section, selected results from each of the Calspan overpressure measurement programs will be presented.

A.3.1 General Electric J-85 Turbojet.

The J85 test series described in Dunn and Rafferty, 1982 pioneered the use of a Ludwig-type shock tube to generate the overpressure and to send this wave system directly into the inlet of an operating engine. The J85 test measurements were performed with the engine off and at various thrust settings from 70 to 94 percent corrected speed, using overpressure pulses from 5.5 kPa (0.8 psi) to 17.2 kPa (2.5 psi) for a duration of about 70 ms. At these exposure levels, the engine experienced no difficulties in that it did not surge, flame out, or suffer structural damage. At the beginning of this program, General Electric and the Air Force indicated that the engine should be able to withstand a 34 kPa (5.0 psi) overpressure without difficulty. However, when the magnitude of the overpressure was increased to about 25 kPa (3.6 psi) the compressor casing displacement approached the red line limit. One additional experiment at 30 kPa (4.4 psi) caused the compressor casing displacement to exceed the red line limit by almost a factor of two. At this last condition the engine experienced severe operational difficulties that were felt to be associated with compressor flutter. Upon post-run review of the data, the test series was terminated and the engine retired from service.

The internal pressure data collected as part of this program suggested that the pressure pulse was not amplified in passing through the compressor. The large compressor casing deflections just described account for part of this observation. In addition, this engine was equipped with fast acting compressor bleed doors because it had been previously used for rotating stall studies. These doors opened during the overpressure tests and are believed to be responsible for relieving some of the pressure.

A.3.2 Williams International F-107-WR-102 Turbofan.

The results of this measurement program are reported in detail in Padova and Dunn (1984) and Dunn, Padova, and Adams (1987). The engine was heavily instrumented with pressure transducers and accelerometers. Total and static pressure measurements were obtained within the engine. In addition, a forty-probe dynamic-pressure rake was located just upstream of the first-stage fan. From these measurements, the fan-face pressure history was determined before, during, and after the shock-wave arrival. The engine had accelerometers located at strategic locations.

Hypodermic tubing was used to transmit the pressure pulse from the internal portion of the engine to the externally mounted pressure transducers. The calculated response time for the indicated pressure to reach 95 percent of the equilibrium pressure level was a maximum of approximately 0.25 milliseconds, which was satisfactory for the purposes of these measurements. The transducers from the high-pressure compressor discharge rearward through the engine were water cooled because of the hot-gas environment.

Measurements were performed with either an extended bellmouth or a S-type inlet (same as on missile) mounted to the engine. Further, with both of these configurations, measurements were obtained with the engine at either 0° yaw or 20° yaw.

The data presented in Dunn, Padova, and Adams (1987) are far more detailed than can be presented here. However, a few representative records will be presented to provide an indication of the data that are available. Figure A-6 presents a typical pressure history obtained from one of the total pressure rakes located just upstream of the fan face. The engine core speed for this particular case was 61,540 rpm. The result shown in Figure A-6 illustrates the pre-experiment pressure level, the early time engine response to the overpressure immediately after shock arrival, and the succeeding steady-state engine response. The discussion presented in Dunn, Padova, and Adams (1987) is separated into the following subsections: (1) typical wave diagram of the engine/facility response to the shock-processed gas and the early-time inlet data and (2) the steady-state engine response to the shock-processed gas.

Note from Figure A-6 that at about 135 ms the pressure begins to fall rapidly from a relatively steady value. It was initially thought that the engine operation might have been more sensitive to the pressure fall associated with the shock wave. However, the engine handled this pressure decrease without any indication of a problem. Wave diagrams are presented in Dunn, Padova, and Adams (1987) to illustrate the origin of the pressure spikes during the early-time response shown on Figure A-6. The steady-state portion of the record is used to describe internal stage-by-stage engine response, to obtain a measure of the pressure distortion at inlet, to obtain a comparison between bellmouth and S-type inlet response, to obtain an indication of the influence of yaw angle on the engine/inlet behavior for both the early engine response period and the steady-state response period, and to summarize facility parameters.

A particular engine component responds to a pressure-pulse disturbance within a time period on the order of several revolutions. It is, therefore, helpful to put the time periods shown on Figure A-6 in perspective by comparing the early-time (~28 ms) and the steady-state (~43 ms) durations with typical engine characteristic times. Table A-1 presents such a comparison for one revolution of the main core and for one revolution of the fan. The shock wave system is moving through the engine at an axial rate of approximately a foot per millisecond. Each encounter of the shock wave with an engine component results in a reflected wave and a transmitted wave. These secondary waves become weaker and weaker with multiple reflection and transmission. The times/rev given in Table A-1 correspond to flow distances of tens of chord lengths and it would be anticipated that steady-state operation would be achieved after a time interval corresponding to several revolutions as stated in the opening sentence.

Table A-1. Engine characteristic times.

Core Speed (rpm)	Time/rev (ms)	Fan Speed (rpm)	Tim/rev (ms)
61,600	1.0	31,900	1.9
55,500	1.1	28,700	2.1
48,700	1.2	25,900	2.3

It was noted early in this section that the specific configuration of the inlet is important in determining the quality of the flow at the engine face. The inlet used in these experiments was S-shaped inlet of the Tomahawk cruise missile and because of the missile configuration the inlet makes a transition from rectangular at the entrance to circular at the outlet (engine face). Surface pressure measurements made along the inlet flow path can be used to infer the quality of the flow in the inlet. Figure A-7 presents pressure histories for two transducers located near the inlet entrance. The upper trace suggests that the flow is well behaved, but the lower trace suggests difficulty in initially establishing a stable condition. Eventually, the flow at this lower location does stabilize. By contrast, Figure A-8 illustrates the surface pressure history at four circumferential locations near to the engine face. These pressure signatures are all very similar suggesting that the inlet flow has been well adjusted in moving from the entrance to the exit of the S-shaped inlet. The pressure data collected in the inlet, at the

fan face and internal to the engine are used to construct wave diagrams to explain the events during exposure of the engine to the pressure field.

It is inevitable that the missile will fly a trajectory which includes yawing and/or pitching maneuvers. To determine the influence of the pressure pulse on the engine operation in the event that the relative angle of encounter between the wave system and the missile was different than 0° , experiments were run by placing the engine at a yaw angle of 20° relative to the shock wave. Figure A-9 is a series of pressure measurements comparable to those given in Figure A-8, but for 20° yaw instead of 0° yaw. A comparison between Figures A-8 and A-9 (note the different time scales) does not indicate any dramatic influence of yaw angle on the flow characteristics obtained at station #3 within the inlet. This result suggests that the inlet is well designed and that it is of sufficient length for flow disturbances associated with the yaw angle to dampen by the time the flow reaches the fan entrance. At locations nearer the inlet entrance, the influence of yaw angle is pronounced.

One of the principal objectives of this measurement program was to investigate the response of a turbofan engine to an overpressure imposed at the inlet face. Specifically, the question to be answered was: if an overpressure of ΔP were imposed on the fan face, then would this overpressure be increased by the appropriate pressure ratio for the respective stages of the machine? One must also consider the question of how much the unloading of the fan and compressor due to the shock-wave passage changes the relative position on the operating map. The performance maps necessary for this determination were supplied to Calspan by Williams International for this machine.

To illustrate the result, the steady-state increase in pressure for a given stage, ΔP_i , normalized by the averaged increase of the 40-probe rake, ΔP_2 , as a function of machine stages has been plotted and is given in Figure A-10. This plot includes the theoretical performance value for the engine in the absence of a shock wave. This theoretical value was experimentally verified during the course of the measurement program.

The engine results obtained with the extended bellmouth and with the S-type inlet at 0 deg yaw angle for engine speeds of 0 rpm and 55,500 rpm are presented in Figure A-10. The multiple data points indicate different runs and not different measurement positions within a given component. The results shown in Figure A-10 are generally independent of the inlet type. However, the bypass fan discharge and the core fan discharge appear to be influenced differently by the

shock-wave system. The core fan-discharge results are in reasonably good agreement with the predicted response, but the fan bypass discharge result is less than anticipated. The measurements obtained downstream of the axial compressor and downstream of the centrifugal compressor were both below the theoretical value with the most noticeable difference occurring after the centrifugal compressor. The turbine discharge and bypass discharge results are also low, but they are influenced by the upstream compressor and fan discharge, respectively.

As noted above, it was necessary to consider the question of whether or not a change of location on the performance map could explain the observed result. When the shock wave passed through the engine, the fan speed was observed to increase by about 4 or 5 percent while the core speed increased by about 0.2 or 0.3 percent. The performance maps were used to conclude that the observed results could not be explained on the basis of a temporary change in operating point. A more detailed calculation procedure than the simple quasi-steady one-dimensional approach attempted in Dunn, Padova, and Adams (1987) using Rae, Batcho, and Dunn (1988) is required to explain the observations. At the present time, the author is not aware of a code that can satisfactorily treat the physical problem encountered here, though there are codes that have attempted portions of the solution, Sugiyama, Hamed, and Tabakoff (1978), Jansen, Swarden, and Carlson (1971), Peacock, DAS, and Erlap (1980), Tesch and Steenken (1976), and Reynolds and Steenken (1976).

Inlet distortion is an important consideration to the missile designer because it provides an indication of how well the engine should perform under stressed conditions, such as those associated with an overpressure system. For the measurements reported in Dunn (1981), the fan face distortion index was calculated from the pressure rake data. The distortion index is defined as the local pressure normalized by the average pressure over the fan face. Two examples of these distortion patterns are given here on Figure A-11 and A-12 for the S-type inlet at 0° yaw and 20° yaw. Isobars are drawn on the plots in order to better visualize the results. When viewed through the eyes of an engine inlet person, the distortion patterns shown on these figures could be a potential problem. In the absence of experimental data to the contrary, there were those who felt that the engine would experience difficulty.

Figure A-11 presents the distortion index pattern for the S inlet at 0° yaw angle. The lower quadrant contains a sizable region of higher pressure.

However, the remainder of the face is essentially at uniform pressure slightly below average. Figure A-12 presents a similar plot for the S inlet at 20° yaw. Note that the engine speed and overpressure values are slightly different for these two cases, but not sufficiently so to make a major difference. Figure A-12 indicates an elevated pressure region in the lower quadrant of the inlet as was seen at 0° yaw, but a reduced pressure region has developed in the upper quadrant. Examples of the fan face distortion are shown here, but many additional ones are given in Ref. 6 for many other conditions. In all cases for which measurements were performed, the engine was able to accommodate the yaw and overpressure induced distortion. At no time did the engine stall or surge.

On the basis of the F-107 measurement program it was concluded that:

- (1) The flow field near the leading edge of an S-type inlet is three-dimensional for both 0 deg and 20 deg yaw angle and local flow separation appears to occur.
- (2) For the S-type inlet, a significant radial pressure gradient exists at the engine face as a result of communication between the engine and the inlet.
- (3) The turbofan stage-by-stage compression of the imposed pressure pulse is significantly less than the stage compression ratios. A quasi-steady state one-dimensional calculation does not satisfactorily explain the results.
- (4) Potential engine vibrations as a result of the overpressure pulse are not a problem area for this particular engine.

A.3.3 Pratt and Whitney TF-33-P-3 Turbofan Engine and J-57 Turbojet Engine.

The TF-33 and the J-57 engines were both tested in the same facility using the techniques described in Section A-2. The pressure history at the engine face shown in Figure A-5 was obtained for the TF-33 engine operating at military rated thrust with an imposed 1.54 psi overpressure. It is appropriate to return to Figure A-5 and to explain additional portions of the lower pressure history record in terms of the TF-33 conditions. Shortly after arrival of the shock wave (~2.5 ms) the overpressure level is increased by reflection of the pressure pulse from one of the internal components. This reflection is felt to have come from the first or second-stage fan. About 5 ms are required for the engine to accommodate to the overpressure pulse. A series of expansion and

compression waves travels into and out of the engine during the test time. Note that the time between pressure peaks during the test time is on the order of 2.7 ms corresponding to a frequency about 370 Hz. The time required for the LP compressor to make one revolution at the thrust setting consistent with the data of Figure A-5 was about 9 ms and the time for the HP compressor was about 6 ms. The frequency of these pressure fluctuations is such that, if they are related to rotating stall, then it would have to be a multicell stall condition. However, if multicell stall were present, it did not manifest itself in a destructive manner. Neither the preshock nor the post-shock pressure record shown on Figure A-5 illustrates the 370 Hz pressure fluctuation that was observed during the test time. However, the character of this fan face pressure record is dependent upon the magnitude of the overpressure pulse as illustrated by comparison of Figure A-5 and Figure A-6, which were obtained for overpressures of 1.54 psi and 2.31 psi, respectively. The pressure history shown in Figure A-6 does not contain orderly pressure fluctuations in the pre-shock region or in the test time region, but the periodic pressure fluctuations do appear during the expansion portion of the pressure pulse. The period of the pressure fluctuation is consistent with that observed for Figure A-5. The pulse decays at the end of the test time and behaves similar to the shock-tube pressure record. The pre-shock fan face pressure record shows evidence of more acoustic noise input than was observed at the shock-tube location, but this input does not degrade the overall signal.

Previous measurements described in Section A.3.1 for the GE J-85 turbojet indicated that displacement of engine components could be a difficulty when flying through overpressure environments. For both the TF33 and the J57, accelerometers were located on the inlet casing, the diffuser casing, and the turbine casing, and the output of these devices was doubly integrated to give an indication of radial displacement of the respective casing.

Figure A-13 is typical of the measured displacement histories for the TF33 turbofan. This particular record is for a fan face overpressure of 2.31 psi for a time period of approximately 20 ms. After decay of the flat-topped portion of the pressure history, the overpressure level remains at about 1 psi above the preshock level for the duration of the record. The casings begin to respond upon arrival of the shock wave, but continue to flex for some time after the peak pressure has subsided. The turbine casing displacement is small, not being much in excess of the preshock value. The diffuser casing displacement is much larger and the maximum peak-to-peak displacement occurs about 100 ms after

shock-wave arrival. The inlet casing displacement is less than the diffuser displacement and requires more time to develop. The inlet casing displacement reaches a maximum value of about 120 ms after shock-wave arrival. These histories are all interesting but the important consideration is how the displacement magnitudes compare with red-line values.

The results presented in Figures A-14 are a summary of the influence of overpressure and engine thrust on the induced casing displacements compared to the preshock and respective red-line limits for the TF33 turbofan engine. In all cases, the displacements given are peak-to-peak radial values. This particular engine was in good physical condition and all of the pre-shock displacement values were well below the limits. For the engine-off condition, the inlet and turbine displacements were well below the NRT, MRT, and TRT pre-shock values. However, even for the engine-off case, the diffuser casing displacement exceeded the limit. Figure A-14 illustrates that below 10.4 kPa (1.5 psi) the inlet casing displacement remained at or slightly below the red-line value. For overpressures above 10.4 kPa, the red-line limit was exceeded by about 50 percent for both NRT and MRT settings. The second portion of Figure A-14 presents a similar comparison for the diffuser casing and shows that the limit displacement was exceeded by about 200 percent at 6.9 kPa (1.0 psi) and by more than 300 percent at 16.0 kPa (2.3 psi). This figure also illustrates that the higher thrust setting results in increased displacement for overpressures above 13.8 kPa (2.0 psi). The trend of the MRT and TRT results is to increase rapidly with increasing overpressure. It is not unreasonable to expect the diffuser casing displacement to increase with increased thrust setting. The compressor discharge pressure level also increases with thrust increase and if the overpressure is amplified in proportion to the overall compression ratio, then the discharge pressure is going to be increased accordingly. The turbine casing displacement shown in the third part of Figure A-14 doesn't exceed the red line regardless of the thrust setting. The pressure in the turbine section did increase as indicated by the exhaust gas total pressure increase and some influence of this increase can be seen in the results.

With the engine operating, the J57 was subjected to overpressure values as high as 18.1 kPa (2.7 psi) at MRT without adverse effect; measured radial displacements are shown on Figure A-15. Also indicated on this figure are data from engine-off measurements successfully performed at overpressures in

excess of 18.7 kPa (2.8 psi). These high overpressure runs with the engine off were performed at the very end of the test series.

A video camera was used to monitor the engine exterior and the tail pipe during all of the overpressure testing. On one of the repeat runs with the engine operational (prior to the engine-off runs described above) at an overpressure level of 14.1 kPa (2.1 psi) a small flame streak (see Figure A-16) and a surge (see Figure A-17) were observed to exit the tail pipe. The overpressure was then increased to about 18.1 kPa (2.7 psi) and a shower of sparks was observed to exit the tail pipe. These sparks were probably the result of an internal rub.

The engine surge experienced in the J57 overpressure experiments was not an operation-limiting event. Only a single surge would occur during each acceleration and it was possible to drive through the event and obtain satisfactory engine operation. The engine was then turned off and allowed to remain inactive for a 24-hour period. When it was again started and allowed to warm up, a series of rapid accelerations produced only a single surge, suggesting that the surging problem had cleared itself.

In conclusion, the response of both a TF33 turbofan engine and a J57 turbojet engine to overpressure pulses has been evaluated for overpressures from 6.9 kPa (1.0 psi) to 19.4 kPa (2.8 psi) at thrust settings from engine-off to TRT. No engine failures were encountered with either engine. The key indicators monitored for incipient engine damage were the exhaust gas total pressure, the exhaust gas total temperature, the HP compressor speed, the bleed valve position, the inlet casing radial displacement, the diffuser casing radial displacement, and the turbine casing radial displacement. For both engines, the exhaust gas total pressure probe indicated passage of the overpressure pulse even though the frequency response of the manifold system was relatively low. However, the HP compressor speed, the bleed valve position, and the EGT were all insensitive to the pressure pulse. While the transient diffuser casing radial displacement exceeded the manufacturer's steady-state maximum value by more than 300 percent, the deflection was damped before permanent engine damage could result. It is difficult to speculate how far one could push the overpressure level before permanent engine damage might occur.

A.3.4 Observations and Suggestions for the User.

At the present time, there are no gas turbine engines in the military inventory that have been designed and tested to an overpressure specification.

UNCLASSIFIED

The F101 engine was designed to be hard to overpressure, but the test phase of the engine development was satisfied on the basis of a paper study. The experimental data relevant to overpressure effects on the operation of gas turbine engines are composed of the extensive data base obtained at Calspan and the limited data obtained at Holloman AFB. On the basis of this experimental work, it has become clear that there are many important parameters to consider, e.g., the strength of the overpressure wave, the angle at which the overpressure wave intercepts the engine, the thrust condition at which the engine is operating upon encounter, the altitude of the encounter, and the configuration of the inlet. The engine measurements performed to date have been done for overpressure values equal to or greater than the values to which the aircraft on which they are mounted have been hardened.

From an engine viewpoint, it is best to take an overpressure wave from the rear (180°) while operating at high thrust level. At this thrust condition, the turbine is generally choked and for overpressure waves that the airframe can withstand, it is virtually impossible to unchoke the machine. The second preference would be to intercept the overpressure wave front-on (0°). At this condition, flow distortion within the inlet would generally be less severe than it would be at other intercept angles. If possible, it would reduce the load on the internal engine structure if the thrust setting could be reduced for this particular encounter. The reason for this is that the compressor tends to amplify the overpressure and at high thrust setting, the compression ratio is greater than it is at lower thrust.

The specific engines that have been tested to date and which are of specific interest to this discussion are the J57 turbojet, the TF33 turbofan, and the F107 turbofan. In all cases, the engines were tested without failure at overpressures greater than that to which the airframe is known to be hardened.

The altitude of the encounter is felt to also be of some importance since it is well known that most gas turbine engines are more sensitive to surge and flame out at high altitude than they are at low altitude. If it is possible to predict the approximate time of encounter, then the crew should be prepared for an engine restart.

In the case of the engine for which a problem was encountered (J85), the problem came in the form of very large engine vibrations while and shortly after the overpressure wave was passing through the engine. The operator action was to immediately retard the throttle to idle which did not produce an immediate

result. However, within a short period of time, recovery was complete and the engine was operational.

It was noted above that the inlet configuration is important. If the inlet happens to have a low value of length to diameter (L/D) and if the yaw angle is other than 0° or 180° , then the distortion at the engine face can be significant resulting in operational difficulties. On the other hand, for large values of L/D the flow in the inlet duct can adjust to the leading edge separation and the inlet distortion does not have as important an influence on engine operation.

A.4. CONCLUSIONS.

The available experimental data regarding the response of gas turbine engines to blast wave environments typical of those associated with the detonation of nuclear devices have been reviewed. All overpressures were low enough to be consistent with airframe survival. The specific engines for which data are available are: the J85 turbojet, the TF-33 turbofan, the J-57 turbojet, and the F-107 turbofan. Permanent damage was sustained only by the J85 turbojet. Beyond this, general conclusions regarding each of these engine measurement programs are difficult to state. Therefore, the approach taken here has been to provide these conclusions on a specific engine basis in the section in which that engine is discussed.

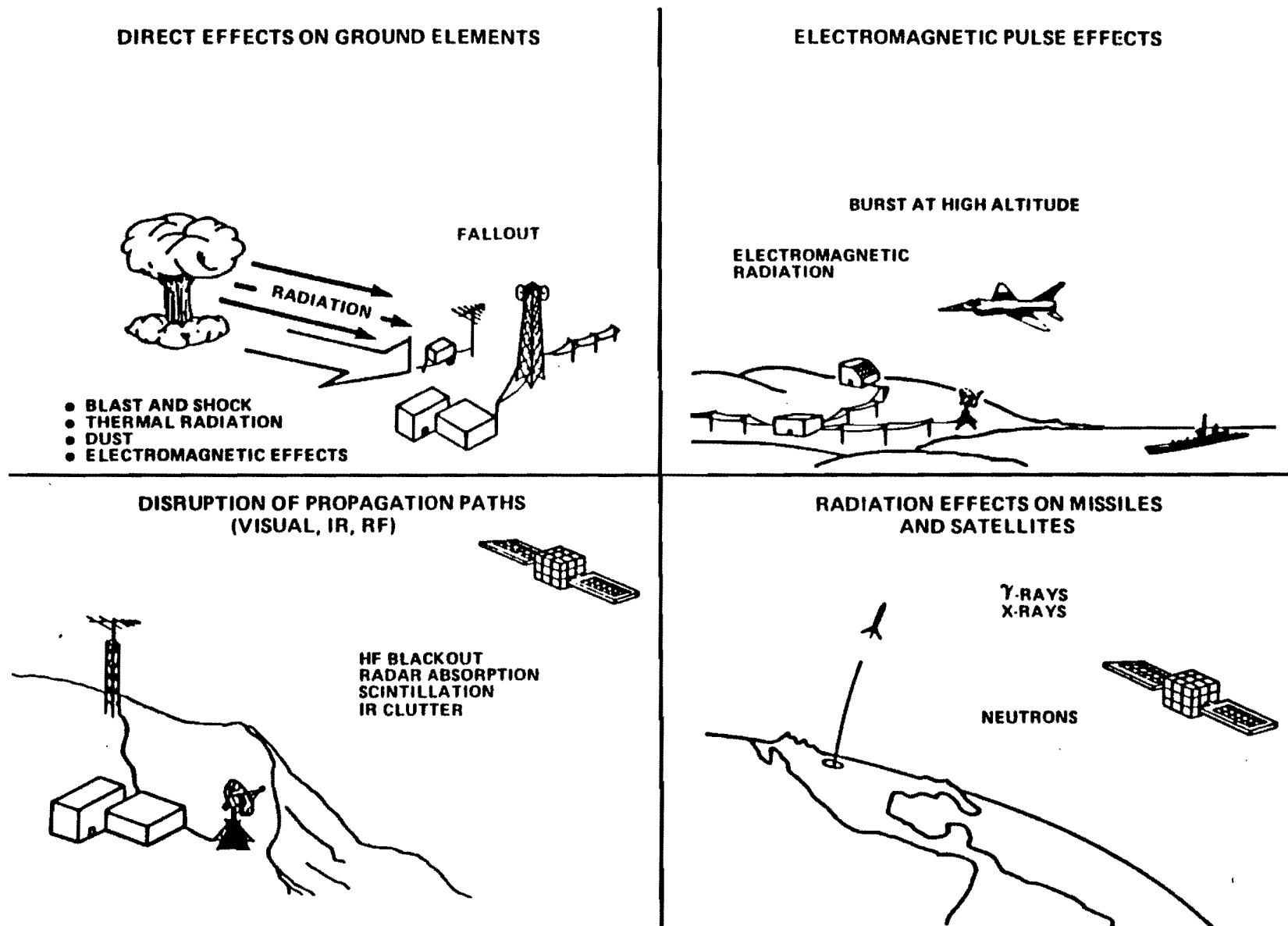
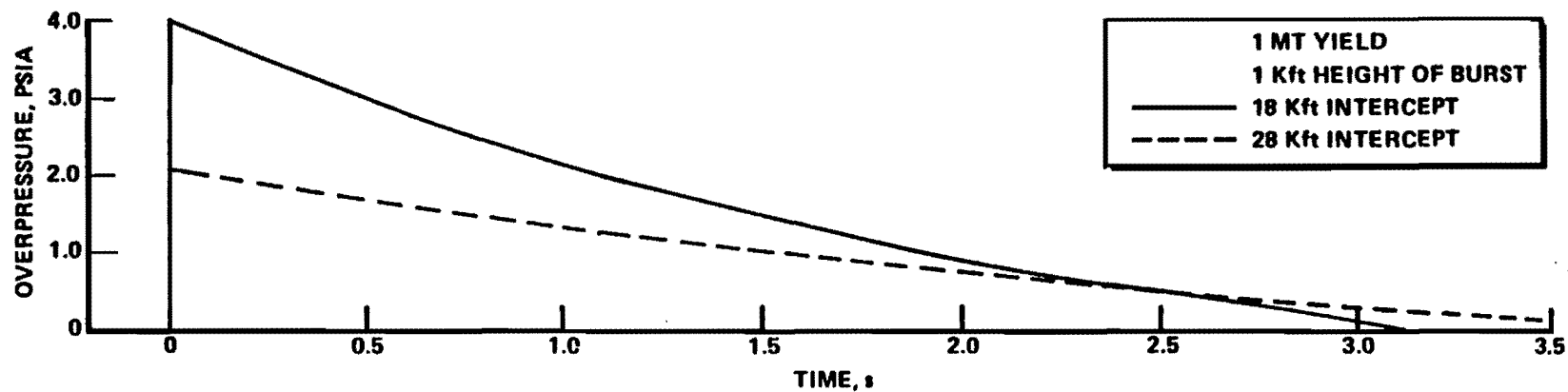


Figure A-1. Nuclear weapon effects.

a) TYPICAL NUCLEAR OVERPRESSURE PULSE



b) TYPICAL SHOCK-TUBE PULSE

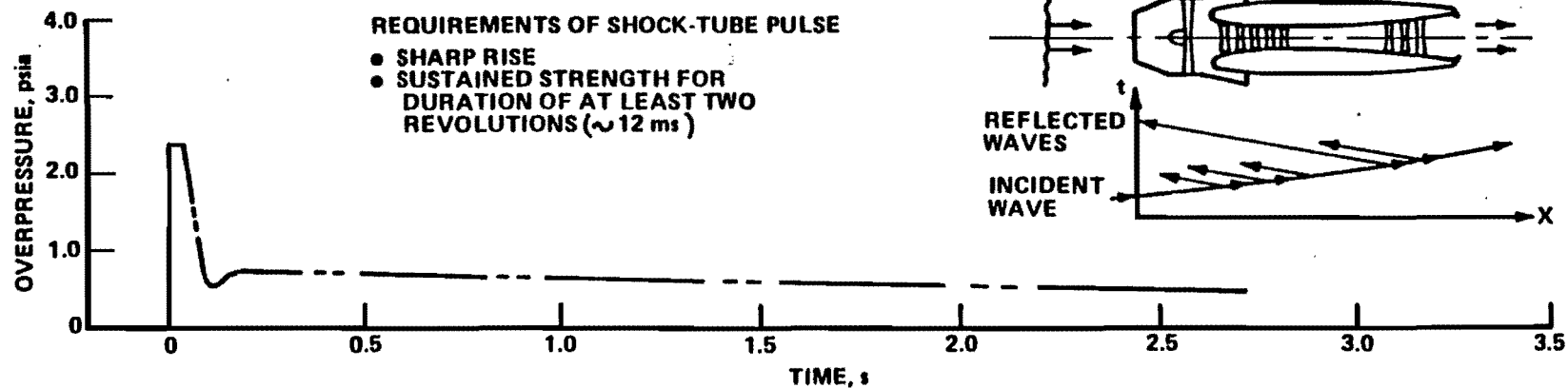


Figure A-2. Pulse requirements.

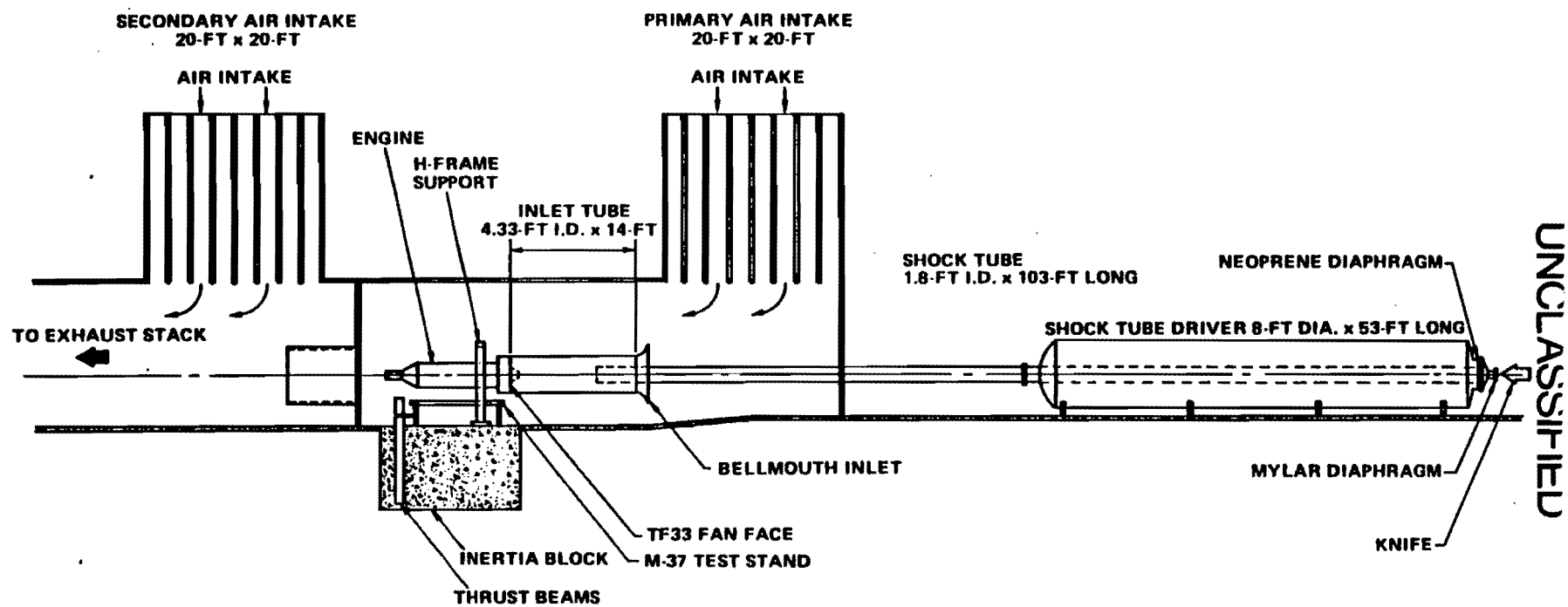
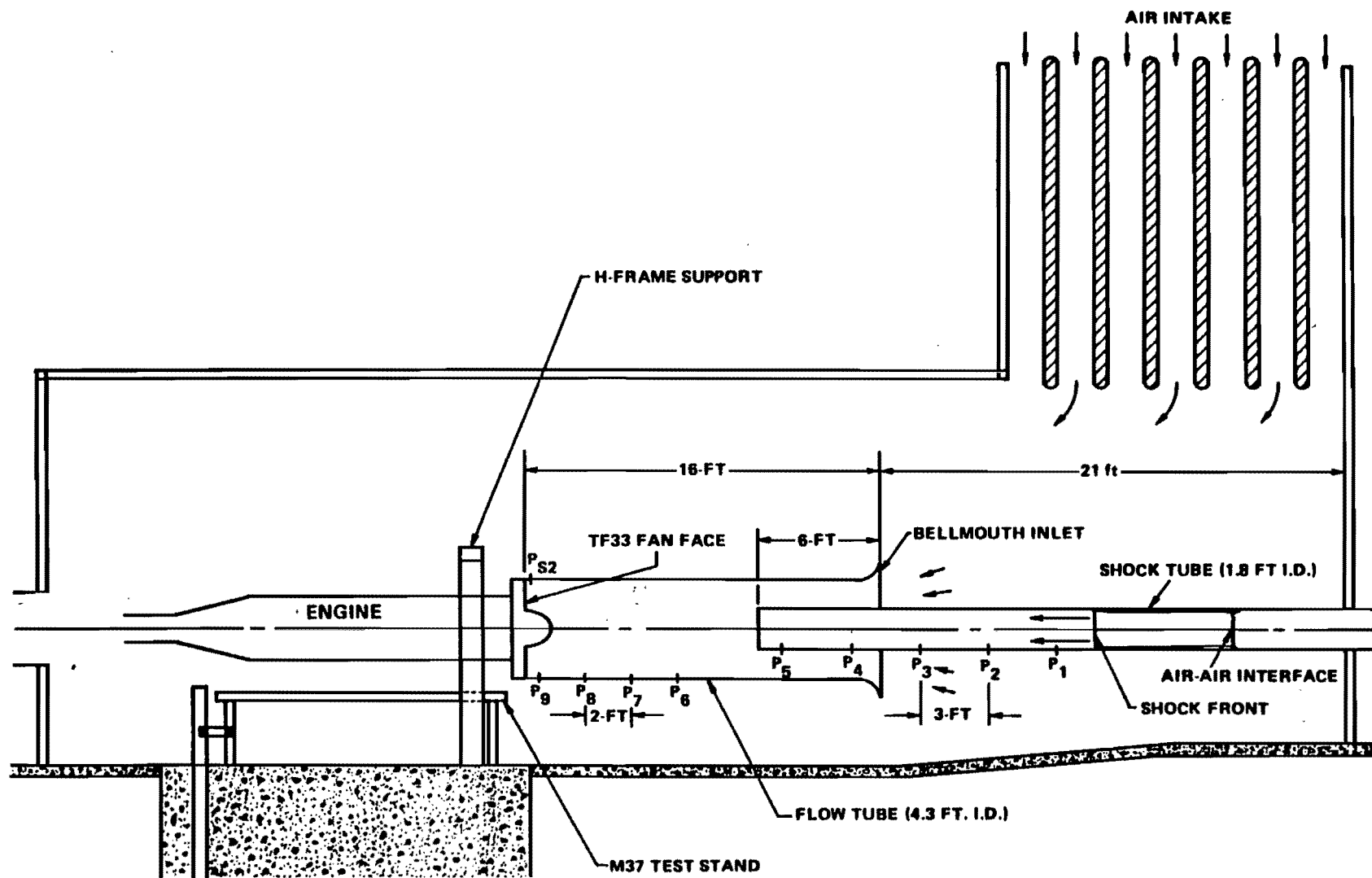


Figure A-3. Sketch of chock tube and test cell configuration.

UNCLASSIFIED

77



UNCLASSIFIED

Figure A-4. Sketch of test cell configuration.

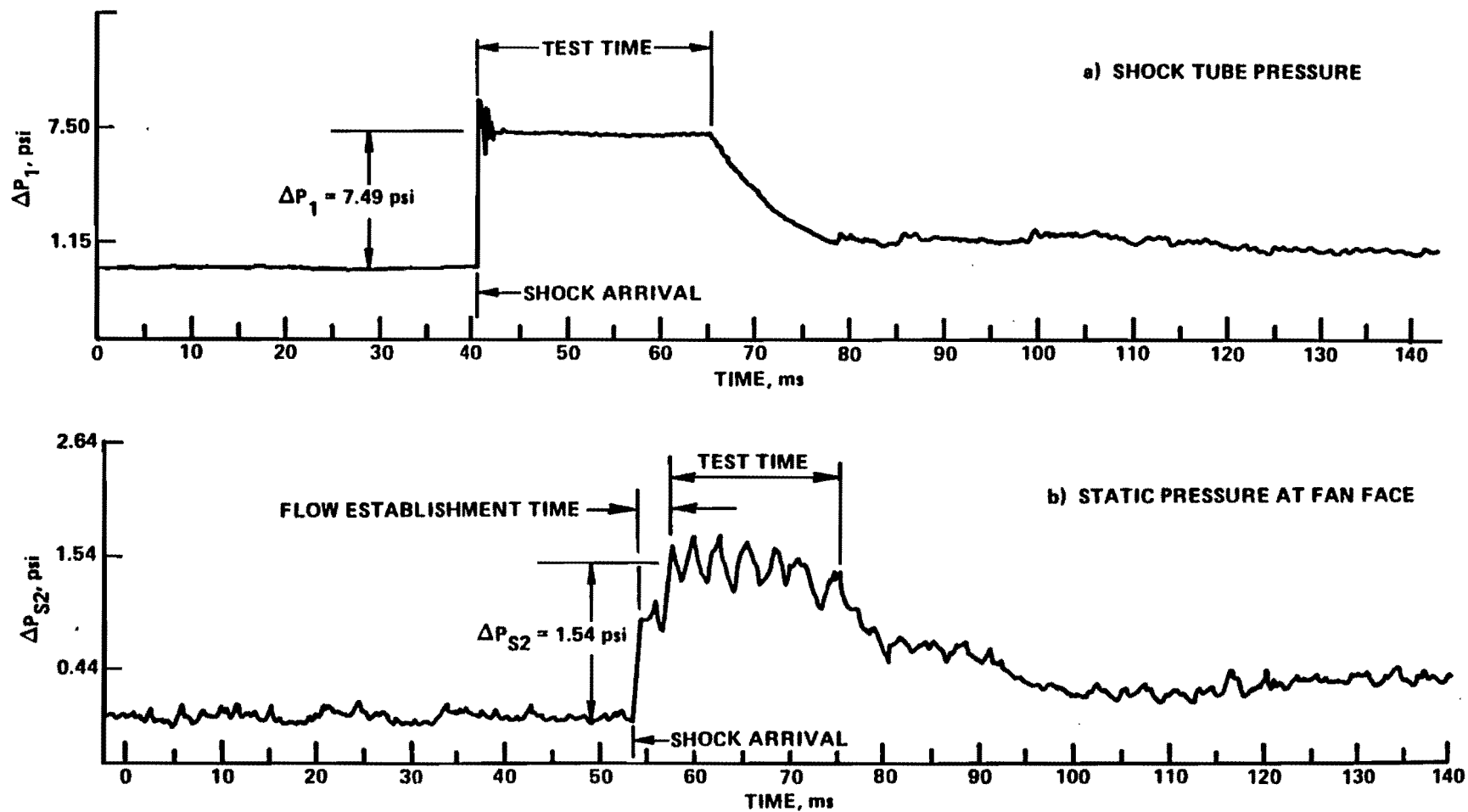


Figure A-5. Typical shock tube and fan face static pressure records for TF33 at MTR setting.

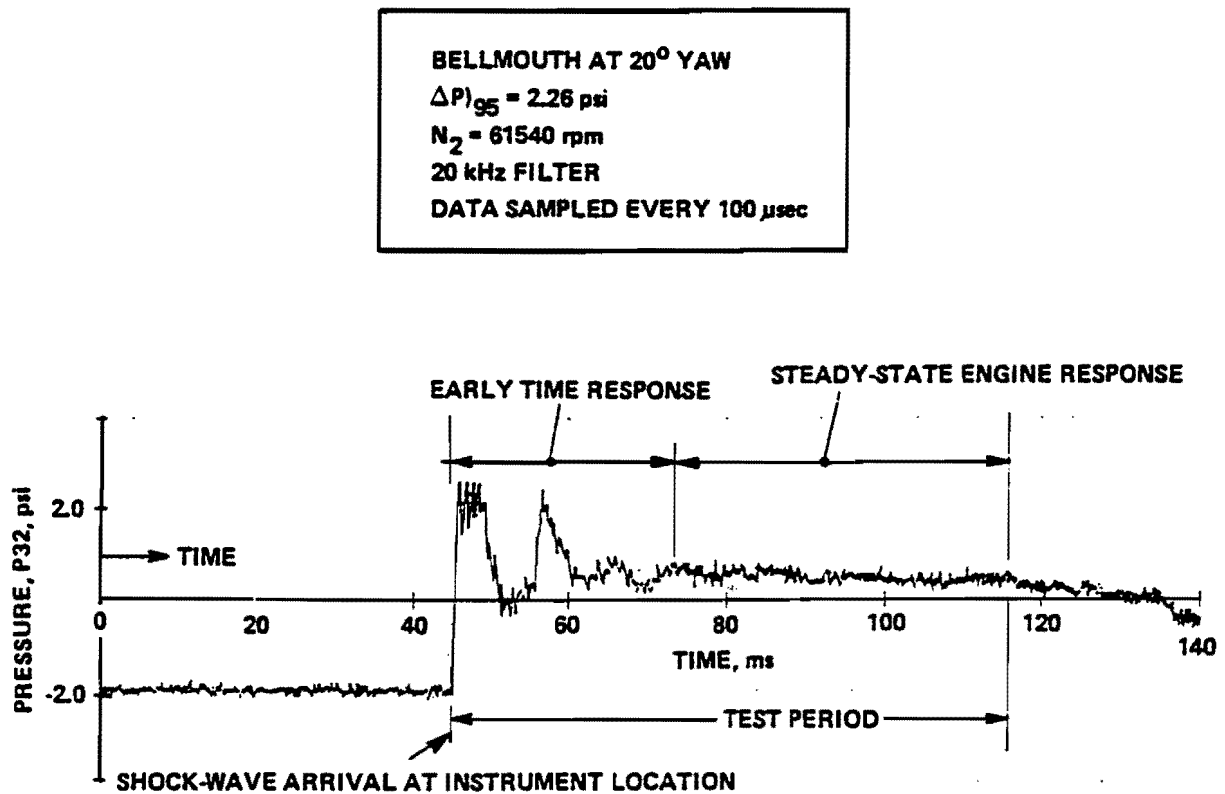


Figure A-6. Typical pressure history.

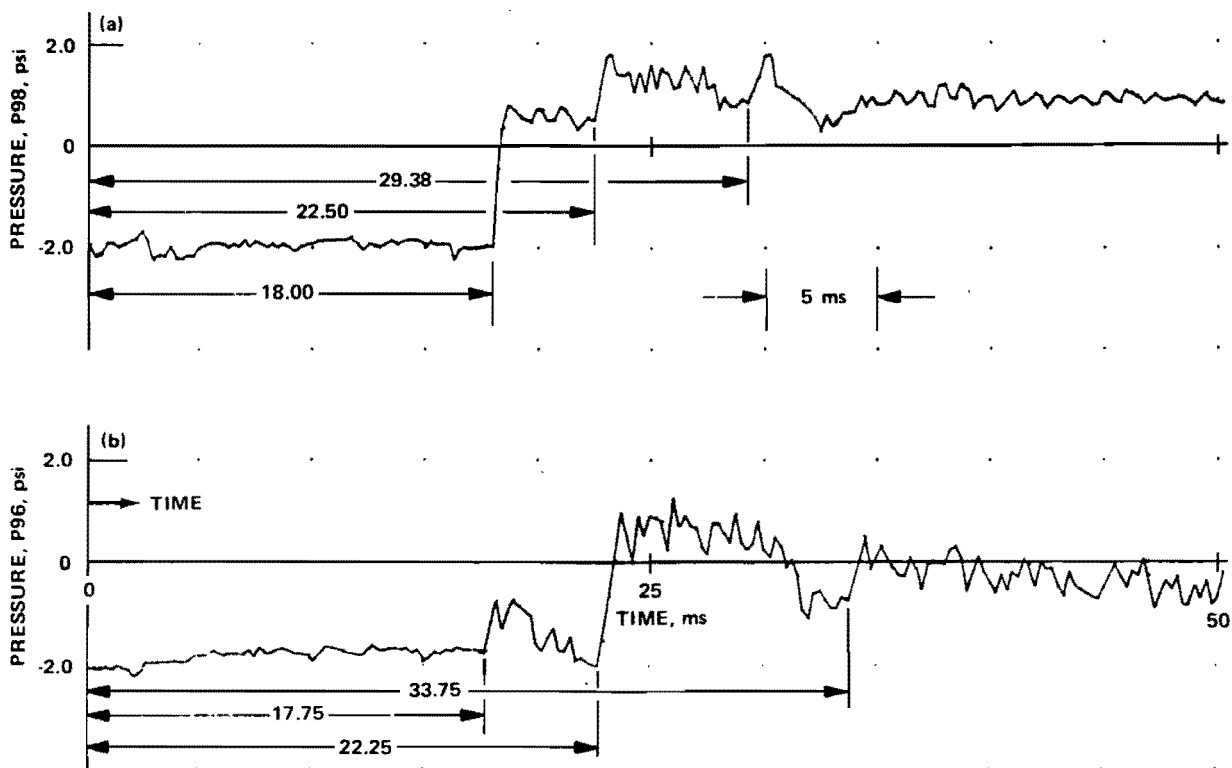
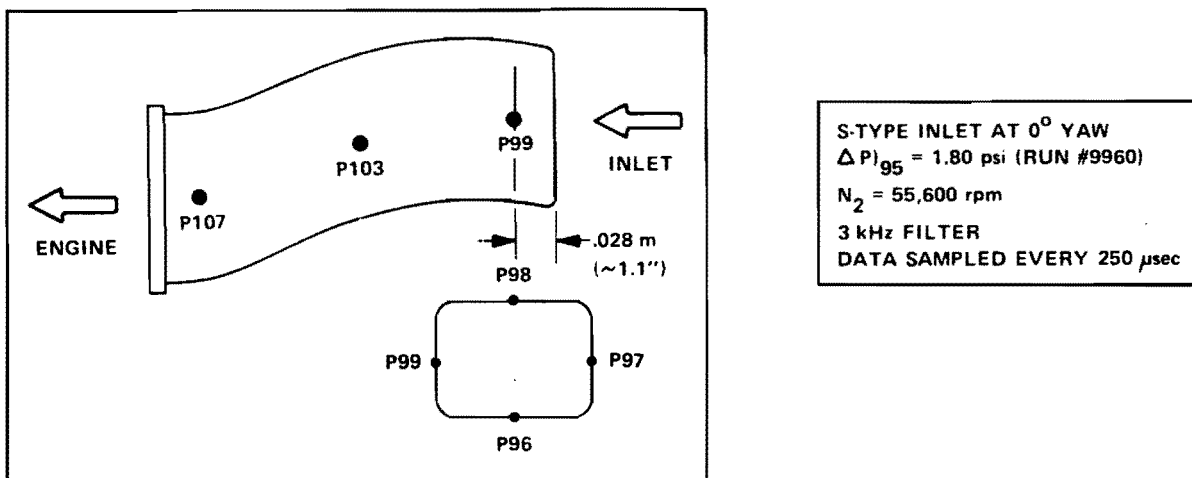


Figure A-7. Typical pressure-data history for station #1 in S-type inlet at 0 deg yaw.

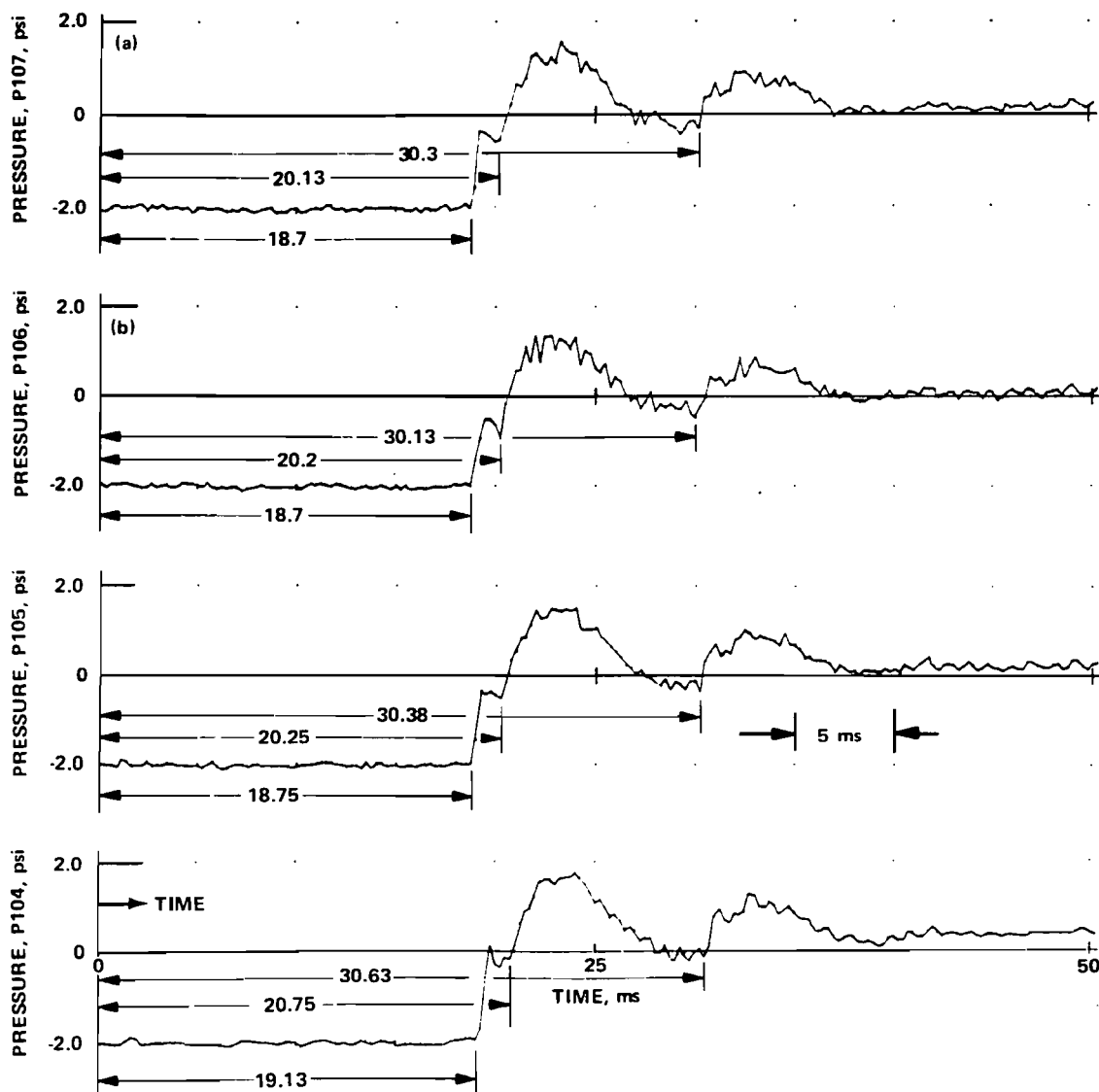
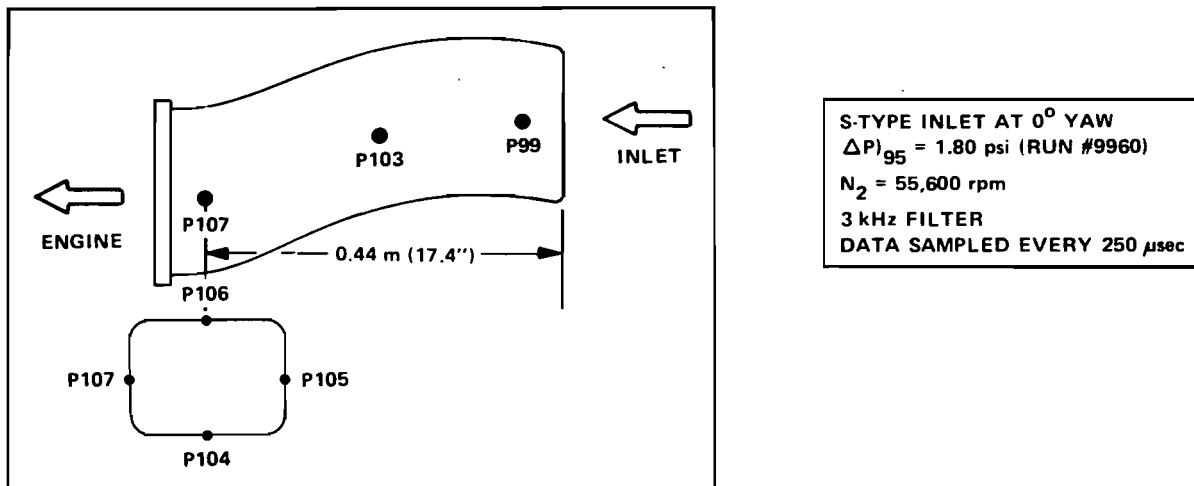


Figure A-8. Typical pressure-data history for station #3 in S-type inlet at 0 deg yaw.

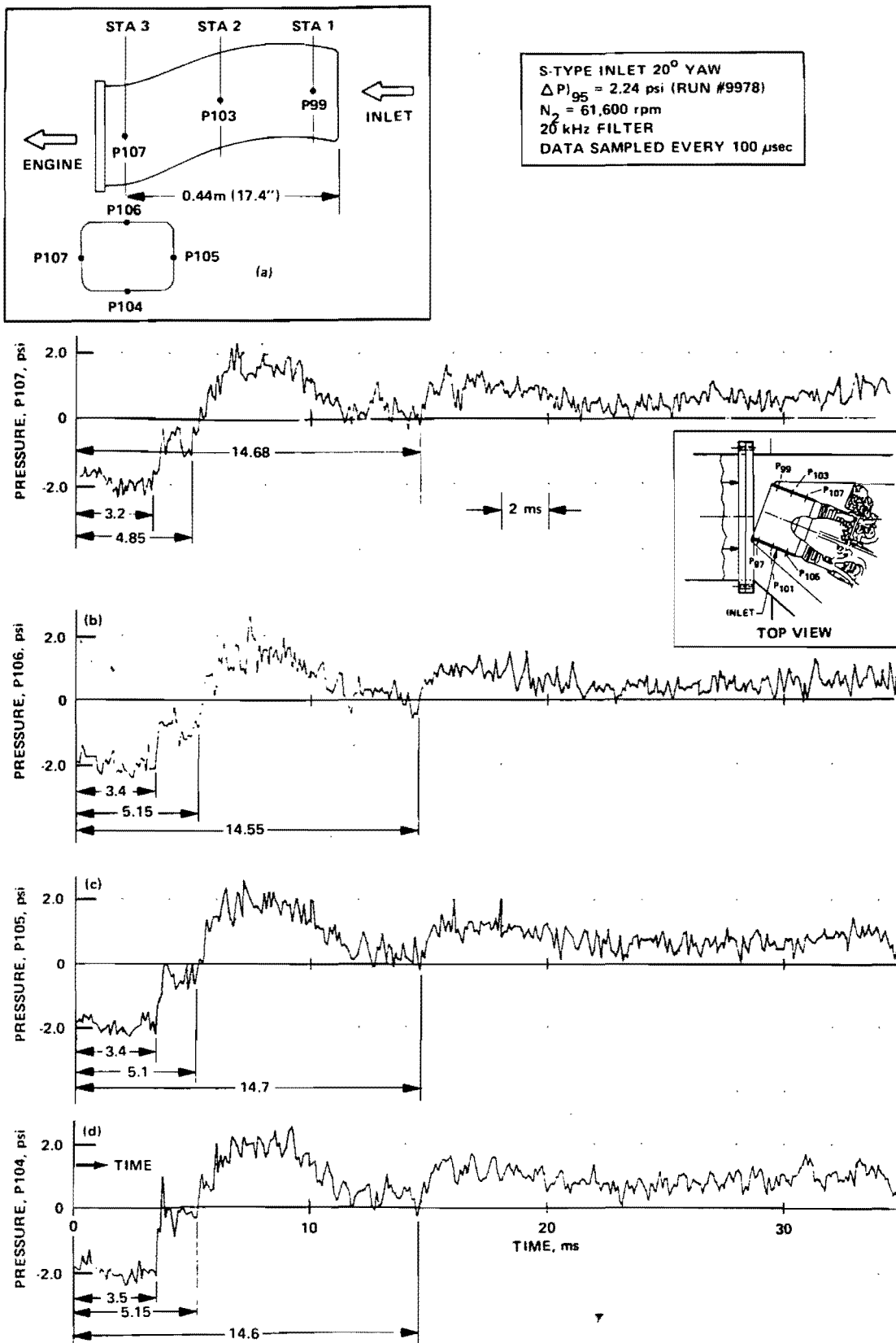


Figure A-9. Typical pressure-data history for station #3 in S-type inlet at 20 deg yaw.

UNCLASSIFIED

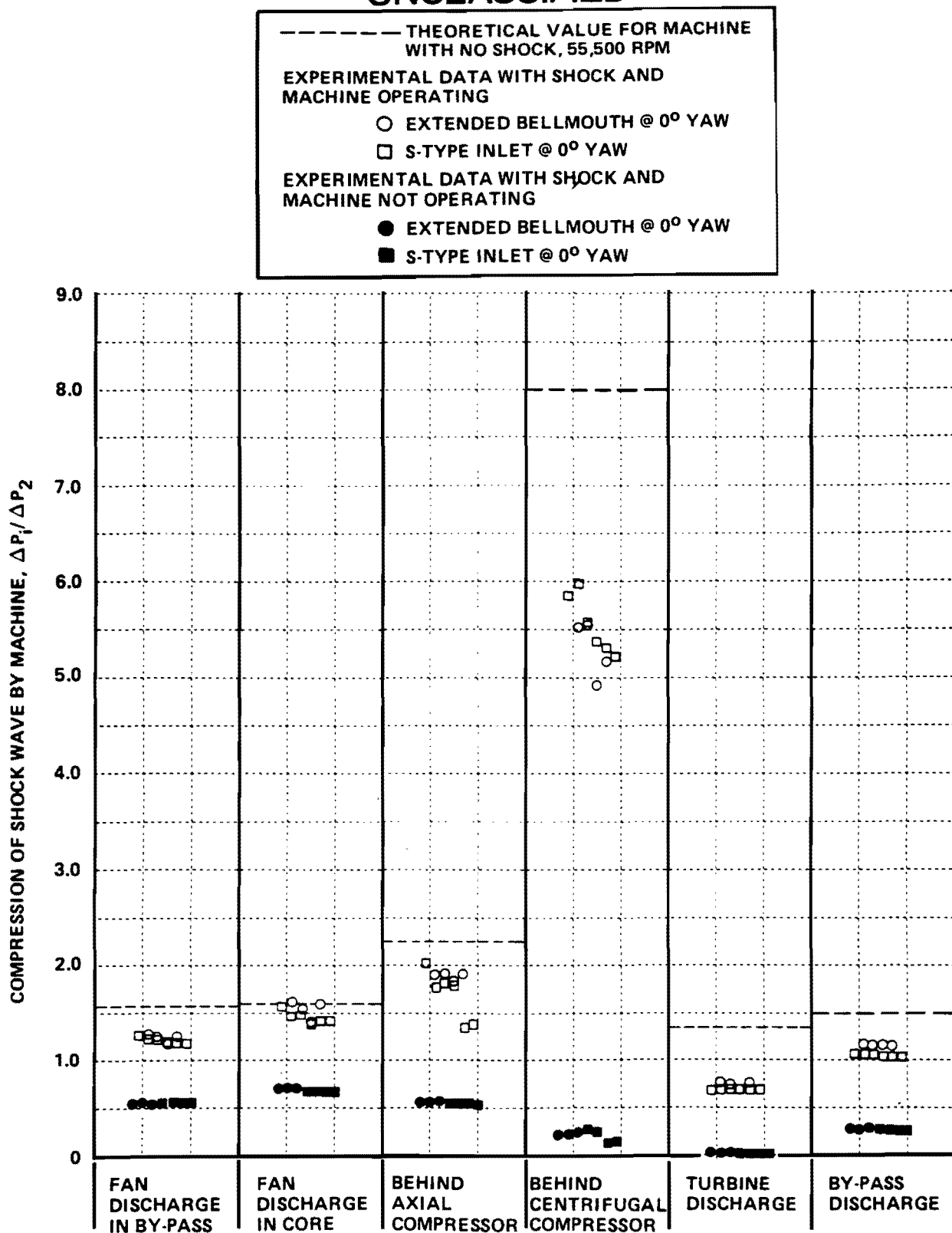


Figure A-10. Engine pressure results for core speed of 55,500 rpm.

UNCLASSIFIED

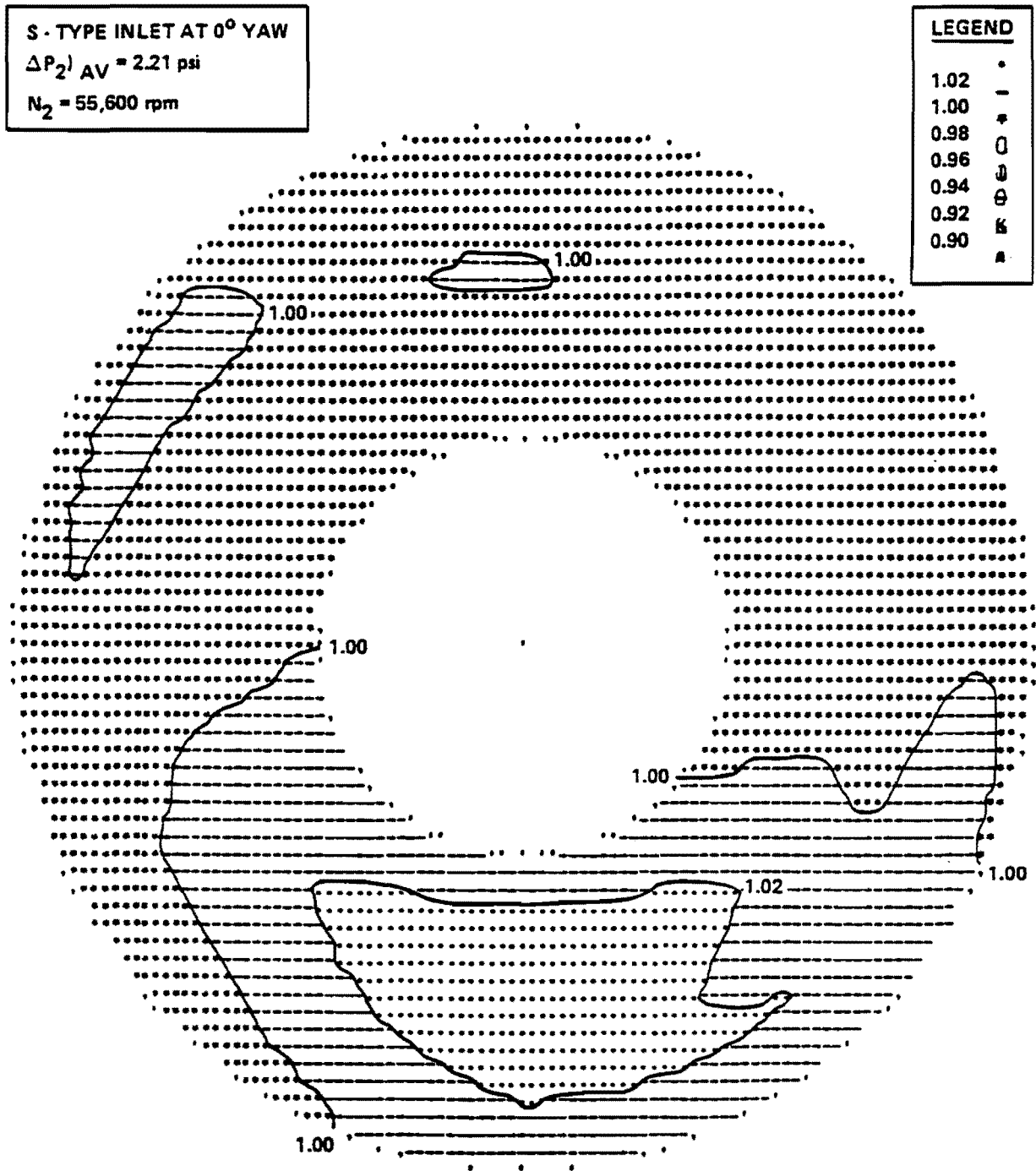


Figure A-11. Distortion index for S-type inlet at 0 deg yaw.

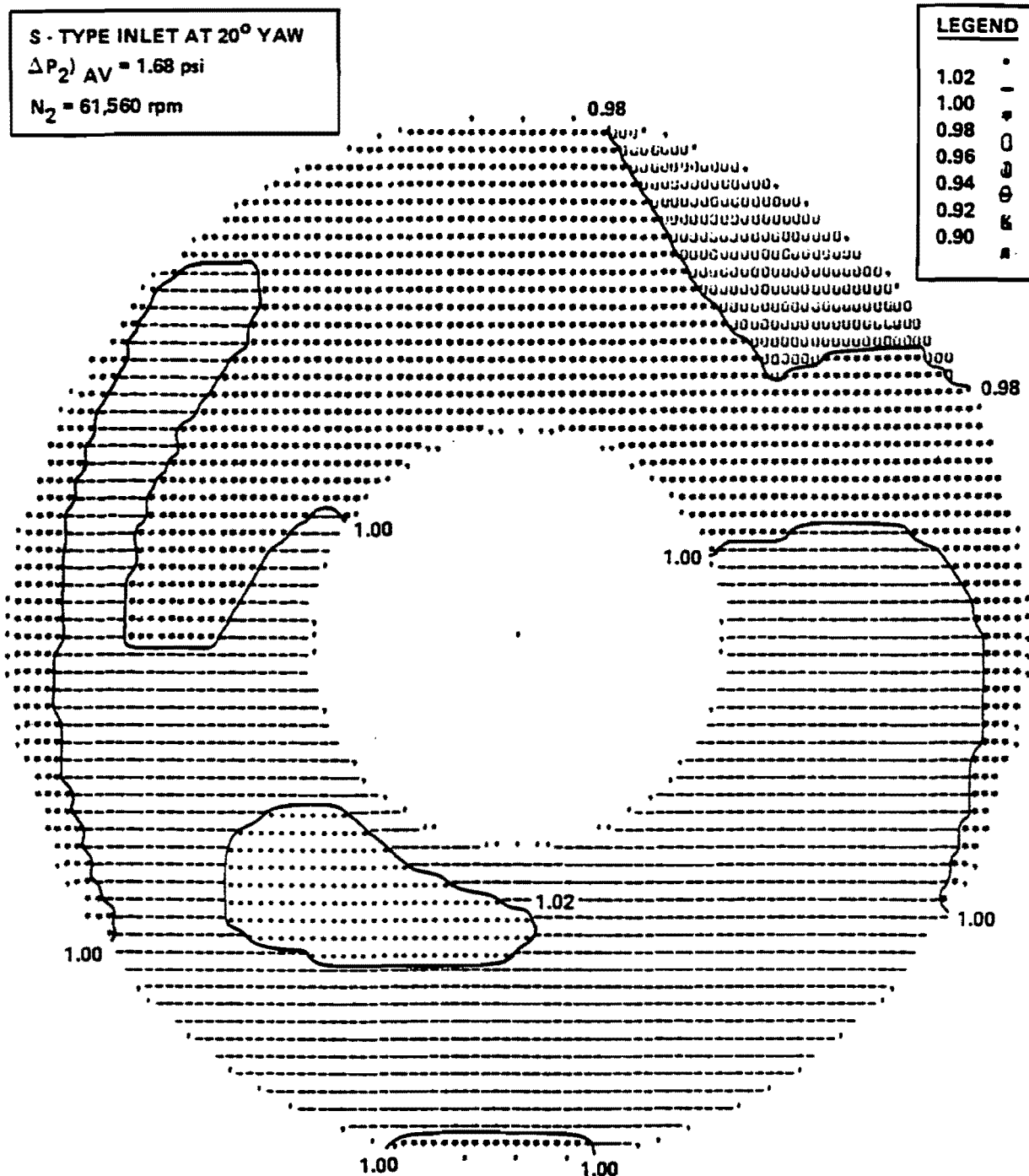


Figure A-12. Distortion index for S-type inlet at 20 deg yaw.

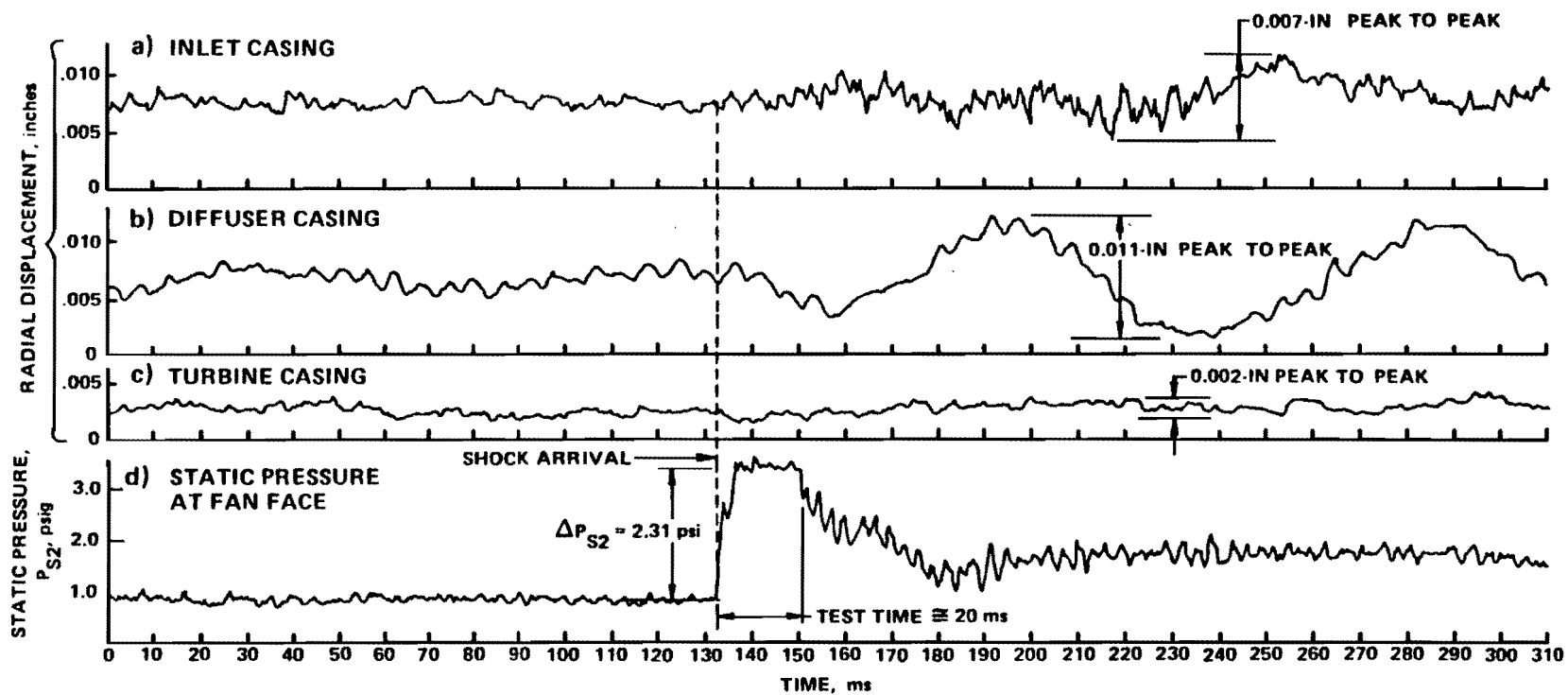


Figure A-13. Typical component radial displacement histories for TF33 at MFT setting.

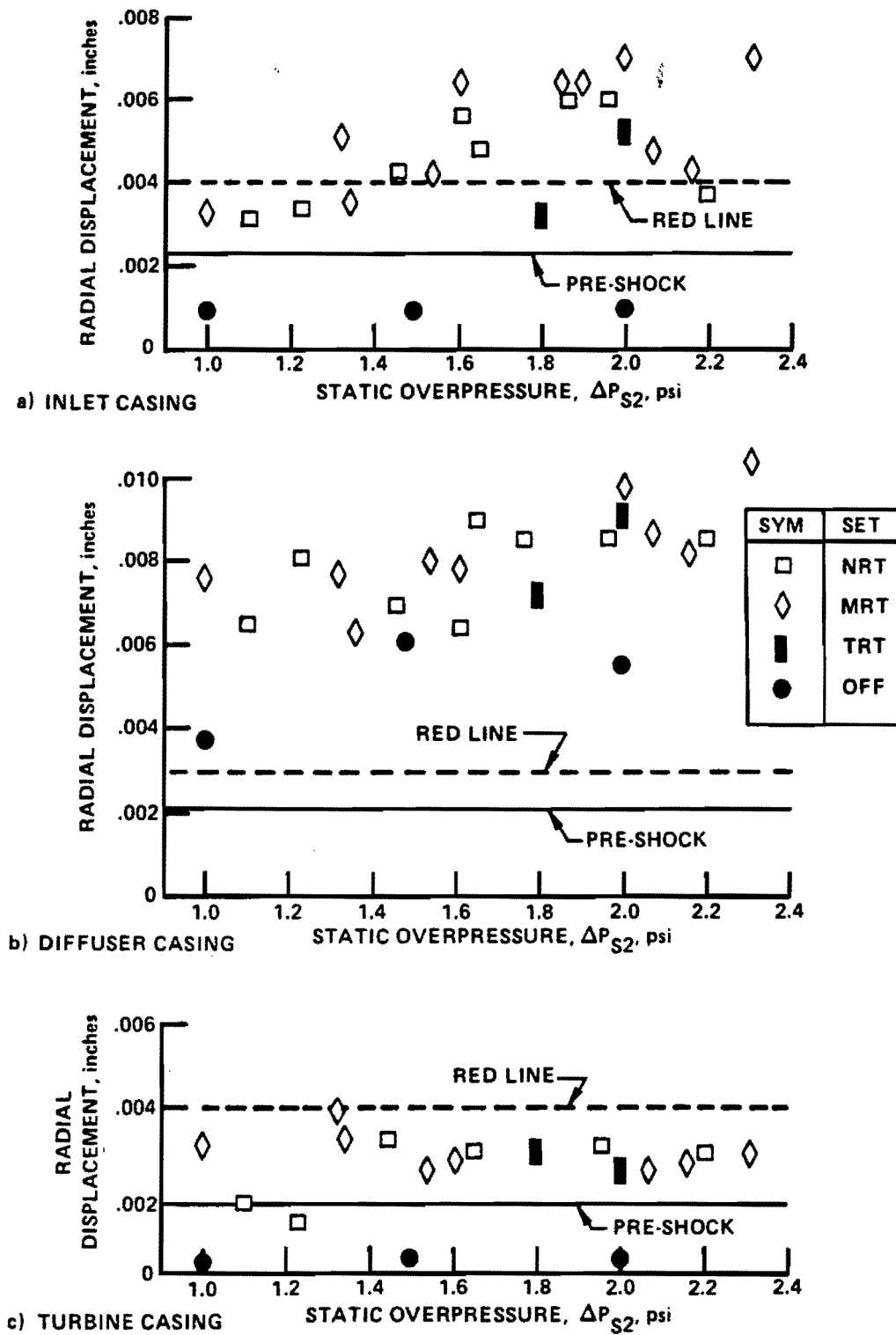


Figure A-14. Influence of overpressure on TF33 inlet, diffuser, and turbine casing displacement.

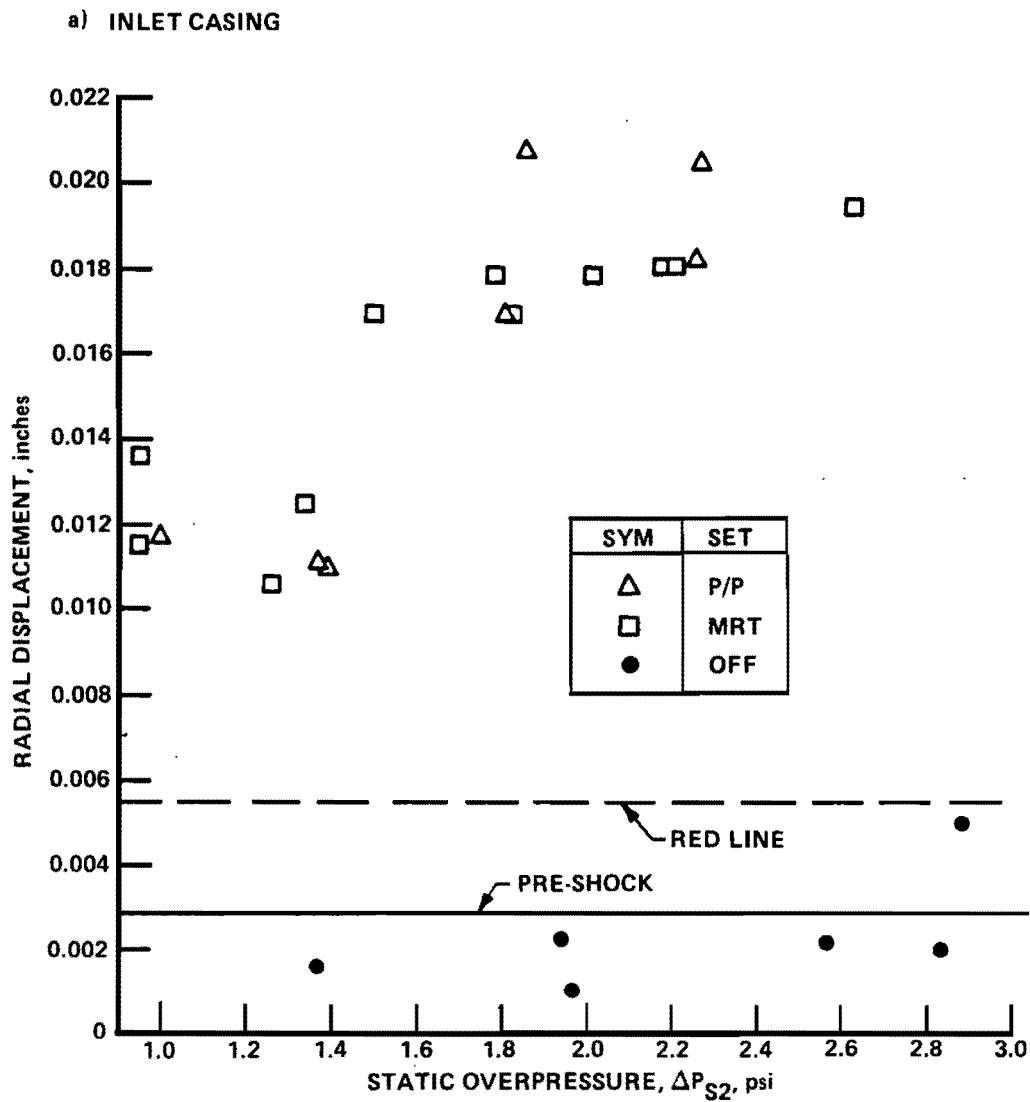


Figure A-15. Influence of overpressure on J57 inlet, diffuser, and turbine casing displacement.

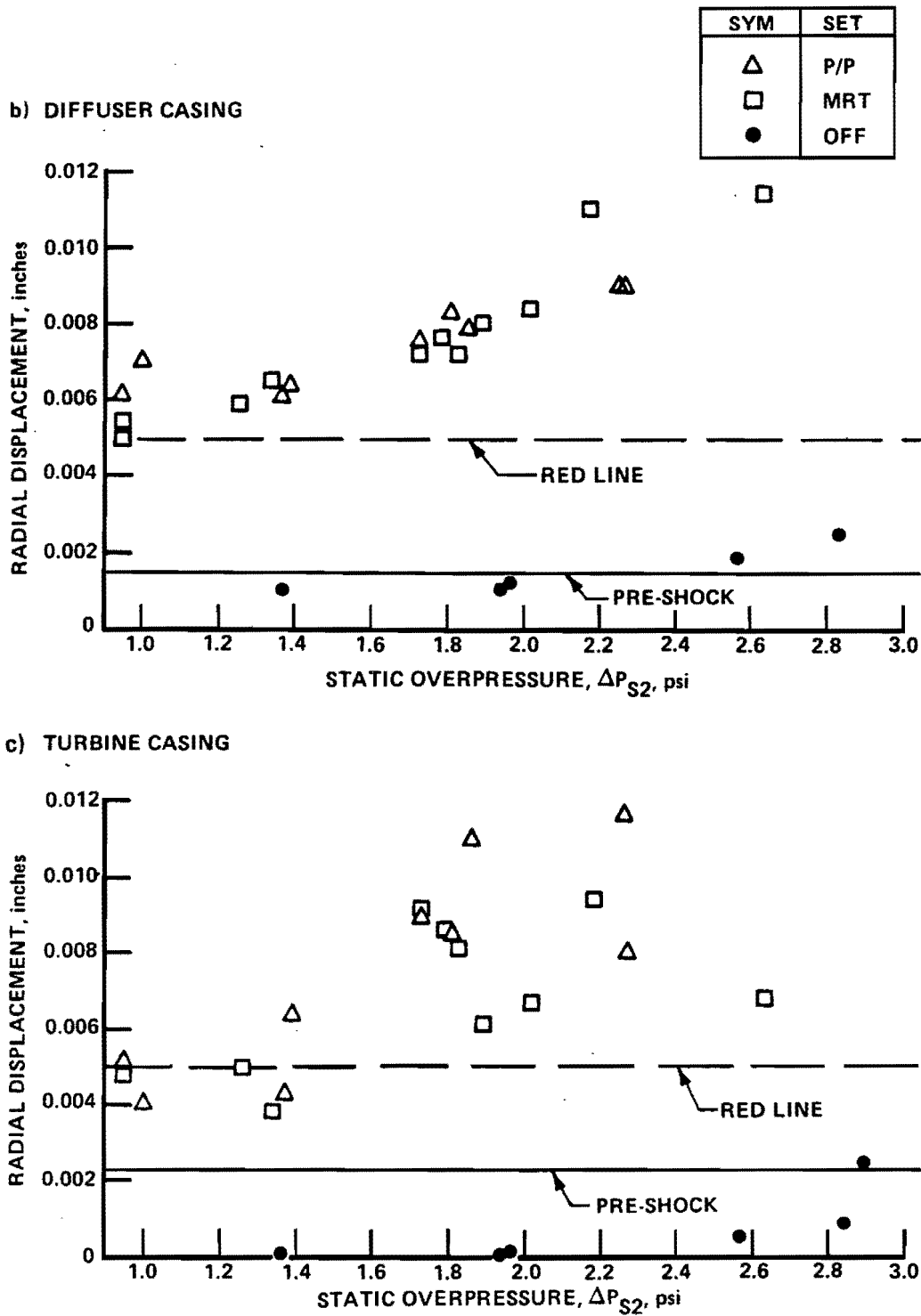


Figure A-15. Influence of overpressure on J57 inlet, diffuser, and turbine casing displacement (Continued).

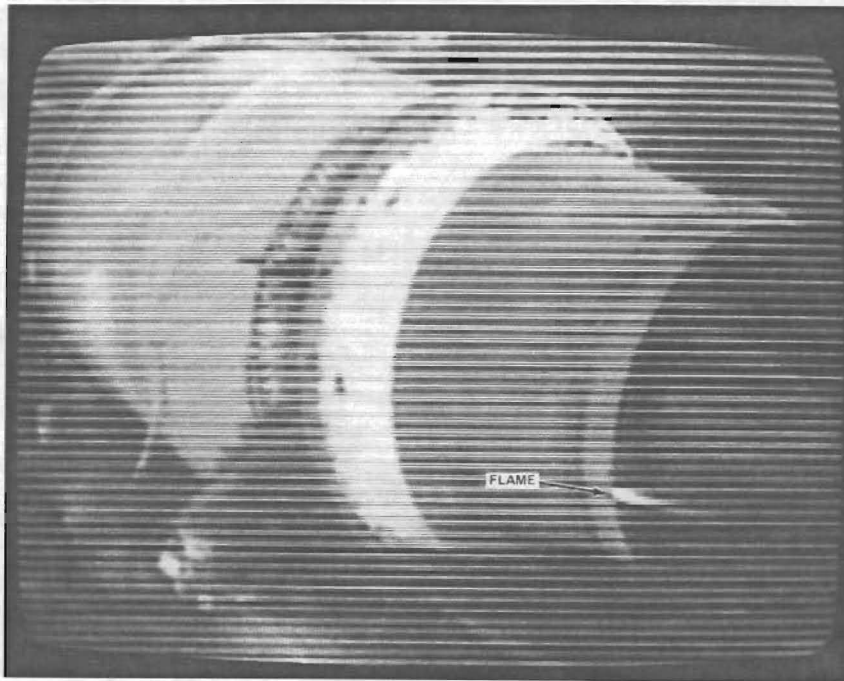


Figure A-16. Photograph of initial tailpipe flame for 2.1 psi overpressure.

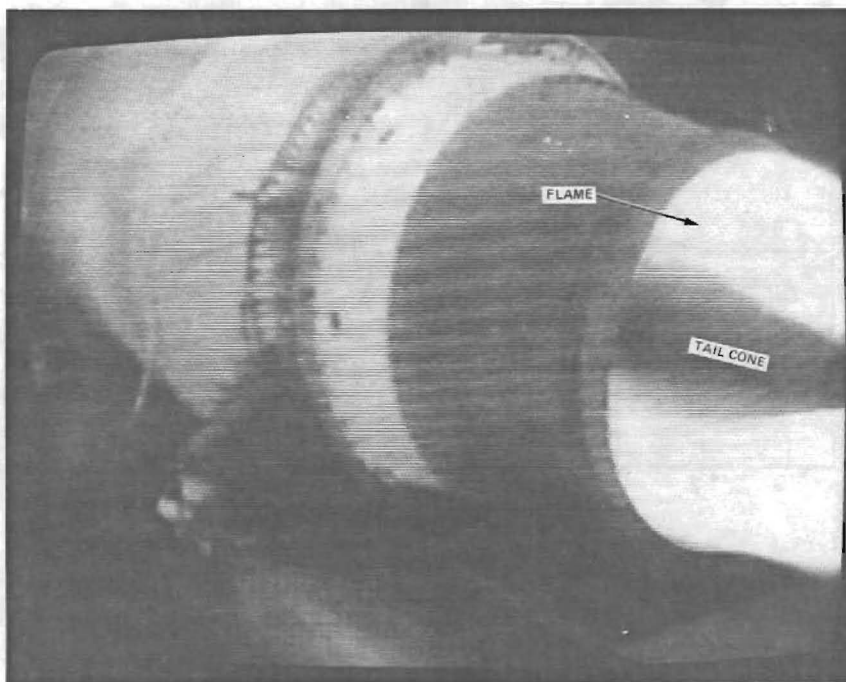


Figure A-17. Photograph of tailpipe surge during acceleration.

UNCLASSIFIED

DISTRIBUTION LIST

DNA-TR-93-2

(This List Is Unclassified)

DEPARTMENT OF DEFENSE

ASSISTANT TO THE SECRETARY OF DEFENSE
ATTN: EXECUTIVE ASSISTANT

DEFENSE INTELLIGENCE AGENCY
ATTN: DIW-4

DEFENSE NUCLEAR AGENCY
ATTN: NASF
ATTN: OPNA
2 CY ATTN: SPWE
2 CY ATTN: TITL

DEFENSE TECHNICAL INFORMATION CENTER
2 CY ATTN: DTIC/OC

DEPARTMENT OF THE ARMY

ARMY RESEARCH LABORATORIES
ATTN: SLCSM-SE

U S ARMY NUCLEAR & CHEMICAL AGENCY
ATTN: MONA-NU DR D BASH

US ARMY CHEMICAL SCHOOL
ATTN: COMMANDING OFFICER

DEPARTMENT OF THE NAVY

NAVAL RESEARCH LABORATORY
ATTN: CODE 7920

OFFICE OF CHIEF OF NAVAL OPERATIONS
ATTN: NUC AFFAIRS & INTL NEGOT BR

DEPARTMENT OF THE AIR FORCE

AERONAUTICAL SYSTEMS CENTER
ATTN: ASD/ENSS HUGH GRIFFIS

AIR UNIVERSITY LIBRARY
ATTN: AUL-LSE

HQ USAF/XOFN
ATTN: XOFN

OKLAHOMA CITY AIR LOGISTICS CTR
ATTN: OCALC/LAS M BUTLER
ATTN: OCALC/LPAAM S GARDNER
ATTN: OCALC/LTAJM J CRIBBS

OTHER GOVERNMENT

CENTRAL INTELLIGENCE AGENCY
ATTN: OSWR/NED

DEPARTMENT OF DEFENSE CONTRACTORS

AEROSPACE CORP
ATTN: D LYNCH

APPLIED RESEARCH INC
ATTN: J BOSCHMA

CALSPAN CORP
2 CY ATTN: M DUNN

GENERAL ELECTRIC CO
ATTN: D KUEHNER
ATTN: K KOCH
ATTN: Z PRZEDPELSKI

HORIZONS TECHNOLOGY, INC
ATTN: E TAGGART

JAYCOR
ATTN: CYRUS P KNOWLES

KAMAN SCIENCES CORP
ATTN: D COYNE

KAMAN SCIENCES CORP
ATTN: R HARDY

KAMAN SCIENCES CORP
ATTN: DASIAAC

KAMAN SCIENCES CORPORATION
ATTN: DASIAAC

LOGICON R & D ASSOCIATES
ATTN: J DRAKE
ATTN: LIBRARY

LOGICON R & D ASSOCIATES
ATTN: E FURBEE
ATTN: J WEBSTER

MCDONNELL DOUGLAS CORPORATION
ATTN: L COHEN

NORTHROP CORP
ATTN: G CURRY

PACIFIC-SIERRA RESEARCH CORP
ATTN: R LUTOMIRSKI
ATTN: S FUGIMURA

PACIFIC-SIERRA RESEARCH CORP
ATTN: M ALLERDING

PHYSITRON INC
ATTN: M PRICE

Dist-1

UNCLASSIFIED

UNCLASSIFIED

DNA-TR-93-2 (DL CONTINUED)

SCIENCE APPLICATIONS INTL CORP
ATTN: J COCKAYNE
ATTN: P VERSTEEGEN

SRI INTERNATIONAL
ATTN: E UTHE
ATTN: J PRAUSA
ATTN: M SANAI

TOYON RESEARCH CORP
ATTN: J CUNNINGHAM
ATTN: T GEYER

UNITED TECHNOLOGIES CORP
ATTN: BEN KOSS

W J SCHAFER ASSOCIATES, INC
ATTN: D YOUMANS
ATTN: W BUITENHUYS

WILLIAMS INTERNATIONAL CORP
ATTN: D FISHER

Dist-2

UNCLASSIFIED


DECLASSIFIED

DECLASSIFIED
